

Interstellar molecule reactions*

William D. Watson†

Departments of Physics and Astronomy, University of Illinois at Urbana-Champaign, Urbana, Illinois 61801

Considerable progress has been made during the past five years toward a quantitative understanding of the formation and destruction processes for interstellar molecules. Two areas have been most successful—investigations of the formation process for molecular hydrogen on the surfaces of dust grains and studies of reactions involving positive ions in the gas. Laboratory measurements for ion–molecule reaction rates have provided strong support for the latter. Extensive studies at ultraviolet wavelengths from the *Copernicus* satellite make possible detailed comparisons between predictions and observations for H₂ and other species in the diffuse interstellar gas. These confirm that a hydrogen atom is converted into an H₂ molecule at approximately every collision with an interstellar dust grain. In the more dense interstellar gas, observations with radio telescopes provide vast data on complex molecules and have recently identified a number of reactive intermediate species—HCO⁺, N₂H⁺, HNC, CCH—whose presence strongly supports the proposed reaction processes. The quite recent development of laboratory methods to measure the microwave frequencies of reactive molecules and molecular ions has been an essential contribution to these identifications. Observed fractionation of (deuterium/hydrogen) and possibly (carbon-13/carbon-12) in certain interstellar molecules provide additional challenges and information for studies of reactions. Although there is semiquantitative agreement between predictions and observed abundances for a wide range of small molecular species, the tests are sufficiently precise in only a few cases to reach reasonably definitive conclusions. To a large degree this is due to poor knowledge of the physical conditions in the gas where the molecules are located. Certain laboratory data are needed—especially, photodissociation cross sections and radiative lifetimes in the ultraviolet, as well as some charge-transfer and reaction rate coefficients under low temperature/density conditions. Information on surface reactions applicable to the astrophysical situation is also desirable. At present the chief problems for interstellar molecule reactions are understanding the formation of larger molecules (larger than triatomic), and the role of surface reactions on dust grains for molecules other than H₂. A lengthy introduction to the interstellar medium is provided for the nonastronomer. The status of information on the basic surface and gas phase processes is reviewed. Finally, the reaction schemes which seem to be of most importance for the major species of small interstellar molecules are discussed and quantitatively compared with observations when possible. Reactions that produce isotope fractionation are treated in some detail.

CONTENTS

I. Introduction	513	D. Electron–ion recombination: Radiative and dissociative	537
A. Nature of the interstellar medium	513	E. Photodissociation/photoionization	538
B. Observation of interstellar molecules	518	IV. Comparison of Predicted and Observed Molecular Abundances in the Interstellar Gas	540
C. Introduction to reactions of interstellar molecules	523	A. Diffuse interstellar clouds	540
II. Physical Processes Relevant to Reactions at the Surfaces of Interstellar Grains	524	B. Dense interstellar clouds	544
A. Temperatures of interstellar grains	525	C. Fractionation of isotopes (dense clouds)	547
B. Electric potential of interstellar grains	525	V. Summary	549
C. Grain surfaces and binding energies of particles to grains	526	References	550
D. Sticking of atoms and molecules onto grain surfaces	528		
E. Mobility of atoms on grain surfaces	529		
F. Processes for ejecting adsorbed particles from grains	530		
G. Summary and conclusions for reactions on interstellar grain surfaces	531		
III. Physical Processes for Reactions in the Gas Phase	533		
A. Cross sections for chemical reactions	533		
B. Charge transfer	534		
C. Radiative association	535		

*Some sections of this paper are based on lectures by the author presented at the 1974 Les Houches Summer School for Theoretical Physics (Les Houches, France). The text of the lectures appears in *The Proceedings of the Les Houches Summer School of Theoretical Physics, XXVI*, "Atomic and Molecular Physics and the Interstellar Matter," edited by R. Balian, P. Encrenaz, and J. Lequeux (North-Holland, Amsterdam, 1975). Supported in part by NSF Grant MPS 73-04781.

†Alfred P. Sloan Foundation Fellow.

I. INTRODUCTION

A. Nature of the interstellar medium

Near the sun the mean separation of stars is about 1 parsec (3×10^{18} cm \approx 3 light years), whereas stellar radii are comparable to the solar radius ($\sim 10^{11}$ cm). In the 1930's, the presence of an interstellar medium (ISM) in this void gained general acceptance. Optical absorption lines of ionized calcium in the stellar spectra of types O and B stars were found to increase in strength with stellar distance as well as to exhibit the pattern of Doppler shifts appropriate for galactic rotation of a uniform gas. During the same period, evidence for a general interstellar extinction of starlight due to small, solid particles (dust grains) became convincing. However, both calcium and dust grains are by mass minor constituents of the ISM (less than a few percent). Detection of the chief component occurred in the early 1950's with the observation of the 21 cm, hyperfine transition of atomic hydrogen. Though some half-dozen interstellar molecules were detected before 1970, these

were of low abundance and most astronomers considered the interstellar gas to be chiefly in atomic form. The large fractional abundances of H_2 and CO that have been detected by observations above the atmosphere and by millimeter wavelength radio telescopes, respectively, now establish that the mass fraction of the ISM in molecular form is at least comparable to that in atoms. Thus the study of chemical reactions in the ISM is of astrophysical interest. General references for the topics discussed in Sec. I.A include Spitzer (1968), and Kaplan and Pikelner (1968). Recent conference and summer school proceedings that contain up-to-date summaries have been edited by Kerr and Simonson (1974), Pinkau (1974), Verschuur and Kellerman (1974), Balian, Encrenaz, and Lequeux (1975), and Wilson and Downes (1975).

1. Distribution of the ISM within the galaxy

The ISM represents about ten percent of the mass of stars in our galaxy. This fraction varies both with distance perpendicular to the galactic plane and with radial distance from the galactic center. Whereas the half-width of the ISM perpendicular to the plane is approximately 200 pc, the half-width averaged over stellar type is near three times this value. At the location of the sun roughly 10 kpc from the galactic center, ISM mass/stellar mass is ~ 0.1 . Toward the galactic center this ratio seems to decrease and reaches $\sim 10^{-3}$ at the center. In the neighborhood of the sun, the average density of the ISM corresponds roughly to one hydrogen atom per cm^{-3} . It does not, however, vary monotonically in the galactic plane, but is associated with the spiral arms and is an order of magnitude or more greater in these arms than in the interarm region (Fig. 1). In fact, except in the local region of the galaxy, the

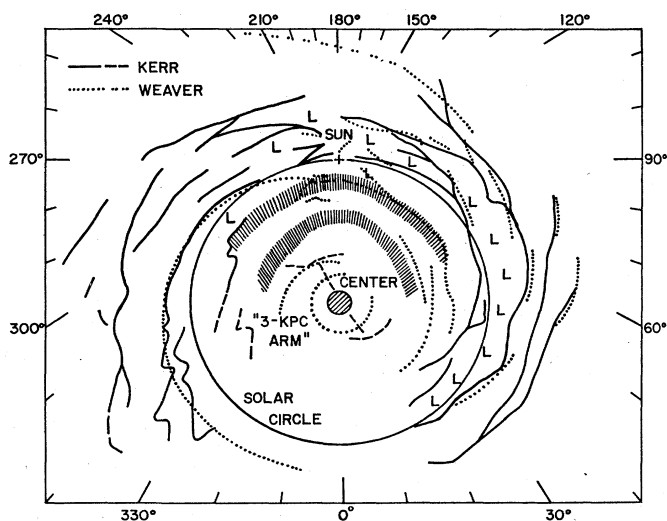


FIG. 1. Superimposed maps of the neutral, atomic hydrogen in the galaxy as interpreted by Kerr and by Weaver. The points marked "L" denote regions that are interpreted as markedly deficient in hydrogen. Dashed lines and hatched areas indicate regions where the location is uncertain, not regions where the hydrogen is weak or strong. The radius of the solar circle is 10 kpc. Galactic longitude is shown around the edge of the map. (from Simonson, 1970).

21 cm transition of interstellar hydrogen is the tracer that is employed to delineate the arms. Recent studies find that the molecular fraction (mainly H_2) of the interstellar gas increases dramatically toward the galactic center and reaches a peak of ~ 0.9 at about 5 kpc in comparison with ~ 0.5 near the sun (Fig. 2).

2. Mass exchange between the ISM and stars

The galaxy began as interstellar gas of which ninety percent has been converted to stars in the lifetime of the galaxy ($\sim 10^{10}$ yr). Whether a net conversion of gas to stars continues is unclear. If star formation rates for the solar neighborhood based on the abundance of young stars are extrapolated to the entire galaxy, the rate at which mass is taken from the gas for star formation is one solar mass (2×10^{33} g) per year. Mass is returned to the gas from stars in a number of ways, though the chief contribution probably comes when stars of one to five solar masses reach the top of the red giant branch. A star evolves off the main sequence to the giant branch when hydrogen is exhausted in its core. Mass is lost continuously from the extended envelopes of these red giants, ultimately leaving in large fraction of the stars ($\sim 1/2$) only the hot, dense core which becomes a planetary nebula. The overall mass return to the ISM is uncertain. Estimates also yield approximately one solar mass per year so that the direction of the net flow of mass between the stars and gas is unclear. In addition, high velocity gas clouds of hydrogen at high galactic latitudes have been interpreted by some investigators to represent a net infall of material into galactic plane. This rate might also be as high as one

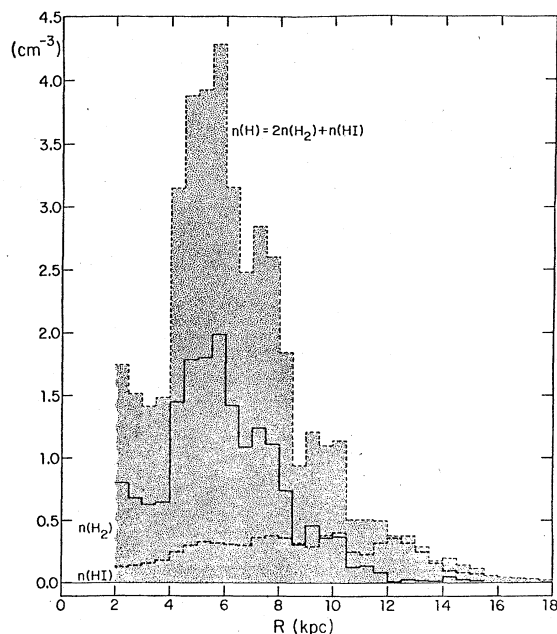


FIG. 2. Radial distribution of the interstellar gas. Observations of radio emission from CO enable a derivation to be made of the large-scale distribution of molecular hydrogen. The number density of H_2 shown here is obtained with the assumption $[H_2]/[CO] = 1.7 \times 10^4$. Also shown is the number density of atomic hydrogen (HI) obtained from 21 cm observations (from Gordon and Burton, 1976).

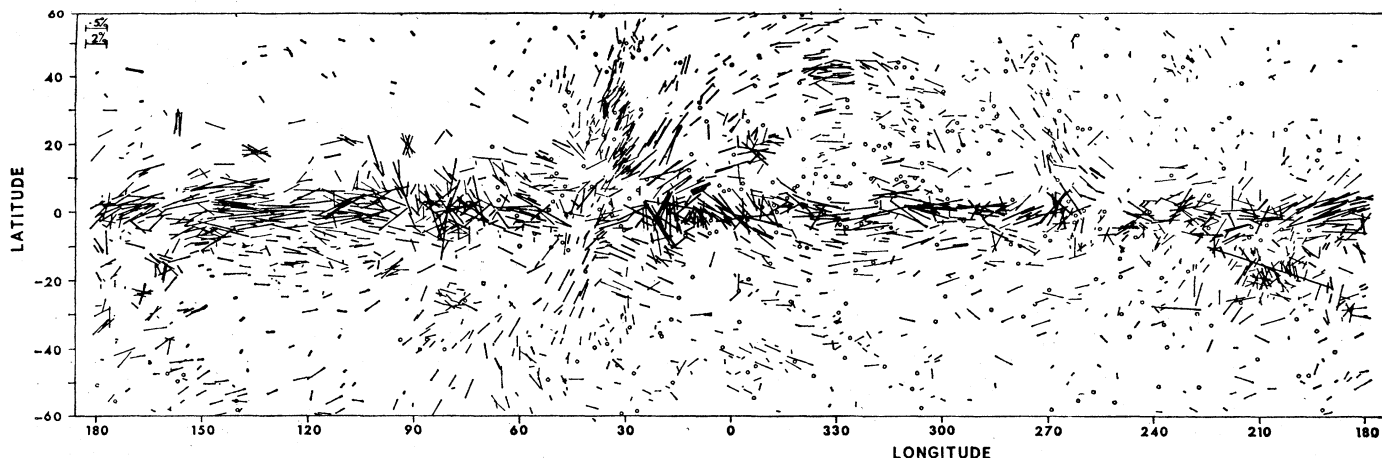


FIG. 4. Interstellar polarization of optical starlight. Direction of polarization is indicated by the lines. Coordinates are galactic latitude and longitude (from Mathewson and Ford, 1970).

[energy]⁻³) as well as the decrease in the ionization cross section, the low energy end of the spectrum dominates the ionization of the ISM. At low energies (≤ 1 MeV/nucleon) the spectrum must turn over due to the weak penetrating ability of cosmic rays at these energies. Unfortunately, the solar magnetic field modulates galactic cosmic rays by a large and uncertain factor at energies below a few hundred MeV/nucleon so that only a lower limit can be estimated by extrapolating the measurements at higher cosmic ray energies. This limit corresponds to an ionization rate $\sim 10^{-17}$ to 10^{-18} ionizations (H atom sec)⁻¹ in the ISM. Element abundances in cosmic rays are roughly similar to cosmic abundances with nuclei $Z \geq 6$ being enhanced by an

order of magnitude or so.

The interstellar radiation spectrum is shown in Fig. 5. Cosmic blackbody radiation at 2.7 K has little influence in the ISM except to populate certain low-lying molecular states associated with radio transitions. Ultraviolet starlight and soft x-rays are of major importance for ionization and dissociation of atoms and molecules, as well as for heating the dust grains. Although the ultraviolet radiation spectrum (~ 1000 – 2000 \AA) is not measured directly, stellar fluxes and statistics along with interstellar extinction are adequately known to allow determinations to factor of two accuracy in the general ISM. Within condensations (clouds) of the ISM, extinction due to dust grains can

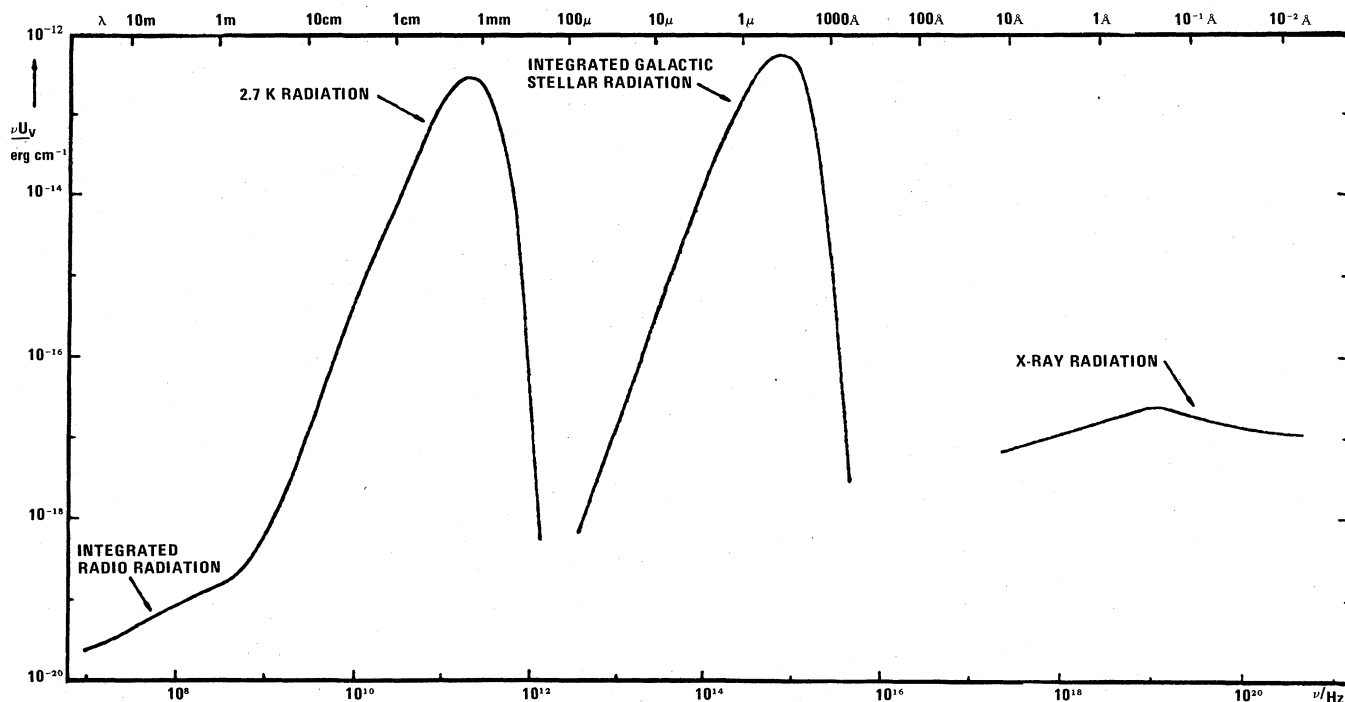


FIG. 5. Radiation density per frequency interval νU_ν , as estimated or measured for the vicinity of the sun.

cause attenuation of the starlight by orders of magnitude and introduce severe uncertainty. Except within these clouds, starlight is quite uniform and is estimated to vary by less than a factor of two within ninety percent of the galactic disk. Atomic hydrogen absorbs starlight at energies greater than 13.6 eV near the stars and thus causes the radiation spectrum in the general ISM to cut off at that energy. Atoms with ionization energies greater than hydrogen are normally neutral in the general ISM, whereas those with lower energies are ionized. Soft x-rays at energies below 100 eV are the main cause for photoionization of hydrogen and helium. Although, the intensity of x-rays at this energy has not yet been measured directly, observations at slightly higher energies indicate a steeply rising spectrum toward lower energy. The measured flux is estimated to yield an ionization rate in the ISM $\approx 10^{-16}$ (H-atom s) $^{-1}$. At these low energies, the penetrating ability of x-rays is quite weak and corresponds to a column density of hydrogen $\approx 10^{19}$ cm $^{-2}$ ("column density" = number density \times path length). In comparison, column densities of typical interstellar clouds are $\geq 10^{21}$ cm $^{-2}$. The source for these x-rays is unclear, though it may be bremsstrahlung from a hot ($T \sim 10^5$ – 10^6 °K) component of the ISM whose presence is suggested by quite recent observations of interstellar OVI.

5. State of the interstellar medium

Hot stars (mainly mainsequence O and B stars, planetary nebulae) produce sufficient radiation at energies greater than 13.6 eV to ionize fully the ISM within perhaps 10 pc of the star. These H II regions or Stromgren spheres produce a rich spectrum of emission lines as well as optical, infrared, and continuum radiation. Valuable information on chemical abundances, stellar properties and interstellar gas dynamics can be obtained from analysis of these data. Such regions comprise about ten percent of the ISM. Arguments supporting the presence of a region around main-sequence O and B stars with a gas temperature $\sim 10^5$ – 10^6 K have been presented quite recently. The chief evidence is the observed OVI mentioned below. A recent review by Osterbrock (1974) of topics related to H II regions is available. For the general ISM (that excluding H II regions), observations have for about ten years indicated that there is a division into hot, dilute ($T \sim 10^4$ °K, $n \sim 0.1$ cm $^{-3}$) and cold, dense ($T \sim 10^2$ °K, $n \geq 10$ cm $^{-3}$) components. Evidence for the cold component is extensive and includes interpretation of 21 cm observations of atomic hydrogen, ratios of *ortho*- to *para* hydrogen, electron densities, and populations of rotational states for molecules. Observational evidence for the hot or intercloud component is more controversial and is based mainly on the difference in line profiles between 21 cm radiation seen in emission and that seen in absorption against a strong source of continuum radiation in the background. High abundances of OVI (approximately one part in 10^4 of the ISM oxygen) have quite recently been observed in the directions of most bright O and B stars in the solar neighborhood. Ultraviolet absorption of OVI appears in spectrum of these stars when observed with the Copernicus satellite. It is argued that the OVI is truly interstellar and not asso-

ciated with the outer layers of the star. OVI cannot be present in adequate quantities in the phases of the ISM discussed above, and a third phase at temperatures $T \approx 10^5$ – 10^6 °K has been proposed. Collisional ionization then produces the OVI and bremsstrahlung from this gas will be the previously unknown source for the soft x-rays in the galaxy. In addition to the stars mentioned above, supernovae blasts are a proposed origin for this hot gas.

Until about 1970, the accepted picture of the general ISM was that of an intercloud region (temperature $\approx 10^4$ K, number density ≈ 0.1 cm $^{-3}$) containing diffuse clouds for which the properties typically are: number density ≈ 10 cm $^{-3}$, kinetic temperature ≈ 100 K, radius ≈ 7 pc, mass ≈ 400 solar masses, visual extinction ≈ 0.2 magnitudes. Except for hydrogen which can be partly in molecular form, the gas is mainly atomic. The spatial density of such clouds is $\approx 5 \times 10^4$ (kpc) $^{-3}$ and they contain a mass comparable to that of the intercloud region. Detection of certain millimeter wavelength molecular transitions now implies that regions of much higher gas density ($\approx 10^3$ – 10^5 cm $^{-3}$) also occur. Higher densities are required to excite these transitions in collisions with other gas particles. The total mass of such regions is probably comparable to that in diffuse clouds and in the intercloud medium. Many of these dense regions are known to be associated with bright stars and are likely to be influenced significantly by stars. Ignore for the moment these higher density clouds and consider the general ISM of diffuse clouds and intercloud matter which is likely to be relatively unaffected by stars and comprises most of the volume of the galactic disk, at least near the sun.

Efforts to understand the state of the general ISM have occupied a large fraction of the theoretical and observational work in the ISM for the past ten years (see e.g., Dalgarno and McCray, 1972; Field 1974). In particular, the focal question has been the source for heating and ionization of the gas. Pulsar dispersion measures and ratios of atomic ionization states have been interpreted to imply electron densities ≈ 0.04 cm $^{-3}$ in the ISM. Ionization of hydrogen is thus indicated, which requires a new ionizing agent since starlight beyond 13.6 eV is expected to be negligible in the general ISM. Further, estimates for the energy loss rates at observed temperatures in diffuse clouds, due mainly to collisional excitation of the $C^+(^2P_{3/2})$ state followed by radiative decay, give losses considerably in excess of known sources of energy input. These difficulties, as well as the temperature/density contrast between diffuse clouds and the intercloud region, led to proposals that an intense flux of low-energy cosmic rays or x rays is present at unobservable energies. An equation of state for the ISM is then obtained as shown in Fig. 6. Point C is thermally unstable, and points B and D agree well with diffuse cloud and intercloud parameters. This *steady-state* model in which diffuse clouds and intercloud gas coexist in pressure equilibrium is highly appealing. However, a number of serious objections can be raised; e.g., soft x rays cannot penetrate diffuse clouds, the total energy of the cosmic rays places severe demands on the unknown sources, to obtain proper cloud temperatures the relative abundance

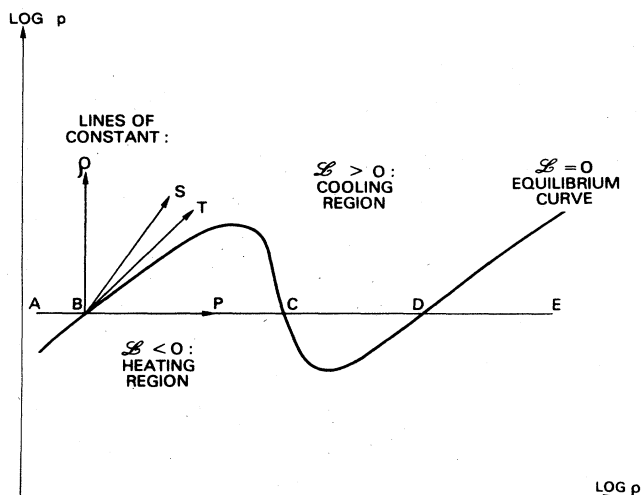


FIG. 6. The "equation of state", p (pressure) vs ρ (density) for the time-independent model for the heating and cooling of the interstellar medium. \mathcal{L} is the net cooling. The curve $\mathcal{L}=0$ divides the p - ρ plane into cooling and heating regions. S is the entropy and T , the temperature (from Field, 1975).

of carbon must be a factor of 10 or more below its cosmic abundance. More directly, the abundance of molecular HD is sensitive to the ionization rate of hydrogen and can be interpreted as strong evidence against any significant enhancement in diffuse clouds of the cosmic ray or x-ray flux beyond that which is observed. The two-phase, steady-state model remains attractive due to its ability to account naturally for the hot and cold regions. It is likely that the basic features of this model are relatively insensitive to the exact energy source or combination of sources present in the general ISM.

The low densities of the ISM cause the equilibration time scales to be quite long, and possible time-dependent effects must be considered. For typical parameters, the time scale for cooling in both diffuse and intercloud regions is about 10^5 yr. The electron recombination time is 10^6 yr under normal intercloud conditions. Supernova explosions seem to be the most important cause for disturbance in the ISM. In particular, the same supernova which are normally assumed to produce the postulated cosmic rays of the steady-state model must have some effect. According to detailed studies, whether time-dependent effects are dominant depends upon the exact supernova rate in the galaxy and the manner in which the supernova energy is deposited. It is possible that they are of major importance. The *time-dependent* model for heating of the ISM is qualitatively similar to the two-phase model in that it predicts a bimodal temperature distribution for the gas. The result follows from the probability distribution for the ages of regions exposed to supernova x-ray flashes and the temperature dependence of the energy loss for a hot gas. Difficulties seem to arise in attempts to obtain the proper cloud sizes in present time-independent models.

The presence of OVI in the ISM discussed above now tends to support the idea that time-dependent effects are important. Calculations indicate that supernova

blasts can also produce appreciable quantities of the very hot ($\approx 10^5$ – 10^6 K) gas that will account for the OVI. An alternative possibility—that the OVI is associated with intense stellar winds from the hot stars in whose spectra the absorption lines are measured—also has implications for the general ISM. The intense wind can sweep up low-density gas in a snowplow effect to produce the "diffuse clouds" at ~ 10 pc from the star. Data on OVI is quite recent and has not been fully digested.

The presence of interstellar clouds with much greater optical extinction (≥ 3 magnitudes) than the diffuse clouds has been recognized for some time from statistical studies of optical star counts in different directions. Because of the dependence of such studies on optical radiation, information was limited to the local region of the galaxy. Only in the past few years with the aid of numerous molecular transitions at radio wavelengths have these more dense parts of the ISM been fully appreciated, if not understood. These regions can be classified according to their activity into either "dark clouds" or "molecular clouds." The latter are associated with active phenomena—bright O and B stars, HII regions, infrared emission, or continuum radio emission—and exhibit broad spectral lines corresponding to turbulent velocities of 4–40 km/s. In contrast, dark clouds are not associated with activity but are quiescent with linebreadths indicative of only 1 km/s internal velocities. Furthermore, molecular clouds have higher kinetic temperatures (50–100 K vs 10–20 K), are larger (10–30 pc vs 1–5 pc), can be more dense (10^3 – 10^6 cm $^{-3}$ vs 10^2 – 10^4 cm $^{-3}$), and may be more massive (10^2 – 10^6 solar masses vs 10^2 – 10^4 solar masses). Both types are mainly molecular hydrogen, though for other molecules larger abundances and greater complexity are found in the molecular clouds. Star formation may be in progress in molecular clouds. In fact, in the absence of rotation, magnetic fields, turbulence, etc., to inhibit contraction, the collapse time for a dark or molecular cloud due to its own self-gravitation is only about 10^6 yr. Since the rate of star formation would then exceed the observed rate by a factor of about 10^4 , factors which inhibit star formation must be present. Evidence from the residual gas associated with young star clusters and the masses of the clusters indicates that no more than about ten percent of the cloud mass collapses all the way to stellar densities. Reasonable values for magnetic fields or rotation rates can provide the remaining needed retardation of cloud collapse.

To summarize, the ISM can be divided for convenience into HII regions, a possible "third phase," an intercloud medium, and three type clouds—diffuse, dark and molecular. In practice, discrete classes do not exist and the three type clouds form a relatively continuous sample.

B. Observation of interstellar molecules

Energies associated with electronic transitions in molecules are much greater than the kinetic energy in ISM clouds where molecules are located. Thus, molecular emission at optical and ultraviolet wavelengths is not detectable. Absorption due to molecules can, however, be observed at these wavelengths in the spectra of bright, O and B type stars. To observe the line

absorption, the continuous absorption due to dust grains in the cloud must be small. Optical and ultraviolet investigations are then limited to the diffuse clouds. Furthermore, the general extinction of 1 magnitude/kpc in the galactic plane restricts these studies to the ISM within approximately one kiloparsec of the sun. In contrast, the galactic attenuation at wavelengths for radio-frequency transitions in molecules is negligible, and observations of molecules in the ISM throughout the galaxy can be made using radio-telescopes. Velocity differences between the various clouds along a line of sight are normally sufficient to prevent the radio frequency lines of one cloud from shielding those of another. However, except in a few cases at longer wavelengths where a source of strong continuum radiation is present behind the cloud, the gas density must be high enough that the molecular transition will be collisionally excited. This normally restricts radio observations to the dark and molecular type clouds. Summaries of optical and ultraviolet data include those by Morton (1975), Spitzer and Jenkins (1975), as well as the classic study by Herbig (1968). Reviews of measurements and their analysis at radio-frequencies have been given by Heiles (1971), Turner (1974), Zuckerman and Palmer (1974), and Penzias (1975).

1. Diffuse clouds

Although the first three interstellar molecules (CH, CH⁺, CN) were detected by ground-based optical telescopes and identified around 1940, no others were found until OH was detected this year at 3078 Å. Molecules that are abundant in the optically accessible diffuse clouds do not have strong transitions at wavelengths longer than the atmospheric cutoff at about 3000 Å. The launch of the *Copernicus* satellite in 1972 made it possible to explore in detail the ultraviolet (~1000-1500 Å) region which contains the electronic transitions of abundant molecules. A few rocket flights of short duration had provided a glimpse of the rich, ultraviolet spectrum. Measurements of H₂ as shown in Fig. 7 established its abundance as a component of the ISM comparable to atomic hydrogen. Extensive studies of the populations of the rotational states of H₂ have provided data on physical conditions in the

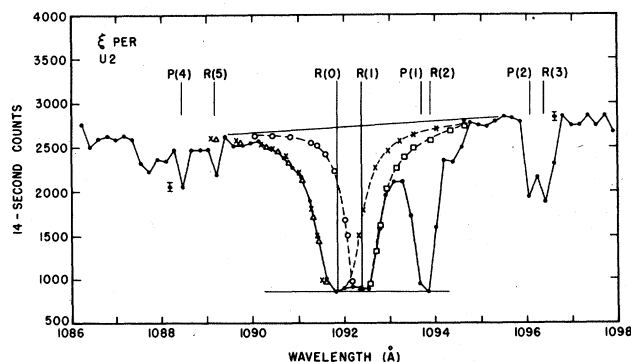


FIG. 7. Absorption spectrum and profile fitting for interstellar H₂ lines in a limited part of the spectrum as observed toward the star ξ Per. Except for P(4) and R(5) all lines are associated with the (1-0) vibrational branch (from Spitzer *et al.*, 1973).

ISM. In addition, carbon monoxide has been studied in detail. HD and quite recently OH have been detected. Potentially valuable upper limits to the abundances of a number of molecular species including CH₂, C₂ and H₂O have also been established. Unfortunately, lack of knowledge of the oscillator strengths prevents investigators from assessing the significance of these limits. Except possibly for CO, uncertainties concerning optical depth, line shape and excitation do not present critical problems in determining abundances from optical and ultraviolet measurements. Nevertheless, optical depths in the center of the strong lines of H₂ can be about 10⁶. A problem that does arise is delineating at what location along the line of sight the particles occur. There are often two or more such gas clouds whose spectra are found to be superimposed when examined with sufficient resolution to separate the various velocity components. Conditions may be quite different from one component to another. For example, the velocity dispersion for the CH⁺ molecule is much greater than for CH, CN, and OH and indicates that CH⁺ is less localized in the gas. Most ultraviolet measurements suffer to some extent from this type ambiguity. Radio detections of OH, CO, and probably H₂CO also exist for diffuse clouds.

Fractional abundances of molecules and other relevant properties for the cloud(s) toward the star Zeta Ophiuchi—a representative diffuse cloud—are presented in Table II. This cloud contains all type molecules that are found in diffuse clouds, as well as all type molecules detected at optical and ultraviolet wavelengths.

2. Dark and molecular clouds

From a comparison of the number of molecules observed by radio telescopes (Table III) with those observed at optical and ultraviolet wavelengths (Table II), it is evident that molecular astrophysics is dominated by radio astronomy. This conclusion is even stronger when the numbers of sources, molecular transitions and

TABLE II. Properties of the cloud(s) in the direction of the star Zeta Ophiuchi—a representative diffuse cloud in the ISM. Fractional abundances are given for the molecules, in addition to the visual extinction A_v (magnitudes) through the cloud due to dust grains, the total gas density $[n]$, the electron density $[e]$ and the gas kinetic temperature T . Except for OH (Snow, 1976, based on the oscillator strength of Ray and Kelly, 1975; Crutcher and Watson, 1976a) and NH (Crutcher and Watson, 1976b) data are from Morton (1975).

A_v	1
$[n]$ (cm ⁻³)	~10 ³
$[e]$ (cm ⁻³)	~0.2
T (K)	~50
H ₂	0.3
H	0.4
HD	1 × 10 ⁻⁷
CO	(0.8 - 4) × 10 ⁻⁶
CH ⁺	7 × 10 ⁻⁹
CH	3 × 10 ⁻⁸
CN	6 × 10 ⁻⁹
OH	~3 × 10 ⁻⁸
NH ^a	≤ 5 × 10 ⁻¹⁰

^a Toward XI Persei.

TABLE III. Interstellar molecules that have been detected at radio frequencies. An estimate for the fractional abundance by number of each molecular species is given in the parenthesis (x) = 10^x . The gas is mainly H_2 in the regions where these molecules are observed, though the H_2 is not observed directly.

CH	Methylidyne (-8)	(CH_3) ₂ O	Dimethyl ether (-10)
CN	Cyanogen (-8)	CO	Carbon monoxide (-4)
CS	Carbon monosulphide (-7)	OH	Hydroxyl (-7)
SO	Sulphur monoxide (-7)	SiO	Silicon monoxide (-7)
SiS	Silicon sulphide (-7)	NS	Nitrogen sulphide (-8)
HDO	Heavy water	H ₂ S	Hydrogen sulphide (-8)
HCN	Hydrogen cyanide (-6)	HNC	Hydrogen isocyanide (-6)
OCS	Carbonyl sulphide (-8)	SO ₂	Sulphur dioxide (-7)
N ₂ H ⁺	Protonated nitrogen (-7)	HCO ⁺	Protonated carbon monoxide (-7)
C ₂ H	Ethynyl (-7)	HCO	Formyl (-8)
NH ₃	Ammonia (-6)	H ₂ CO	Formaldehyde (-8)
H ₂ CS	Thioformaldehyde (-10)	HNCO	Isocyanic acid (-9)
HCOOH	Formic acid (-10)	HC ₃ N	Cyanoacetylene (-8)
NH ₂ CN	Cyanamide (-9)	CH ₂ NH	Methanimine (-10)
CH ₃ OH	Methanol (-7)	CH ₃ HCO	Acetaldehyde (-10)
NH ₂ HCO	Formamide (-10)	HC ₅ N	Cyanodiacetylene (-10)
CH ₃ C ₂ H	Methyl acetylene (-9)	HCOOCH ₃	Methyl formate (-10)
CH ₃ NH ₂	Methylamine (-10)	CH ₃ CH ₂ OH	Ethanol (-10)
CH ₂ CHCN	Vinyl cyanide (-10)	CH ₃ C ₃ N	Methyl cyanoacetylene (-10)

isotopic species are included. Although the first radio detection occurred in 1963 with the OH radical (Weinreb *et al.*, 1963), the explosive growth in radio observations really began in 1968-69 with detections of NH₃ (Cheung *et al.*, 1968), H₂CO (Snyder *et al.*, 1969), and H₂O (Cheung *et al.*, 1969). The last is not a true interstellar molecule in the sense that it is detected only in compact, masering sources whose physical conditions and dimensions are drastically different from those of interstellar clouds. Since 1969, some 34 new chemical species and numerous isotopic forms have been found. Representative molecular lines as observed by a radio telescope are shown in Fig. 8. Here, the slightly greater linebreadth of the U 90.66 line in comparison with HCN and HCO⁺ is evidence in support of HNC as the proper molecular identification for this line. The quadrupole splitting which produces three lines for HCN is much smaller in HNC and appears only as an enhanced linebreadth. Subsequent laboratory measurements of the HNC frequency established beyond doubt that U 90.66 is due to HNC. With increasing gas density, the ability to detect molecules is normally improved both by the higher excitation rates and an increased rate for chemical reactions which produce the molecules. The two most favorable galactic sites for molecule observations are the gas cloud(s) in the Orion Nebula and Sagittarius B2 cloud(s) near the galactic center. These also seem to have the highest gas densities, though the observability of the Orion Nebula benefits as well from the relative closeness of the nebula to the sun ($\sim \frac{1}{2}$ kpc). The spatial extent of various molecules along one axis passing through the molecular peak is shown in Fig. 9 for the Orion Nebula. In total, there are several hundred interstellar gas clouds in which molecules have been detected with radio telescopes.

Unlike the optical and ultraviolet measurements, there is often significant uncertainty in relating radio frequency data to the molecular abundances. Consider the transfer of radiation of intensity I_ν associated with a transition between an upper level (u) and lower level (l)

as it propagates through a homogeneous medium of thickness L representing an interstellar cloud. Radio astronomical measurements at frequency ν are usually expressed in temperature units $J(T_B) = c^2 I_\nu / 2k\nu^2$ where the brightness temperature T_B is defined in terms of the Planck function $B_\nu(T_B)$

$$I_\nu = B_\nu(T_B) = (2h\nu^3/c^2) / (e^{h\nu/kT_B} - 1). \quad (1.1)$$

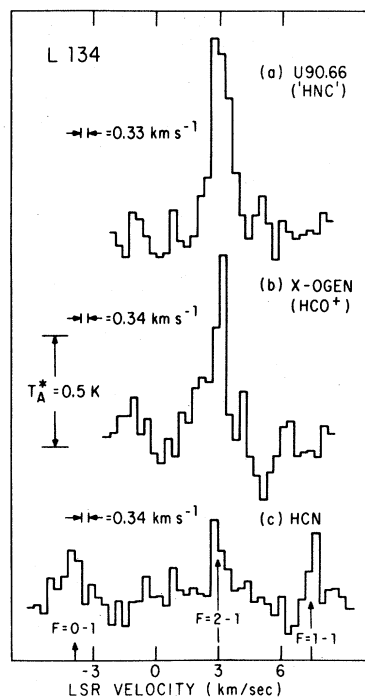


FIG. 8. Observed emission spectra from the interstellar cloud L134 for (a) U90.66 now identified as HNC (b) X-ogen now identified as HCO⁺, and (c) HCN. All are $J=1-0$ transitions. The ordinate can be considered as relative intensity and the abscissa is the velocity of the gas in relation to the local standard of rest LSR (from Snyder and Hollis, 1976).

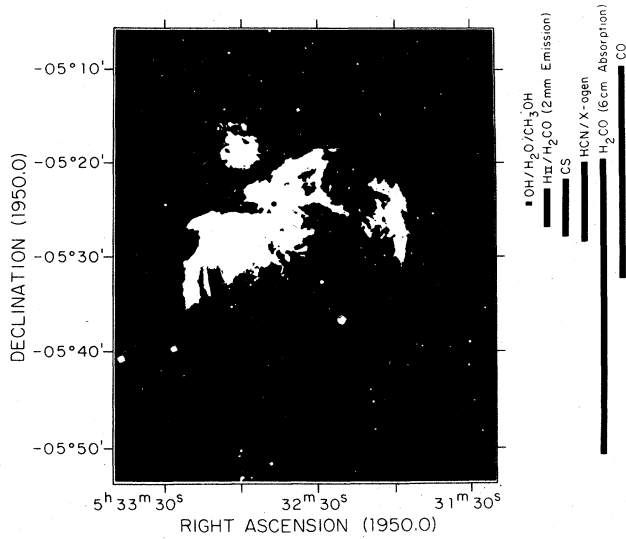


FIG. 9. The Orion Nebula. A region of bright stars and ionized gas with which a molecular cloud is associated. The extents along one axis of the emission from various molecular transitions are indicated by the bars. Axes are astronomical coordinates in degrees and minutes, and hours, minutes and seconds, of arc.

Thus T_B is the temperature of a blackbody that subtends the same solid angle as the source and emits the same radiative intensity at frequency ν . Frequently the Rayleigh-Jeans limit is applicable so that $J(T_B) \approx T_B$. The quantity obtained in molecular line measurements is the difference between the intensity on the line at an adjacent frequency for which the brightness temperatures are $T_{B,L}$ and $T_{B,C}$, respectively

$$\Delta J = J(T_{B,L}) - J(T_{B,C}) = [J(T_{ex}) - J(T_C)] [1 - \exp(-\tau(\nu))] \quad (1.2)$$

for an optical depth $\tau(\nu)$ given by

$$\tau(\nu) = (c^2 A N_1 g_u / 8\pi \nu^2 g_l) f(\nu) [1 - \exp(-h\nu/kT_{ex})]. \quad (1.3)$$

Here, A is the radiative decay rate for the upper state, N_1 is the column density of molecules in lower state, the g 's are the degeneracies of the states, $f(\nu)$ is a normalized function describing the line shape, T_C is the temperature of any continuum microwave emission located behind the cloud, and T_{ex} is the excitation temperature defined by the populations n of the two states

$$n_u/n_l = (g_u/g_l) \exp(-h\nu/kT_{ex}). \quad (1.4)$$

Thus for a line to be detectable, T_{ex} must be altered from T_C . This normally occurs by collisions with H or H_2 in the gas so that for typical sensitivity of radio telescopes, the excitation rate by collisions must very roughly be comparable with the radiative decay rate A when $\tau < 1$. Excitation cross sections σ have been poorly known, though recent calculations hopefully have alleviated this problem. Typical values are $\sigma \approx 10^{-15} \text{ cm}^2$ for rotational excitations at the relevant temperatures. However, when $\tau \gg 1$, the emitted radiation is reabsorbed a number of times before it escapes the cloud and A is effectively decreased to A/τ . Alteration of T_{ex}

TABLE IV. Spontaneous emission rates A and frequencies ν for representative transitions of interstellar molecules (from compilation by Turner, 1974).

Molecule	ν (GHz)	A (s ⁻¹)
OH	1.667	7.7×10^{-11}
NH ₃	23.694	3.6×10^{-8}
H ₂ CO(2 ₁₁ -1 ₁₀)	140.839	5.3×10^{-5}
H ₂ CO(1 ₁₀ -1 ₁₁)	4.830	4.2×10^{-8}
CO	115.271	7.5×10^{-8}
CN	113.492	1.3×10^{-5}
HCN	88.632	2.4×10^{-5}
HC ₃ N	9.098	4.0×10^{-8}
CS	146.969	6.1×10^{-5}

from T_C becomes easier. Representative values of A are given in Table IV. At millimeter wavelengths the continuum radiation is due to the 2.7 K universal blackbody flux, whereas at centimeter wavelengths galactic and extragalactic radio sources can dominate. Thus, observation of ΔJ does not directly yield the molecular abundance, since, in general, both τ and T_{ex} must be known. Various methods are employed to estimate these. For example, under certain circumstances τ can be estimated from ratios of hyperfine components or isotopic forms for which $\tau \ll 1$ can be studied and these abundances scaled by an assumed isotope ratio. An additional consideration is the possibility that a velocity gradient occurs in the gas cloud and has an important influence on the radiative transfer of the molecular radiation.

As a result of the low ISM densities, surprising molecular excitations as described by T_{ex} can occur. For example, one of the first detected molecular transitions—the 6 cm transition of formaldehyde—has an excitation temperature T_{ex} less than the 2.7 °K of the universal blackbody radiation. The observed transition is between the 1₁₀ and 1₀₀ states shown in Fig. 10. An

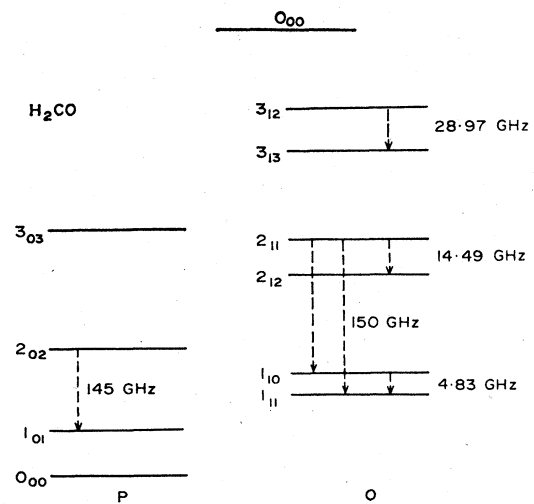


FIG. 10. Energy level diagram appropriate for microwave transitions of formaldehyde, a slightly asymmetric rotor. Ortho and para states are indicated by O and P, respectively. Transitions between these are negligible.

asymmetry in the collision cross sections tends to populate the 2_{12} state preferentially over the 2_{11} state in collisions with molecular hydrogen when the formaldehyde is initially in the 1_{10} or 1_{11} state, as it is mainly. Radiative deexcitation dominates collisional deexcitation and leads to an enhanced population in the 1_{11} state due to selection rules that allow $2_{12} \rightarrow 1_{11}$, but not $2_{12} \rightarrow 1_{10}$ transitions. The asymmetry in the collision cross sections and its influence on formaldehyde excitation was originally recognized by Townes and Cheung (1969) from classical considerations. Detailed calculations have verified that an asymmetry of the appropriate magnitude does occur (Augustin and Miller, 1974; Evans, 1975; Garrison *et al.*, 1975). Astrophysical evidence also supports strongly this explanation.

As a result of the low gas densities in the ISM, the abundances of reactive radicals and molecular ions are often comparable with the abundances of the relatively unreactive molecules that are readily available in the laboratory. A major problem has been the determination of microwave frequencies for the reactive molecules. Typically, an accuracy $\Delta\nu/\nu \approx 10^{-4}$ is needed in order to perform a sensitive observation with a radio telescope. The reliability of calculations is normally $\Delta\nu/\nu \approx 10^{-2}$ to 10^{-3} . A recent breakthrough in the ability to measure microwave frequencies of reactive molecules has recently been made by C. Woods and collaborators. Their measurements include HCO^+ , DCO^+ , HNC , and N_2H^+ (e.g., Woods *et al.*, 1975; Saykally *et al.*, 1976).

3. Isotope abundances

Isotope abundances throughout the galaxy are of particular interest as a result of their relation to mass exchange between stars and the ISM. In addition, the deuterium to hydrogen ratio is relevant to cosmological questions. With the exception of atomic deuterium in the local region of the galaxy, only molecular observations are able to detect the less abundant isotopes. Measurements of $^{13}\text{CH}^+$ at optical wavelengths, as well as ^{13}CO and HD in the ultraviolet, have been obtained with the usual limitation to about 1 kpc from the sun. Excluding some upper limits, the remaining information on isotopes is due to radiofrequency observations of interstellar molecules. Factor of 2 or so deviations from solar system isotope ratios is what is normally expected. At this level of precision, uncertainties in the radiative transfer discussed in the previous section cause difficulties. To some extent this problem is alleviated by studying hybrid ratios (e.g., $^{13}\text{C}^{16}\text{O}/^{12}\text{C}^{18}\text{O}$) where the lower abundances reduce the influence of saturation on the molecular line intensities. Bertojo, Chui and Townes (1974) recently summarized the observational status of isotope abundances in the ISM. As a result of the ^{13}C abundance, $^{13}\text{C}/^{12}\text{C}$ is the most extensively studied isotope ratio.

Hydrogen/deuterium. The atomic (D/H) ratio in the interstellar gas is measured by the *Copernicus* satellite to be 2×10^{-5} (Rogerson and York, 1973). Although the measurement is for the local region of the galaxy, the ratio is probably typical of the galactic disc as a whole if the galactic center is excluded. Radio mea-

surements in distant regions of the galaxy employing the 92 cm hyperfine transition of the deuterium atom yield upper limits, $<1/13,000$ toward Cassiopea A (Weinreb, 1962) and $\approx 1/2000$ at the galactic center (Pasachoff and Cesarsky, 1974). Interstellar HD is also observed at ultraviolet wavelengths and found to have an abundance that is typically 10^{-6} to 10^{-7} that of H_2 in diffuse clouds (Spitzer *et al.*, 1973). Self-shielding by molecular H_2 at the wavelengths for its ultraviolet photodissociating transitions slows the dissociation of H_2 but not HD. When this difference is included, the observed ratio actually implies that HD is produced at a rate $\sim 10^3$ faster than H_2 per D or H atom, respectively. Radio observations have detected DCN (Jefferts, Penzias and Wilson, 1973; Penzias *et al.*, 1976), HDO (Turner *et al.*, 1975), DCO^+ (Hollis *et al.*, 1976), and obtained upper limits to OD/OH ($\approx 1/400$ in the galactic center, (Allen, Cesarsky and Crutcher, 1974); $\approx 1/30$ toward 3C123, (Dickel and Radick, 1976). The detections yield $\text{DCN}/\text{HCN} \sim (2-5) \times 10^{-3}$ in the six locations studied and $\text{DCO}^+/\text{HCO}^+ \sim 0.1$ to 1 in three locations if HCO^+ is optically thin. Since H_2O is detected only in masers and not in clouds, no HDO/ H_2O ratio can be determined. Clearly, large effects of chemical fractionation are present in DCN and DCO^+ . The fractionation can be understood as a result of ion-molecule exchange reactions and the difference in zero-point vibrational energies of hydrogen and deuterium in molecules (see Sec. IV.C).

Carbon isotopes. Radio observations of carbon isotopes are based mainly on H_2CO , CO, CS and HCN. Bertojo, Chui and Townes (1974) conclude that the evidence does support a "factor of two" enhancement in the $^{13}\text{C}/^{12}\text{C}$ ratio over the solar system value of 1/90. Since their review, a number of observational studies—with CO (Wannier *et al.*, 1976a); with H_2CO (Wilson, T. *et al.*, 1976 and Matsakis *et al.*, 1976); with CS (Wilson, R. *et al.*, 1976); with HCN (Linke *et al.*, 1975)—seem to provide support for the idea that this "factor of two" enhancement prevails throughout much of the galaxy. There are indications of source-to-source variations. In contrast, optical observations in the solar neighborhood for $^{13}\text{CH}^+ / ^{12}\text{CH}^+$ (Bartolot and Thaddeus, 1968; van den Bout, 1972; Hobbs, 1973) are in some disagreement but tend to support a solar system value. These observations should be influenced less by line saturation than the radio measurements. Chemical fractionation may also be a significant, and possibly dominant, effect in $^{13}\text{C}/^{12}\text{C}$ ratios from interstellar molecules. Preliminary data indicate that the abundance of $\text{H}^{13}\text{C}^{12}\text{C}^{12}\text{CN}$ is half that of $\text{H}^{12}\text{C}^{12}\text{C}^{13}\text{CN}$ or $\text{H}^{12}\text{C}^{12}\text{C}^{13}\text{CN}$ (Churchwell, Walmsley and Winnemisser, 1976). A likely mechanism to produce chemical fractionation of carbon isotopes has also been suggested (see Sec. IV.C).

Other isotopes. Other rare isotopes that have been observed in interstellar molecules are ^{17}O , ^{18}O , ^{15}N , ^{33}S and ^{34}S . Recent work includes that of R. Wilson *et al.* (1976) for sulfur isotopes and Wannier *et al.* (1976b) for oxygen isotopes. These isotope ratios for O, N, and S are less well studied than carbon, but are generally similar to solar system values. Evidence for deviations does exist.

C. Introduction to reactions of interstellar molecules

Reactions involving molecules in the ISM occur under drastically different conditions from those in the laboratory. Thus it is desirable at the outset to recall the relevant physical conditions. For convenience of discussion, two general type conditions that are representative of the ISM are considered: diffuse clouds and dense clouds. The latter represent the previously discussed "dark" and "molecular" clouds taken together. Gas temperatures less than 100 °K and grain temperatures 10°–20 °K are assumed for both. At these temperatures and the low ISM densities, reactions must in practice be exothermic to be important. Particles with internal excitation are quite rare and have not been found to influence molecule formation and destruction. Reactions under high temperature can be important in cloud–cloud collisions (Aannestad, 1973a) and in interstellar masers (Goldreich and Scoville, 1976), but will not be considered here since both influence only a small fraction of the ISM. Gas densities 10–10³ cm⁻³ are representative of diffuse clouds, whereas 10³–10⁶ cm⁻³ are more typical for dense clouds. However, the essential difference between the two type regions is the presence of galactic, optical, and ultraviolet starlight in the diffuse clouds which can ionize and dissociate the atoms and molecules. With the exception of hydrogen which is perhaps half molecular, the gas is mainly in atomic form, and those atoms whose ionization energies are below 13.6 eV are ionized. The occurrence of carbon primarily as C⁺ is particularly important for reactions. In dense clouds, optical and ultraviolet radiation is assumed to be excluded as a result of the large optical depths at these wavelengths. Because of this obscuration and their distance from the sun, the dense regions are not well understood so that in practice the assumed absence of starlight is open to some question. Bright stars and infrared radiation from hot grains are normally observed in the neighborhood of molecular clouds. It is unclear whether they are sufficiently close to the molecular regions to affect reactions involving the observed molecules.

It is clear from the foregoing that the physical state of the ISM is far from thermodynamic equilibrium. The ionization state is dramatically altered by the radiation from that which would prevail at the kinetic temperature of the gas. Similarly, the atoms in interstellar clouds would all be tied up in molecular form. Finally, in thermodynamic equilibrium, elements other than hydrogen and helium will be frozen out onto the cold dust grains, probably as H₂O, CH₄ and NH₃. This is prevented in part by the dis-equilibrating effect of starlight and cosmic rays, and in part because the time to reach full equilibrium is comparable with or longer than cloud lifetimes. In the dense clouds from which starlight is excluded, high-energy cosmic rays (≥100 MeV/nucleon) seem to provide adequate stimulation for the reactions that prevent the molecular abundances in the gas from attaining thermodynamic equilibrium.

Consider now the approximate time scales for major competing processes relevant to interstellar molecule reactions. When appreciable ultraviolet radiation is present, destruction of molecules is often due to photo-

dissociation which occurs in a typical time

$$t_{\text{diss}} \approx 300 \text{ yr } (AB + h\nu \rightarrow A + B) \quad (1.5)$$

per molecule in the unshielded galactic radiation flux. A particular atom or molecule collides with some other particle (mainly hydrogen) on a short time scale,

$$t_{\text{coll}} \approx 300/n \text{ yr } (A + B \rightarrow A + B) \quad (1.6)$$

in a gas of density n (cm⁻³). In most such collisions no new molecule is produced. To form a molecule when A and B are atoms, it is necessary to lose the excess energy either through emission of radiation for which,

$$t_{\text{rad}} \approx 3 \times 10^9/n \text{ yr } (A + B \rightarrow AB + h\nu) \quad (1.7)$$

per atom in the ISM for this type collision, or to the surface when the collision between A and B occurs on a dust grain. For reactions on a grain surface, the analogous time scale is

$$t_g \approx 10^9/n \text{ yr } (A + B + \text{grain} \rightarrow AB + \text{grain}). \quad (1.8)$$

In the ISM, three-body reactions in the gas can be neglected

$$t_{3\text{-body}} \approx 3 \times 10^{23}/n^2 \text{ yr } (A + B + M \rightarrow AB + M). \quad (1.9)$$

If either A or B is a molecule, exchange reactions become possible. The time scale for a particular particle of type A to produce a new molecule through such an exchange reaction can be as short as

$$t_x \approx 10^3 \text{ yr}/f_{BC} n, \quad (A + BC \rightarrow AB + C). \quad (1.10)$$

Although this formation process seems fast in comparison with Eqs. (1.7) and (1.8), the fractional abundance f_{BC} of particles that can react by exchange reactions in the ISM is small and the net molecule formation through (1.10) is normally comparable with other processes. For example, most reactions with H₂ are endothermic or have activation energy barriers unless particle A is ionized. With the exception of chlorine, atoms whose ionization energy is below 13.6 eV and can thus be ionized by starlight do not react exothermically with H₂. The ionization rate for some atoms (e.g., D, O) can however be large enough that exchange reactions with H₂ are somewhat faster than competing reactions. Certain other type exchange reactions are also somewhat faster than competing reactions and are of major importance in producing new molecules from old ones. Radiative association reactions probably also are faster when one particle is already in molecular form. A cross section has been proposed for the radiative association C⁺ + H₂ → CH₂⁺ + hν that is 10³ greater than employed for Eq. (1.7). Molecular ions now seem to play a major role in reactions in the ISM. Their lifetime is usually governed by dissociative electron recombination for which the lifetime per ion is typically,

$$t_{\text{de}} \approx 0.1/[e] \text{ yr } (AB^+ + e \rightarrow A + B) \quad (1.11)$$

at an electron density $[e]$ cm⁻³. For comparison, the analogous time for radiative electron capture by the ion is roughly

$$t_r \approx 3000/[e] \text{ yr } (A^+ + e \rightarrow A + h\nu) \quad (1.12)$$

In *diffuse clouds*, comparison of Eqs. (1.5) and (1.7)

or (1.8) indicates that only about $10^{-7}n$ of the atoms are expected to be in atomic form in a steady state. For molecular hydrogen, self-shielding increases Eq. (1.5) by $\sim 10^3$ to 10^4 , so that $H_2/H \sim 1$ frequently occurs. These predictions are in qualitative agreement with the observations (Table II). Steady state is a good approximation for molecular abundances in most diffuse clouds since the mean time between disruptive events—cloud–cloud collisions, collision with a star, cloud collapse—is greater than about 10^7 years. For *dense clouds*, the lifetimes of molecules are normally much longer so that the contributions of certain phenomena with long time scales must, in principle, be considered. For example, molecules are observed in the atmospheres of cool stars from which mass is being blown into the ISM. If the lifetimes of molecules in dense clouds are essentially the lifetime of the cloud, injection by stars might be significant. One such example where this seems to occur is the region IRC +10216. However, in general, the mass loss rate is not great enough to have wide influence for molecules in the ISM. In addition the presence and abundance of certain molecular species—DCN, DCO^+ , HNC—indicates that molecules in dense clouds are produced in the low temperature/density environment where they are observed. The high DCN/HCN and DCO^+/HCO^+ ratios are apparently thermal effects due to the difference in zero-point energies and thus require low temperatures. HNC is readily rearranged by collisions into the lower energy structure HCN. From Sec. IV.B, the characteristic time for the main gas-phase reaction chains that are stimulated by cosmic ray ionization in dense clouds can be estimated to be about 10^7 years. If interstellar clouds are collapsing at near their maximum rate (i.e., free fall), the molecules produced by gas-phase reactions will not reach quasistatic abundances. The rate at which particles stick to grains always becomes faster than cloud collapse at the higher densities and suggests that surface reactions do reach a quasistatic situation. In the dense clouds, the optical extinction through the clouds indicates that optical depths at ultraviolet wavelength are greater than ten. A comparison of the lifetime against photodissociation (i.e., Eq. (1.5) increased by a factor of 10^4 or more) and formation rates (Eqs. (1.7) and (1.8)) suggests that dense clouds in the ISM are mainly molecular—a conclusion that is consistent with observations.

Historically, the first comprehensive study of interstellar molecule reactions seems to be that of Bates and Spitzer (1951) directed toward understanding the abundances of CH and CH^+ in diffuse clouds. These authors recognized the possible importance of most processes considered at present and concluded that serious difficulties arise. Since that time the CH/ CH^+ question has received more attention than any other abundance problem. Nevertheless, the abundance of CH^+ is not understood in terms of its relevant reactions at present unless $CH^+ + e \rightarrow C + H$ is unusually slow despite theoretical conclusions to the contrary. A second phase of study concerning interstellar molecule formation began in the early 1960's in relation to the H_2 molecule. Detection of H_2 requires observation of its ultraviolet absorption spectrum from above the atmosphere. This had not yet

been achieved and it was supposed that a large fraction of the galactic mass might be hidden as H_2 . Radiative association and all other gas phase processes are completely negligible for H_2 formation. Detailed investigations concluded that essentially every H atom that hits a dust grain will stick and be converted into H_2 through reactions on the surface (Hollenbach, Werner and Salpeter, 1971). This prediction has now been confirmed by observation of interstellar H_2 beginning in 1970. In response to the rapid expansion in molecule observations beginning in 1968–1969, re-investigations of both gas and surface reactions were undertaken. The chief success seems to be in the consideration of reactions between molecules and positive ions which are produced directly or indirectly by cosmic rays. Most small molecules can be produced as a consequence of “ion–molecule” reactions. A number of successful, semi-quantitative confrontations with observational data have been formulated. Some successful predictions have even been made in an area long dominated by the observations. Basic work on the application of “ion–molecule” reactions in the ISM includes Black and Dalgarno (1973), Herbst and Klemperer (1973), and Watson (1973d, 1974a).

The elementary processes relevant to surface and gas-phase reactions in interstellar clouds are discussed in Secs. II and III. These processes are then applied in a straightforward manner in Sec. IV to interstellar clouds. For simplicity, the emphasis is toward the most abundant elements H, He, C, N, and O. Recent reviews of interstellar molecule reactions include Dalgarno and Black (1976), Herbst and Klemperer (1976) and Watson (1975). The last reference considers in more detail many of the topics in Secs. II and III.

II. PHYSICAL PROCESSES RELEVANT TO REACTIONS AT THE SURFACES OF INTERSTELLAR GRAINS

A first consideration is simply the rate at which a gas atom will hit a grain since this determines an upper limit to the influence of surface reactions. Based on the dust-grain surface area per H atom discussed in Sec. I.A, a typical atom or molecule of atomic weight A in the gas [temperature $T(K)$, number density n] strikes a grain in a mean time t_g

$$t_g \approx 10^9 / \sqrt{(T/100A)n} \text{ yr.} \quad (2.1)$$

For positive ions, Eq. (2.1) is sensitive to the charge on the grain and may be increased by a factor up to about 4 or decreased drastically if the grain is positively charged (Sec. II.B). The similarity between this time scale and that of competing processes [Eq. (1.7) and (1.10)] requires that surface reactions be considered.

The probable presence of inert grain surfaces in astrophysical situations where surface reactions are of interest is fortunate since the processes may then be relatively insensitive to the precise surface structure and to unpredictable surface chemistry. For reactions of gas atoms to occur at the grain surfaces, the gas particles must stick when they hit. This question has been debated especially with regard to the sticking of H atoms, but now seems settled with H atoms sticking in

perhaps one-third of their collisions under typical conditions (Sec. II.D). Grain temperatures (Sec. II.A) must be sufficiently low that thermal evaporation will not eject an adsorbed particle before other particles stick and react with it. Surface mobility of the adsorbed particles must be considered, especially for hydrogen (Sec. II.E). After reactions at the surfaces, the product molecules must be returned to the gas. At the average grain temperatures characteristic of the general ISM, thermal evaporation seems inadequate except for H_2 . Nonthermal ejection processes are uncertain (Sec. II.F). In any event, we conclude (Sec. II.G) that essentially every reactive particle (except possibly positive ions) incident on an interstellar grain does react with some other particle from the gas (it just may not be returned to the gas). Attachment of H atoms to any incident atom seems to be the dominant occurrence, and it is difficult to go beyond this first level of complexity. At present one can only speculate on the mechanisms by which complex molecules might be formed on the cold grain surfaces of the general ISM. Near intense sources of starlight, grains in the interstellar clouds may be hot enough ($T_g \gtrsim 75$ K, perhaps) to catalyze surface reactions through bonds to the surface of chemical strength as occurs under laboratory conditions (Brecher and Arrhenius, 1971; Anders *et al.*, 1974; Bar-Nun, 1975; Iguchi, 1975). Only processes relevant to the cold grain surfaces of the general ISM are included here.

A. Temperatures of interstellar grains

Under conditions of the general ISM, grain temperatures will be determined by the steady state reached in the absorption of starlight at optical wavelengths and the re-emission of this energy as infrared radiation. The steady state for a grain at temperature T_g is then given by

$$\int F(\lambda)Q(\lambda)d\lambda = \int B(\lambda, T_g)Q(\lambda)d\lambda,$$

where $B(\lambda, T_g)$ is the Planck function for blackbody radiation at temperature T_g and wavelength λ . Here $F(\lambda)$ is the radiative flux incident on the grain. At an average point in the galactic disk, $F(\lambda)$ in the optical region has a shape similar to that of a blackbody at 10^4 K, but reduced in intensity by a factor of approximately 10^{14} . Interstellar grains are much smaller than the wavelength of the infrared radiation which they emit and are thus hotter than the equivalent blackbody temperature for the starlight energy density (~ 3 K). Some representative values for the absorption efficiency $Q(\lambda)$ are presented in Fig. 11 (see also van de Hulst, 1957). Calculations for temperatures of grains with various compositions have been performed by a number of investigators (e.g., Werner and Salpeter, 1969; Greenberg, 1971). For grains of standard size (radius ≈ 500 – 100 Å), average temperatures are 10–20 K relatively independent of reasonable uncertainty in composition. Purcell (1969) has deduced minimum grain temperatures (≈ 6 K) from limits on $Q(\lambda)$ implied by the Kramers-Kronig dispersion relations, though temperatures greater than 10 K are again more realistic. Calculations show that grain temperatures decrease somewhat (\sim factor of 2) inside interstellar clouds due to the shielding of starlight, though

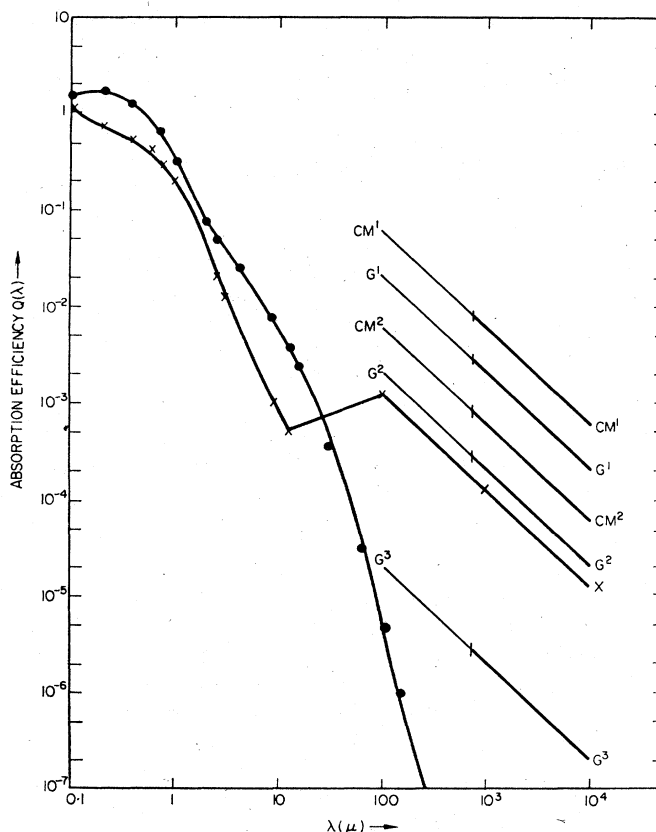


FIG. 11. Absorption efficiency as a function of wavelength for the grain-models studied: ●—● 0.05μ pure graphite grains; ×—× 0.15μ core-mantle grains. The diagonal lines between 100μ and $10^4\mu$ show the absorption efficiency for various values of f , the amount of enhancement by impurity oscillators in the far infrared; $f=1$ corresponds to the maximum enhancement permitted in the theory of Field (1969). CM^1, CM^2 : core-mantle grains enhanced with $f=1, 0.1$; G^1, G^2, G^3 : graphite grains enhanced with $f=1, 0.1, 10^{-3}$. The heavy portions of these curves show the efficiency when the enhancement is effective only at $\lambda > 750\mu$ (from Werner and Salpeter, 1969).

the decrease is smaller than might be expected. Infrared radiation emitted by grains on the outside of the cloud penetrates to the interior and heats these grains (Werner and Salpeter, 1969).

The above discussion refers only to time-averaged grain temperatures. Interstellar grain temperatures are well below the Debye temperatures (typically a few hundred K) of the materials so that the specific heat is low. The energy imparted to a grain by, for example, passage of a cosmic ray (Watson and Salpeter, 1972a) is sufficient to cause large temperature increases. For smaller grains (radius $\lesssim 100$ Å), absorption of optical photons causes temperature increase well above the average grain temperature (Duley, 1973; Greenberg and Hong, 1974; Purcell, 1976). Similar temperature pulses occur if most of the recombination energy in molecule formation is imparted to the grain (Allen and Robinson, 1975).

B. Electric potential of interstellar grains

Competition between photoemission of electrons and the sticking of charged particles (mainly H^+ , C^+ and e^-)

from the gas determines the electric potential of grains. Until recently photoemission was ignored. If the sticking efficiency is the same for positive ions and electrons that make contact with the grain surface, the higher velocity of the electrons then causes a negative grain charge. In this case the average grain potential ϕ is (Spitzer, 1948)

$$e\phi/kT_{\text{gas}} = -2.5,$$

when H^+ is the chief positive ion. It is somewhat more negative when heavier positive ions are the most numerous.

Now that ultraviolet data on photoemission are available, it is not clear that the grains are negatively charged in interstellar clouds of low optical depth (Watson, 1972). Although photoemission yields (electrons ejected/photons absorbed) depend upon the poorly known composition of the grains, some generalizations are possible (see Fig. 12). For most refractory materials considered for interstellar grains (e.g., silicates, oxides, silicon carbide and graphite) photoemission yields are about 0.03 to 0.10 at photon energies ~ 10 –13.6 eV. For small grains (radius ≈ 100 Å), the yield will be further increased by geometrical effects. The other major class of likely grain materials—frozen CH_4 , NH_3 , and especially H_2O —probably have weak photoemission below 13.6 eV due to the high ionization energies of the free molecules. If these ices are rearranged in some manner as has been proposed (e.g., radiation processing) into more complex molecules, the photoemission yields may be near 0.1 again (e.g., Fujihira *et al.*, 1973). A surface layer of ten or so monolayers of frozen H_2O would probably serve as an effective barrier to prevent photoelectrons from escaping with high efficiency.

The average cross section for a particle of charge q

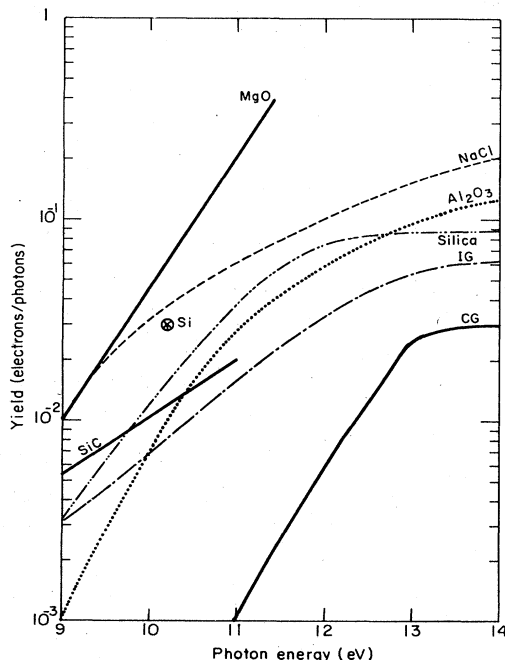


FIG. 12. Photoemission yields that are representative of that expected for interstellar grain materials (from compilation of Watson, 1973a).

from an equilibrium gas to hit a grain with electric potential ϕ is determined from Coulomb orbits and differs from the geometric cross section by a factor

$$1 - \frac{q\phi}{kT_{\text{gas}}}, \quad q\phi < 0; \quad \exp(-q\phi/kT_{\text{gas}}), \quad q\phi > 0.$$

A grain will be positive at a gas temperature of ~ 100 °K if, roughly,

$$1 < \frac{\text{photoejection}}{\text{electron sticking}} = \frac{\int Q(\lambda)F(\lambda)y d\lambda}{[e]v_e S_e} \approx \frac{(y/0.1)}{[e] \text{ cm}^{-3}} \quad (2.2)$$

for photoemission yield y , electron density and velocity $[e]$ and v_e , respectively, and an electron sticking efficiency $S_e = 1$. Electron densities in interstellar clouds seem to be 0.1 to 1 cm^{-3} so that grains may be either positive or negative depending upon y . No data are available for the sticking of electrons to surfaces under the conditions of interest. For the sticking of low-energy (≈ 1 eV) electrons onto neutral surfaces, laboratory data indicate that $S_e \approx 0.3$ for likely surface materials (see Watson, 1972). For positive grains and $kT_{\text{gas}} \approx 0.01$ eV, then $S_e \approx 1$ is a safe assumption. For negative grains, the likely value for S_e is unclear.

C. Grain surfaces and binding energies of particles to grains

Even if the composition of the grain surface were known, in general, the problem of estimating the binding energy D for a reactive atom or molecule to the surface would still be formidable. Laboratory experiments almost always involve either unreactive gas molecules/surfaces or binding energies of chemical strength (≈ 0.5 eV/particle). Possible bond strengths range from that for *chemisorption* (chemical strength) to that of *physical adsorption*. Pure physical adsorption involves only the van der Waals interaction between the surface and the adsorbed particle. Approximate binding energies and surface potentials for physical adsorption are obtained simply by summing independently the van der Waals potential between the adsorbed particle and the individual molecules of the solid. This typically yields a binding energy four to eight times the van der Waals well depth for a pair, or a few tenths eV in most cases of interest except hydrogen for which D is smaller. Additional effects often increase the binding energy above that for pure physical adsorption. These include exposed ions in an ionic solid, a permanent dipole moment of the adsorbing particle, surface irregularities and impurities, and the degree of coverage of the surface.

Although the nature of the binding between gas particles and the surfaces of interstellar grains is highly uncertain, it is nevertheless useful to consider physical adsorption since this represents one limit—the *minimum possible binding*. Further, under conditions in the general ISM surfaces or sites of strong chemical binding will simply become covered over by a chemisorbed monolayer. Additional monolayers will be added until the binding for incident particles is much weaker than for strong chemical binding. This occurs in the laboratory (e.g., Gomer, 1959; Folman and Klein, 1968), and

even for reactive atoms and radicals the binding may be only that for physical adsorption. While it is clear that the binding of a chemically saturated molecule to an inert, molecular crystal is weak, there is little direct evidence concerning reactive atoms and radicals. Clearly the binding of H, C, N, O, etc., atoms to inert grain surfaces such as ice is an essential question. An experiment (Marenco *et al.*, 1972) which measures the energy transmitted to a surface from incident atomic hydrogen indicates that the binding of H atoms to a frozen H₂O surface is comparable to that expected from physical adsorption (see also Klein, 1968).

Since van der Waals attractive forces are proportional to the polarizability of the particles, estimates for physical adsorption energies of various type particles can be made from the measurements with one type adsorbed particle. In Fig. 13 physical adsorption energies for N₂ on various surfaces are presented which can be employed in conjunction with the polarizabilities of Table V for such estimates. Physical adsorption of hydrogen is unusually weak due to the low polarizability of hydrogen, as well as to the large quantal zero-point energy that results from the low mass of hydrogen. If only physical adsorption can occur for H atoms, the formation of molecular hydrogen on grains is sensitive to the exact value of the binding energy. Hollenbach and Salpeter (1970) deduced a well depth of 800 K for the surface potential of the H-H₂O system based on an experimental binding energy for the H₂-H₂O system of 500 K. Their H-H₂O surface binding energy is 450 K when the zero-point energy is included. More recently the binding energy for H₂ on frozen H₂O and on CO has been measured to be 860 K and 350 K (Lee, 1972). For atomic H the analogous energies are then estimated as 750 K and 280 K. If a monolayer of H₂ is first placed on the H₂O surface, binding energies of 650 K and 520 K are found for H₂ and H.

The zero-point energy needed to deduce the binding energy for atomic H from measurements for H₂ or from theoretical calculations of the surface potential has been obtained by Hollenbach and Salpeter (1970). The surface potential not only varies perpendicular to the surface, but is periodic in directions parallel to the surface as indicated in Fig. 14. An energy barrier of perhaps one-

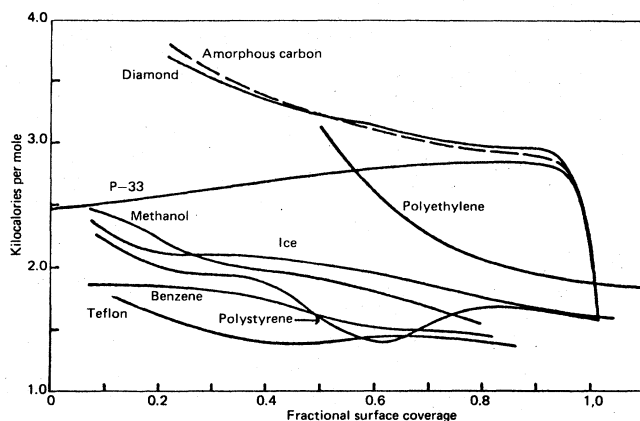


FIG. 13. Heats of adsorption for N₂ on various solids (1 kcal/mole = 0.044 eV/particle). From Dormant and Adamson (1968).

TABLE V. Representative polarizabilities of atoms and molecules.

Particle	Polarizability (10^{-24} cm ³)
He	0.21
Ne	0.41
A	1.6
H ₂	0.81
O ₂	1.6
N ₂	1.7
CO	1.9
NO	1.7
H ₂ O	1.5
NH ₃	2.2
CH ₄	2.6
H	0.67
O	0.73

half the well depth exists between potential wells. A harmonic oscillator treatment to estimate the zero-point energy is inaccurate, and a variational calculation has been performed using a delocalized wave function that has the correct periodic variation along the surface. This yields the 450 K mentioned above.

Based on data such as that in Fig. 13 and that of Lee (1972), we conclude that all reactive atoms of interest, C, N, O, etc., except possible H, will be adsorbed to interstellar grains with binding energies greater than about 800 K per particle. The binding for small molecules, e.g., H₂O, CH₄, NH₃, will be somewhat stronger (≈ 1000 K per particle). If several layers accrue, the more abundant molecules (CO, H₂O, CH₄, etc.) might

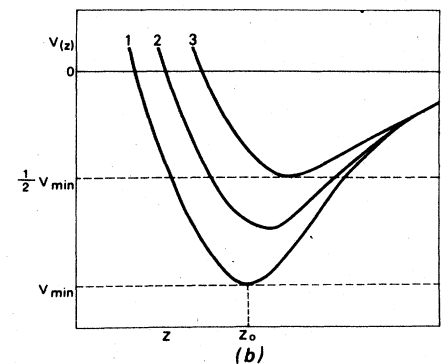
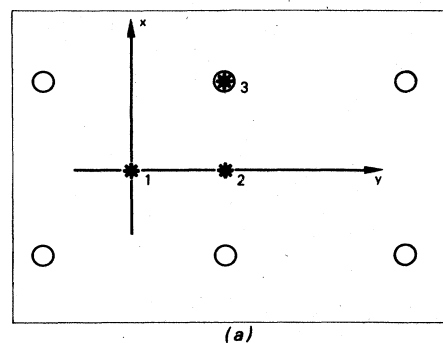


FIG. 14. The physical adsorption potential for H on an H₂O surface as a function of height Z above the surface is shown in (b) for three surface points labeled by numbered positions in (a). Open circles in (a) denote the surface atoms of the lattice.

TABLE VI. Critical temperatures T_C for various gases to freeze onto interstellar grains if they form pure crystals. The hydrogen density is taken as 10^4 cm^{-3} , and that for the other gases is 1 cm^{-3} .

Substance	T_C (K)
H ₂	< 2.5
N ₂	13
CO	14
CH ₄	19
NH ₃	60
H ₂ O	92

freeze out as pure crystals in which case the critical temperature for freezing onto the grains can be determined from laboratory vapor pressure data (Table VI).

Appreciable migration of particles from the surface into the interior of a grain is possible, as frequently occurs in the laboratory. It is difficult at present to evaluate this effect. If the binding for a particle is greater in the interior than on the surface, the interior probably becomes saturated early in the lifetime of a grain. Alternatively if the binding is greater on the surface, the particle will tend to remain there. Thus migration into the interior is likely to be unimportant in comparison with reactions on the surface.

D. Sticking of atoms and molecules onto grain surfaces

“Sticking” means here that the incident particle becomes thermalized to the grain for at least a brief time. The very weak binding to the surface if only physical adsorption occurs, along with the low ratio of the mass of the H atom to that of the surface particle (e.g., H₂O), suggests that the energy transfer might be quite low for H atoms incident onto an ice surface. In order to stick, the incident particle must transfer its translational energy to the surface before it bounces back off the surface. The problem has been investigated extensively as a topic in surface physics and elaborate, detailed calculations have been performed. To illustrate the essential aspects of sticking under the relevant astrophysical conditions, it is adequate to summarize the classical treatment of Hollenbach and Salpeter (1970) directed toward the sticking of atomic hydrogen onto ice for the formation of H₂.

This calculation is based upon the following:

(1) The collision of the gas atom with the surface can be represented by a gas atom colliding with the repulsive potential of a single surface atom which is at rest at its equilibrium position until the onset of the repulsive collision.

(2) As a first approximation this single atom is attached by a spring of natural frequency ω (the Debye frequency of the solid) to a stationary wall.

(3) The energy of the collision is $(\epsilon + 0.75 V_{\min})$, where ϵ is the kinetic energy of the gas atom outside the range of the surface potential and V_{\min} is defined by Fig. 14.

(4) The repulsive potential of the surface can be approximated by an exponential in the neighborhood of the classical turning point

$$V = -0.75 V_{\min} + (\epsilon + 0.75 V_{\min}) e^{-r/b}.$$

A characteristic collision frequency can then be determined for a collision involving a reduced mass μ

$$\omega_0 = \sqrt{(\epsilon + 0.75 V_{\min}) / 2\mu b^2}.$$

By following the one-dimensional classical trajectory, the energy transferred to the surface atom ΔE_s can be calculated. For sticking under astrophysical conditions of most interest (especially H atoms on frozen H₂O), the calculated ΔE_s agrees well with results of more detailed calculations (e.g., Goodman, 1966) which do include the response of the entire crystal. However, the experimental data often involves systems in which the collision is slow enough that the entire crystal can respond ($\omega_0 \ll \omega$). An analytic expression which reproduces the results of the calculations by Goodman (1966) is

$$\Delta E_s (m_s/m_g) / (\epsilon + 0.75 V_{\min}) = 2\omega_0^3 \omega (\omega^2 - \omega_0^2)^{-2}, \quad \omega/\omega_0 \geq 1.68 \\ = 1, \quad 1 \lesssim \omega/\omega_0 < 1.68. \quad (2.3)$$

To find a sticking probability from ΔE_s , the three-dimensional hopping of the gas atom across the surface must be considered. In order to stick, a particle must survive approximately $(\epsilon/\Delta E_s)$ hops without being scattered into a sufficiently small angle θ from the normal to the surface that it will escape. Instead of calculating and dealing with exact differential scattering cross sections, a probability is introduced for scattering into $\theta \leq \theta_0$ of the form

$$p = (\theta_0/\Omega)^2, \quad (2.4)$$

where Ω (radians) is a parameter near unity. The probability for adsorption of a particle with incident energy ϵ is then (Hollenbach and Salpeter, 1970)

$$P_\epsilon = \exp[-\frac{1}{2}(\epsilon/E_c)^2],$$

where

$$E_c = \Omega(0.75 V_{\min} \Delta E_s)^{1/2}.$$

With $\gamma = E_c/kT$, the sticking probability can then be obtained for a Maxwellian particle distribution with temperature T

$$S(T) \approx (\gamma^2 + 0.8\gamma^3) / (1 + 2.4\gamma + \gamma^2 + 0.8\gamma^3). \quad (2.5)$$

For comparison with laboratory experiments it is desirable to calculate the accommodation coefficient $\alpha(T)$ —the fraction of the energy of the incident particles which is transferred to the surface. This comparison tests many of the approximations involved in finding $S(T)$.

In Table VII, calculated and experimental values for $S(T)$ and $\alpha(T)$ are summarized. These data do support the prediction that H atoms stick to interstellar grains with $S \approx 1/3$. The temperature dependence of $S(T)$ is illustrated in Fig. 15. For atoms and molecules heavier than hydrogen (C, N, O, etc.), all factors—large V_{\min} and m_g —improve the likelihood for sticking. Thus $S(T \approx 100 \text{ K}) \approx 1$ for these particles. For positive ions incident from the gas, evaluation of the sticking is complicated by effects of recombination at the surface. Within the constraints of present information, it seems that $S(T)$ might be quite small or near unity for positive ions.

TABLE VII. Sticking and accommodation coefficients. "Exp." denotes experimental values; "1" and "2" refer to calculations employing $\Omega^2=1$ and $\Omega^2=2$; α_c includes a correction [from Hollenbach and Salpeter, 1970, except (a) from Marenco *et al.*, 1972 and (b) from Day, 1973].

System	D (°K)	b (Å)	ω ($\times 10^{13}$ s $^{-1}$)	ω_0	ΔE_g (°K)	T (°K)	S_{exp}	S_1	S_2	α_{exp}	α_1	α_c		
Xe/W	2400	0.38	2.17	0.75	170	100		0.91	0.96	0.92	0.91	0.92		
						200		0.78	0.85	0.85	0.74	0.85		
						300	0.42	0.64	0.75	0.68	0.57	0.77		
Kr/W	1500	0.38	2.17	0.74	64	100		0.77	0.85	0.77	0.72	0.80		
						200		0.52	0.66	0.57	0.44	0.59		
						300		0.35	0.50	0.46	0.28	0.46		
Ar/W	900	0.38	2.17	0.85	25	100		0.51	0.65	0.49	0.42	0.53		
						200		0.25	0.36	0.33	0.18	0.31		
						300		0.14	0.24	0.29	0.10	0.24		
Ne/W	240	0.38	2.17	0.60	1.3	100		0.025	0.046	0.05	0.014	0.04		
Ne/CO ₂	350	0.35	2.50	0.75	9.5	78	0.21	0.25	0.35					
O ₂ , CH ₄ , CO ₂ /graphite (b)						273				0.78–0.96				
H ₂ /CO ₂	450	0.35	2.50	2.80	21	78	0.48	0.44	0.57					
H ₂ /H ₂ O	375	0.30	3.00	3.00	43	78	0.55	0.54	0.66					
H ₂ /H ₂ O (a)						450	0.25			~0.7				
H ₂ /graphite (b)						77				0.8		0.75		
						200				0.4		0.45		
						273				0.4		0.40		
H/H ₂ O	300	0.30	3.00	4.00	17	78		0.32	0.45					

E. Mobility of atoms on grain surfaces

Motion across a surface by adsorbed particles is inhibited by the irregularities of the surface potential that result from the discrete positions of the lattice molecules. For particles to move between adjacent surface minima (a few angstroms), a barrier whose height is typically $E_B \approx V_{\text{min}}/2$ must be surmounted (Fig. 14). When chemisorption dominates, this estimate can be quite poor and E_B may be almost equal to V_{min} or it may be much less than $V_{\text{min}}/2$. An adsorbed particle moves between potential minima as a result of classical, thermal hopping and quantum mechanical tunneling. Thermal hopping is slow, but uncontroversial. Theory and experimental measurements of surface tunneling is

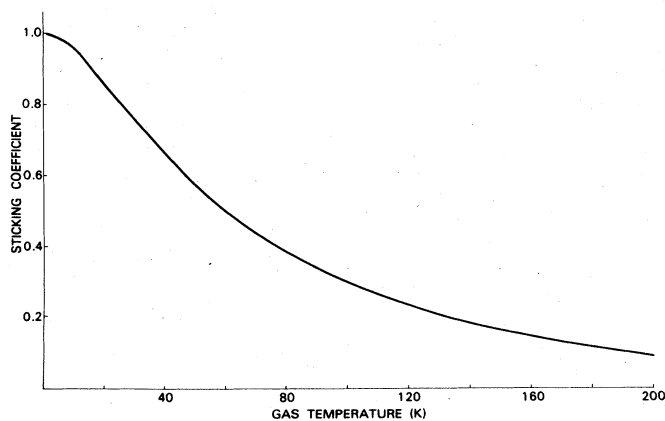


FIG. 15. Semiempirical sticking probability for atomic hydrogen on a graphite surface (from Day, 1973).

still regarded as somewhat uncertain, at least in detail.

In thermal hopping the characteristic time required for an adsorbed particle to acquire an energy greater than the barrier height E_B by thermal fluctuations and hop over the barrier is

$$t_t(1) \approx \nu_0^{-1} \exp(E_B/kT_g), \quad (2.6)$$

where $\nu_0 \approx 10^{12}$ s is the characteristic vibration frequency for the adsorbed particle. Since this is a random process the adsorbed particle requires a time,

$$t_t(N) \approx \nu_0^{-1} N^2 \exp(E_B/kT_g), \quad (2.7)$$

to get to a point N lattice spacings away. Thermal migration of adsorbed particles has been observed in the laboratory (e.g., Gomer *et al.*, 1957; Folman and Klein, 1968) in approximate agreement with Eq. (2.7).

Quantum mechanical tunneling is of particular interest here because the adsorbed atoms are light, and E_B for physical adsorption is relatively small. An estimate can be made from the Wentzel-Kramers-Brillouin approximation (WKB) for a one-dimensional barrier to find the time,

$$t_q \approx \nu_0^{-1} \exp \left\{ -2/\hbar \int |p| dx \right\}, \quad (2.8)$$

required for an adsorbed particle to move between adjacent potential minima. Here $p = \sqrt{2m_g[E - V(x)]}$, where E is the energy of the adsorbed particle, and the integral is over that part of the path between surface wells for which $V(x) > E$. For physically adsorbed atomic H on frozen H₂O, $[V(x) - E] \approx 0.05$ eV over a distance ≈ 2 Å. Then $t_q \approx 10^{-8}$ s. To obtain an accurate value for t_q (which is clearly sensitive to small uncertainties), it

is necessary to obtain the delocalized wave function for the adsorbed particle in the manner of Hollenbach and Salpeter (1970). Then t_q can be determined from the breadth in energy ΔE_b of the lowest energy band,

$$t_q(1) \approx 4\hbar / \Delta E_b. \quad (2.9)$$

Representative values of ΔE_b are presented in Table VIII. Although other calculations for the surface mobility (e.g., Ricca *et al.*, 1969) on different systems are, in general, in agreement with these, the only relevant experimental support seems to be that by Dash and collaborators (e.g., Dash, 1968; Bretz and Dash, 1971). In these experiments the specific heat per adsorbed particle is measured at temperatures near 1 K and is found to be near k (Boltzmann's constant) per particle. The experiments employ the particle/surface combinations He⁴/Ar, He³/graphite and He⁴/graphite. A specific heat near k per particle is expected for a two-dimensional, mobile gas. If the adsorbed particles were tightly bound in the potential wells, a specific heat much smaller than k would result. Quantitative information about ΔE_b can also be obtained from the temperature dependence of the specific heat and is consistent with results from calculational methods similar to that employed to find the ΔE_b of Table VIII.

Unlike thermal motion, the time required for quantum tunneling to a location N surface sites away where a second reactive particle is located is (Hollenbach and Salpeter, 1971)

$$t_q(N) \approx N t_q(1). \quad (2.10)$$

Realistic grain surfaces are probably not uniform as assumed above, but have a number of irregularities due to impurity atoms, ejection of surface atoms by cosmic rays, etc. The particle is then scattered by these irregularities and Eq. (2.10) must be modified

$$t_q(N) \approx N^2 \sqrt{f} t_q(1), \quad (2.11)$$

for a fractional abundance of irregular surface sites f (assumed randomly located).

F. Processes for ejecting adsorbed particles from grains

1. Thermal evaporation

Except for H₂ and possibly CO and N₂, thermal evaporation at the average grain temperature T_g in the general ISM is relatively ineffective for the ejection of adsorbed particles. To an adequate approximation for the purpose here, the average time for an adsorbed particle to gain sufficient energy by thermal fluctuations to overcome the surface binding D is $t_{th} \approx \nu_0^{-1} \exp(D/kT_g)$.

TABLE VIII. Band widths ΔE_b for surface states of adsorbed atoms. V_m = well depth. From Hollenbach (1969); Hollenbach and Salpeter (1970).

Atom/surface	m_g/m_H	V_m (°K)	ΔE_b (°K)
He/Ar	4	200	0.12
H ₂ /H ₂ O	2	800	7
H/H ₂ O	1	800	30
Heavy atom/H ₂ O	20	800	7.5×10^{-4}

Thus an adsorbed particle with $D \approx 800$ K remains on a grain at $T_g = 20$ K for about 10^5 s. The more abundant particles H₂, CO, H₂O, CH₄, etc., might freeze onto grains as relatively pure crystals in which case the more accurate evaporation rates can be obtained from vapor pressure data as in Table VI.

For quite small grains (radius ≈ 100 Å), the excursions from the average T_g mentioned in Sec. II.A when a photon is absorbed or when a chemical reaction occurs on the surface will be sufficient to eject weakly adsorbed particles. Purcell (1976) find that these temperature fluctuations will be able to return the adsorbed particles to the gas if $D \leq 0.1$ eV and the grain radius is ≤ 100 Å. If the binding is as large as 0.3 eV, accretion will not be prevented by this effect for grains with radii ≥ 50 Å. The presence of large numbers of these small grains in the interstellar gas is as yet uncertain. Further, the apparent presence of larger grains in appreciable abundance would in any event be a cause for depletion for atoms from the gas at approximately the sticking rate to grains.

More extreme, but less frequent, temperature fluctuations in grains are caused by the passage of low-energy cosmic rays. Two processes are of possible importance: (1) Evaporation due to the elevated temperature of the entire grain. (2) "Spot heating" which results from the initial depositing of the energy lost by the cosmic ray into a tube of radius ten or so angstroms centered on the cosmic ray path. Before the energy diffuses through the entire grain, the temperature is very high and can cause evaporation of adsorbed particles or of the outer layers of the grain. Processes (1) and (2) have been investigated in detail (Watson and Salpeter, 1972a). For favorable grain properties (composition, binding energy D) and low gas densities, it might be possible to return molecules efficiently to the gas. An accurate knowledge of the low-energy cosmic ray flux is, however, unavailable.

2. Photo-ejection

Arguments have been presented to suggest that ejection of physically adsorbed particles by ultraviolet radiation may be efficient (Watson and Salpeter, 1972a). Since theoretical ideas about surface processes are subject to severe uncertainties, efficient photo-ejection must be regarded with caution until adequate experimental measurements have been performed. The only relevant experiment does suggest that photo-ejection of physically adsorbed particles is efficient (Greenberg, 1973). The astrophysical parameters involved (gas density, radiation flux) are such that ejection of particles by radiation might reasonably keep interstellar grain surfaces "clean" when the interstellar radiation is not severely shielded. It is convenient to employ an efficiency δ such that the rate for photo-ejection of an adsorbed particle is

$$t_p^{-1} = \delta t_\gamma^{-1},$$

where t_γ is the mean time for the particle in the gas phase to absorb an ultraviolet (≈ 6 – 13.6 eV) photon from the average, unshielded galactic radiation ($t_\gamma \approx 10^8$ s, typically).

A model for the ejection process similar to the dissociation of a molecule has been suggested. Absorption of a photon then involves excitation to an electronic state of the adsorbed particle. At the equilibrium separation for the ground state from the surface, the excited state may be repulsive. Ejection will occur if the adsorbed atom is not deexcited by transfer of the electronic excitation into the surface. A semiquantitative examination of the locations of the potential well minima in the ground and excited states, as well as the time scales for dissociation versus that for transfer of electronic excitation, indicates that $\delta \approx 1$ may be typical for physical adsorption. For tight binding to the surface (chemisorption), transfer of excitation into the surface should be faster so that $\delta \ll 1$. The limited experimental data for photo-ejection and electron impact ejection (which may involve a similar mechanism) do yield $\delta \approx 0.01$ for chemisorption (see references in Watson and Salpeter, 1972a; Greenberg, 1973).

Experimental photo-ejection yields for weak binding are presented in Table IX. To convert these yields to δ it is necessary to divide by the fraction of the incident radiation that is absorbed in the adsorbed layer. Such information is not available. Absorption cross sections obtained in the gas phase are not helpful since most of these molecules exhibit little or no absorption at the 2000–2750 Å of the experiment. Greenberg (1973) suggests that a reasonable estimate for the fraction absorbed in his experiment is $\approx 10^{-5}$, though it could be as large as $\approx 10^{-3}$. For the former value $\delta \approx 0.1$ to 1.

3. Ejection in reactions

A discussion of ejection in chemical reactions is given for H_2 molecules by Hollenbach and Salpeter (1970), and for other molecules by Watson and Salpeter (1972a). No direct experiments exist, though measurements by Marenco *et al.* (1972) for the energy transferred to an ice surface ($\ll 4.5$ eV per molecule) indicates that most of the formation energy is retained by the ejected molecule. No experimental constraints are placed on whether it is mainly translational, vibrational, or rotational

TABLE IX. Photoejection yields (molecules ejected per incident photon) for weakly bound gases onto cold fused quartz for radiation of wavelengths 2000–2750 Å (from Greenberg, 1973).

Yield	Molecule
$\sim 1 \times 10^{-5}$	CS_2
$\sim 1 \times 10^{-6}$	$\left\{ \begin{array}{l} CO_2 \\ O_2(O_4?) \\ CO \end{array} \right.$
$\sim 10^{-6} - 10^{-7}$	$\left\{ \begin{array}{l} C_6H_6 \\ C_4H_{10} \\ N_2 \\ CH_4 \\ H_2O \\ CH_3OH \\ NH_3 \end{array} \right.$
$< 10^{-8}$	$\left\{ \begin{array}{l} Cu_2O \\ CdS \end{array} \right.$

energy.

The semiquantitative theoretical discussions examine the magnitudes of the forces, distances and time scales associated with the classical trajectories of physically adsorbed particles. As the molecular potential of two recombining particles on a surface pulls them together, they are pulled against the repulsive potential of the surface. A force E_{\perp} can then occur between the surface and the center-of-mass of the molecule of mass M . This imparts a net momentum

$$p_{\perp} = \int F_{\perp} dt,$$

when the force is integrated over the reaction trajectory. If the resultant energy $E_{\perp} = p_{\perp}^2/2M$ exceeds the binding energy D , the molecule will be ejected directly. For H_2 molecules Hollenbach and Salpeter (1970) estimate $E_{\perp} \approx 0.20$ eV $> D$. The larger mass of heavier atoms (e.g., OH, NH, CH) tends to reduce E_{\perp} so that it is unclear whether E_{\perp} exceeds D . If it does not escape, the "hot" molecule can hop across the surface and convert some additional vibrational energy into translational energy needed for escape. However, due to the large difference between the time scales for vibrational and translational motion, the collisions seem to be quite adiabatic with little energy conversion. Calculations for the recombination process and the subsequent "hopping" have been attempted, but the results are only an indication (Watson and Salpeter, 1972a). It seems likely that both ejection and equilibration to the surface will occur with non-negligible probabilities.

4. Sputtering

The ejection of surface particles through direct collision with an incident gas particle has been discussed most recently by Aannestad (1973b). At average interstellar cloud temperatures (~ 100 K), sputtering is completely negligible based on these rates. However, sputtering may be important in the overall mass balance between the grains and gas by returning atoms to the gas from icy grain mantles during a high temperature phase (i.e., "intercloud") of the gas.

G. Summary and conclusions for reactions on interstellar grain surfaces

Clearly, the uncertainties in the physical processes and astronomical conditions are severe. A detailed investigation of all possibilities is thus hardly worthwhile (even if possible) and I will concentrate on general conclusions. As stated previously, only the cold grains of the general ISM are considered here. Hot grains ($T \gtrsim 50$ K) near intense sources of radiation are ignored. Reactions are assumed to occur on top of the surface, though the general conclusions are not likely to be altered significantly if diffusion into the interior is considered.

First, I wish to emphasize that the occurrence of a grain surface that strongly binds (chemisorbs) the gas particles is no bar to reaction with other particles in the ISM. To prevent reactions, an atom must stick, remain immobile and unreactive, and then be ejected in atomic form. The only process that might eject strong-

ly bound particles rapidly enough to be important is photo-ejection. For this, the rate t_p^{-1} for photo-ejection of an adsorbed particle must be faster than the rate t_s^{-1} at which the site is covered over by one or more monolayers on top of which the binding will be weak. That is,

$$10^{-9}\delta \approx t_p^{-1} > t_s^{-1} \approx 10^{-11}n(\text{cm}^{-3}) \quad (2.12)$$

to prevent reactions. Since probably $\delta \lesssim 0.01$ for chemisorbed particles, Eq. (2.12) is not satisfied at densities $n \gtrsim 1 \text{ cm}^{-3}$ appropriate for interstellar clouds. Strong binding is thus no problem for molecule formation.

1. Reactions to produce molecular hydrogen

The specific parameters for H_2 formation on frozen H_2O surfaces employing only van der Waal's binding for atomic H will be emphasized since this has been studied in detail and is representative of the inert surfaces which are expected to occur. The description here is in the spirit of Hollenbach and Salpeter (1971). An H atom from the gas sticks to the grain in about one of three collisions. Keeping the atomic H bound to the grain until a second H atom sticks has seemed to be the chief problem. That is, for reactions to be efficient, the thermal evaporation time from the surface must at least be greater than the sticking time

$$\nu_0^{-1} \exp[D(\text{H})/kT_g] \gtrsim ([\text{H}] v_H r_g^2)^{-1} \quad (2.13)$$

for a grain of radius r_g onto which H atoms from the gas of density $[\text{H}]$ and velocity v_H are incident. For representative values in Eq. (2.13) ($r_g \approx 10^{-5} \text{ cm}$, $v_H \approx 10^5 \text{ cm/s}$, $[\text{H}] \approx 10 \text{ cm}^{-3}$)

$$D(\text{H})/kT_g \gtrsim 35 \quad (2.14)$$

is needed. Grain temperatures 10 to 20 K then require $D(\text{H})/k > 350$ to 700 K which is consistent with the $D(\text{H})$ deduced in Sec. II.C from the work of Lee (1972). Since the sticking time from Eq. (2.13) is much greater than the time for the H atom to traverse the entire grain surface according to Eqs. (2.7) and (2.10), only two atoms on a grain will be sufficient to find each other and react before evaporating when Eq. (2.13) is satisfied.

At somewhat lower grain temperatures than defined by Eq. (2.14), the situation can be complicated by the presence of molecular hydrogen on the surface. Due to its greater mass and polarizability, molecular hydrogen is normally expected to be bound more tightly by physical adsorption than is atomic H

$$D(\text{H}_2)/k - D(\text{H})/k \approx 100 \text{ K}. \quad (2.15)$$

In analogy with Eqs. (2.13) and (2.14), the surface will be covered over by a monolayer of H_2 when

$$D(\text{H}_2)/kT_g \approx 50. \quad (2.16)$$

If the H_2 monolayer is sufficiently rigid that H atoms cannot replace the molecules, the binding for the atoms on top of the monolayer will be quite small (perhaps 200 K). Equation (2.14) will not then be satisfied except at lower than the usual grain temperatures. Only a few degrees Kelvin separate the temperatures which satisfy Eqs. (2.14) and (2.16). If, however, $D(\text{H}_2)$ de-

creases smoothly near monolayer coverage as suggested by data such as that in Fig. 13 or if the H_2 monolayer is not sufficiently rigid to prevent replacement by H atoms, an H atom that hits a grain will normally remain long enough to react with another H atom before returning to the gas (Watson, 1975).

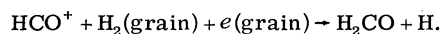
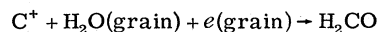
At higher grain temperatures than will satisfy Eq. (2.14) for a regular (no impurities) ice surface ($T_g \gtrsim 20 \text{ K}$), reaction to produce H_2 will be inefficient unless other effects are present. It is probable that a few sites of enhanced binding $D'(\text{H})$ occur. These may be due to ejection of surface particles by cosmic rays, growth irregularities, or impurity atoms which may have a semi-chemical attraction for atomic H. Atomic H is likely to replace molecular hydrogen in such sites as is necessary. The number and strength of such sites is governed by the requirements that an H atom migrate to an enhanced site before it is evaporated from the regular surface and that $D'(\text{H})$ is great enough to prevent evaporation before other H-atoms stick to the grain. Hollenbach and Salpeter (1971) find that a single such site of $D'(\text{H})/k \approx 2000 \text{ K}$ on a grain will be adequate for $T_g \lesssim 40 \text{ K}$.

Independent of which of the above cases does occur, return of the H_2 molecule to the gas presents no problems. The molecule will either be ejected directly in the reaction or by thermal evaporation.

2. Reactions to produce molecules other than H_2

In light of the predicted high efficiency for forming H_2 , reactions of other atoms and molecules must be considered likely. Serious difficulty is encountered, however, in understanding the return to the gas. We follow here the discussion of Watson and Salpeter (1972a, b). Heavier atoms (C, N, O, etc.) easily stick and remain on the grain. Positive ions may encounter some difficulty in sticking and will be strongly repelled if the grain is positively charged. Positive grains may dominate in low-density clouds, but not in clouds with moderate optical extinction. Again, the emphasis is toward inert surfaces with weak binding for reactive particles. Unless the surface has specific chemical properties that prevent reactions between heavy atoms and H atoms, the normal path is for reactive heavy atoms that are incident to become chemically saturated with hydrogen. Reaction with hydrogen is preferred both because of its much greater relative abundance and its greater mobility. From the treatment of H_2 production it is clear that an H atom can always "find" another reactive particle that is already on the surface. The requirement that the heavy atom remain until an H atom sticks is analogous to Eq. (2.14) and is easily satisfied for $T_g \lesssim 22 \text{ K}$ since $D(\text{C}, \text{N}, \text{O}, \text{etc.})/k \gtrsim 800 \text{ K}$ (Sec. II.C). After the heavy atoms have been converted into chemically saturated molecules (e.g., CH_4 , NH_3 , H_2O), further reactions are strongly inhibited by large activation energy barriers ($\approx 0.3 \text{ eV}$). It might be possible for molecules, which are still highly excited immediately (of the order of several vibration periods) after a recombination reaction, to collide with saturated molecules and react. Excitation of the adsorbed molecules by radiation may also provide energy to

overcome energy barriers. Incident C, N, O, etc., atoms might react before they are thermalized with the adsorbed molecules if the activation energy is small. If the incident particle is ionized (e.g., C^+ , HCO^+), there will probably be no energy barrier and reactions seem likely, for example



Direct return of the product to the gas is more likely than in previous cases since the C^+ and HCO^+ are not adsorbed. The possible rates for such processes based on astronomical conditions are competitive, though little information on cross sections is available.

During the reaction process between a heavy atom or radical and hydrogen, an appreciable fraction of the products are most likely ejected nonthermally back to the gas. Some will be ejected in intermediate reactions as OH, CH, CH_2 , NH, NH_2 , etc., while others remain to produce the chemically saturated forms CH_4 , NH_3 , H_2O , etc., of which a fraction are not ejected in the reaction. If these are not returned to the gas, heavy elements will be frozen out of the gas in a time comparable to that usually associated with the lifetime of interstellar clouds. Application of the analog for Eq. (2.16) indicates that thermal evaporation will not eject the particles at normal T_g (≈ 20 K) for typical D (heavy molecule)/ $k \approx 1000$ K. Thus nonthermal ejection mechanisms are needed and photo-ejection must be considered. If $\delta \approx 1$ and the heavy elements in the gas are in atomic form, photo-ejection will prevent significant depletion of the gas when

$$ne^{2.5T} \nu (\text{cm}^{-3}) \approx 10^5 / f. \quad (2.17)$$

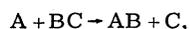
Here sources of radiation are assumed to be outside the cloud, τ_v is the visual optical depth to the cloud center, and f is the fraction of heavy atoms that remain on the grains after all reactions.

In summary, reactive heavy particles are certainly converted into molecules when they hit grains in the general ISM. Hydrides (OH, CH, NH, CH_4 , H_2O , etc.) are mainly produced. The chief uncertainty is in returning the molecules to the gas, though a significant fraction may be returned in the reaction process and by photo-ejection when starlight is present. Temperature fluctuations of very small grains (radius < 100 Å) that result from the energy emitted in the chemical reaction might be able to cause ejection of weakly bound molecules. The presence of such grains is uncertain.

III. PHYSICAL PROCESSES FOR REACTIONS IN THE GAS PHASE

A. Cross sections for chemical reactions

Chemical reactions of the type



where A and BC represent atoms or radicals, and can be neutral or ionized are considered here. Purely theoretical calculations do not normally yield cross sections for such collisions that are sufficiently accurate for practical application. Only a few fully quantum

treatments of reactive collisions are available. These require considerable computational effort and have been applied to only the simplest systems. In addition to treatment of the collision, the equally formidable task of obtaining an accurate adiabatic potential energy surface for a polyatomic must also be met. The most extensive variational calculations normally give energies accurate at best to ≈ 0.05 – 0.1 eV (e.g., Schaefer, 1972). Collision energies in the astronomical context are ≤ 0.01 eV. The ever present possibility for small, "activation energy" barriers in reactions between neutrals is a source of particular concern at these low temperatures. It is evident that uncertainties tend to be greatest at the lower energies where information is needed for astrophysical purposes.

From the experimental viewpoint, essentially no cross sections have been measured at temperatures below 300 °K. Information is often unavailable on the energy dependence. When available it is usually obtained from a fit to the experimental data of the form

$$\alpha = \langle \sigma v \rangle = A \exp(-E/kT) \text{ cm}^3 \text{ s}^{-1} \quad (3.1)$$

in a quite different temperature region from that of the interstellar gas. The "rate coefficient" α in Eq. (3.1) is the product of the cross section and velocity averaged over a Maxwellian distribution. Use of such expressions can yield cross sections that are either too large or too small. The presence of a slower reaction channel that does not dominate at high temperatures, but has little or no activation energy is possible. Low-lying excited states of the reacting particles that are populated at laboratory densities may dominate the reaction. At the low densities of the interstellar gas, these states will be underpopulated in comparison with thermodynamic equilibrium. Excited electronic states are usually much more reactive than the ground state. Further, quantal tunneling through an activation energy barrier might enhance the reaction rate at low temperatures over that given by Eq. (3.2). As indicated by the temperature dependence of the $D + H_2$ reaction shown in Fig. 16, present evidence suggests that such tunneling will not be of major importance in astrophysics.

In the absence of extensive experimental data, semi-empirical guidelines have been employed. Which of

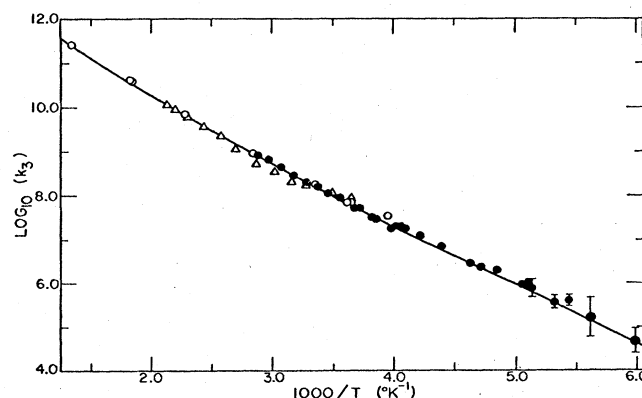


FIG. 16. Experimental data for the reaction $D + H_2 \rightarrow HD + H$. The molar rate coefficient $k_3(\langle \sigma v \rangle = k_3/6 \times 10^{23} \text{ cm}^3 \text{ s}^{-1})$ vs (temperature) $^{-1}$ (from Mitchell and LeRoy, 1973).

numerous competing reactions are likely to dominate can then be delineated in order that the crucial laboratory measurements can be performed. Because of the low collision rate in the interstellar gas, a reaction must usually occur at essentially every "hard collision," as well as be exothermic due to the low temperature, in order to be important. The rate coefficient for "hard collisions" is then a useful value against which to compare reaction rates. Positive-ion reactions with neutrals almost always seem to occur at near this rate when only a few atoms are involved. Neutral-neutral reactions with no activation energy often proceed at nearly every collision. A characteristic difference of one-to-two orders of magnitude exists between ion-neutral and neutral-neutral rate coefficients for collision. A hard collision is considered to be a classical collision in which the impact parameter is small enough that the long-range attractive r^{-n} potential ($n > 2$) will overcome the angular momentum barrier. The particles will then spiral into the chemical region of the potential and form a complex which is likely to decay into products different from the incident particles. For ion-molecule systems, polarization gives a long-range potential at a distance r

$$V_i(r) = -\epsilon e^2 / 2r^4, \quad (3.2)$$

where ϵ is the polarizability of the neutral. In neutral-neutral reactions the long-range attraction is due to the van der Waal's force,

$$V_n(r) \approx -(\epsilon_1 \epsilon_2 / r^6) I. \quad (3.3)$$

These lead to rate coefficients to spiral into the chemical region of the potential

$$\alpha_i = \langle \sigma v \rangle = 2\pi(\epsilon e^2 / \mu)^{1/2} \quad (3.4)$$

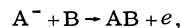
and

$$\alpha_n = \pi 13.5 (\epsilon_1 \epsilon_2 I / \mu)^{1/3} \langle v^{1/3} \rangle, \quad (3.5)$$

for a reduced mass μ in the collision. Representative values—polarizabilities = 10^{-24} cm³, $\mu = 2m_H$, $I = 1$ Ry, and temperature = 100 °K—give $\alpha_i \approx 2 \times 10^9$ cm³s⁻¹, and $\alpha_n \approx 4 \times 10^{-11}$ cm³s⁻¹.

As a working guide, exothermic neutral-neutral reactions whose rates are near α_n under laboratory conditions ($T \approx 300$ °K) probably have similar rates in the interstellar gas. A laboratory rate significantly slower than α_n suggests an activation energy barrier or reaction from an excited state which will normally cause the reaction to be unimportant at the low temperature/density conditions of the interstellar gas. Activation energy barriers usually occur when a chemically saturated molecule is involved (reactant or product), but are likely not to occur in reactions involving only atoms and radicals. In contrast, exothermic ion-molecule reactions involving small molecules usually proceed at near α_i and are temperature independent. It is this convenient property that has made it possible to perform with reasonable confidence detailed studies of ion-molecule reaction schemes in the interstellar gas. To illustrate the general characteristics of reaction rates, we present in Table X and Table XIA-D some representative data.

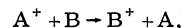
Reactions between negative ions and neutrals



have been considered (Dalgarno and McCray, 1973) and seem to be less important under astrophysical conditions than the reactions discussed above. Only $H^- + H \rightarrow H_2 + e$ will be considered (Sec. IV.A.1).

B. Charge transfer

Because of the simplified geometry, the reaction process in charge-transfer between atoms



is less complex than the molecular rearrangements discussed in the previous section. Charge transfer can be considered as the transition between the two potential energy curves associated with the asymptotic ionization states of the atoms. As in chemical reactions, the transition usually occurs mainly in the neighborhood of the crossing between the two states. A two-state approximation may be adequate in certain low-energy collisions and provides physical insight into the process (e.g., Mott and Massey 1965). Within the Born-Oppenheimer approximation the total wavefunction is taken to be of the form

$$\Psi = \varphi_0(r, R)F_0(R) + \varphi_1(r, R)F_1(R), \quad (3.6)$$

where the φ are electronic wave functions for the two states obtained by ignoring interaction between the states ("adiabatic" states). The F represent the nuclear wave functions which are dependent on internuclear separation R , but not the electron coordinates r . By substituting Ψ into the Schrödinger equation, the coupled equations,

$$(\nabla^2 + k_0^2 - V_{00})F_0 = V_{01}F_1, \quad (3.7)$$

$$(\nabla^2 + k_1^2 - V_{11})F_1 = V_{10}F_0$$

are obtained. Here,

$$V_{ij} = (2\mu/\hbar^2) \int V(R, r) \varphi_i^* \varphi_j d\vec{r}, \quad (3.8)$$

TABLE X. Measured rate coefficients α for representative reactions between neutrals at temperature T . A and E (activation energy) are obtained by fitting to the assumed form $\alpha = A \exp(-E/kT)$.

Reaction	T (K)	α (cm ³ s ⁻¹)	A (cm ³ s ⁻¹)	E (eV)
H + CH ₄			1×10^{-11}	0.51
H + H ₂ CO			2×10^{-11}	0.17
O + HCN			9×10^{-12}	0.35
O + CH ₄			5×10^{-11}	0.23
O + H ₂ CO	300	2×10^{-13}		
O + C ₂ H ₂	300	6×10^{-13}		
O + OCS			2×10^{-10}	0.26
N + C ₂ H ₂	300	3×10^{-13}		
OH + H ₂ → H ₂ O + H	300	7×10^{-15}		
³ CH ₂ + H ₂ → ¹ CH ₃ + H	300	$< 5 \times 10^{-14}$		
OH + N → NO + H	300	7×10^{-11}		
OH + O → O ₂ + H	300	5×10^{-11}		
CN + O → CO + N			1×10^{-10}	0.10
CH ₃ + O → H ₂ CO + H	300	3×10^{-11}		
OH + H → H ₂ + O			1×10^{-11}	0.34
NH + NO	300	2×10^{-10}		

TABLE XI. Measured rate coefficients α for representative ion-neutral reactions at temperatures ≈ 300 °K.

Reaction	$\alpha(10^{-9} \text{ cm}^3 \text{ s}^{-1})$
A. Reactions involving hydrogen transfer	
$\text{H}_2^+ + \text{H}_2 \rightarrow \text{H}_3^+ + \text{H}$	2
$\text{O}^+ + \text{H}_2 \rightarrow \text{OH}^+ + \text{H}$	1.6
$\text{OH}^+ + \text{H}_2 \rightarrow \text{H}_2\text{O}^+ + \text{H}$	1
$\text{H}_2\text{O}^+ + \text{H}_2 \rightarrow \text{H}_3\text{O}^+ + \text{H}$	0.6
$\text{N}^+ + \text{H}_2 \rightarrow \text{NH}^+ + \text{H}$	0.5
$\text{NH}^+ + \text{H}_2 \rightarrow \text{NH}_2^+ + \text{H}$	1
$\text{C}^+ + \text{H}_2 \rightarrow \text{endothermic}$...
$\text{CH}^+ + \text{H}_2 \rightarrow \text{CH}_2^+ + \text{H}$	1
$\text{C}_2^+ + \text{H}_2 \rightarrow \text{C}_2\text{H}^+ + \text{H}$	1.1
$\text{CH}^+ + \text{H} \rightarrow \text{C}^+ + \text{H}_2$	$8 \times 10^{-15} T^{5/4} \text{ }^a$
$\text{H}_3^+ + \text{N}_2 \rightarrow \text{HN}_2^+ + \text{H}_2$	1.0
$\text{HeH}^+ + \text{H}_2 \rightarrow \text{H}_3^+ + \text{He}$	1.8
$\text{HCO}^+ + \text{HCN} \rightarrow \text{H}_2\text{CN}^+ + \text{CO}$	~ 2
$\text{N}_2\text{H}^+ + \text{CO} \rightarrow \text{HCO}^+ + \text{N}_2$	1
B. Reactions involving transfer of atoms heavier than hydrogen	
$\text{CH}_4^+ + \text{CH}_4 \rightarrow \text{CH}_5^+ + \text{CH}_3$	1.2
$\text{CH}_3^+ + \text{CH}_4 \rightarrow \text{C}_2\text{H}_5^+ + \text{H}_2$	0.95
$\text{CH}_3^+ + \text{NH}_3 \rightarrow \text{NH}_4^+ + \text{CH}_2$	0.17
$\rightarrow \text{CH}_2\text{NH}_2^+ + \text{H}_2$	0.66
$\text{NH}_4^+ + \text{CH}_4 \rightarrow \text{NH}_5^+ + \text{CH}_3$	0.39
$\text{C}^+ + \text{NH}_3 \rightarrow \text{H}_2\text{CN}^+ + \text{H}$	1.1
$\rightarrow \text{C} + \text{NH}_3^+$	1.1
$\text{C}^+ + \text{H}_2\text{O} \rightarrow \text{HCO}^+ + \text{H}$	2
C. Reactions involving dissociation by helium	
$\text{He}^+ + \text{H}_2 \rightarrow \text{H}^+ + \text{H} + \text{He}$	$\sim 1 \times 10^{-4}$
$\rightarrow \text{H}_2^+ + \text{He}$	$< 10^{-4}$
$\rightarrow \text{HeH}^+ + \text{H}$	$< 10^{-4}$
$\text{He}^+ + \text{CO} \rightarrow \text{C}^+ + \text{O} + \text{He}$	1.4
$\text{He}^+ + \text{N}_2 \rightarrow \text{N}_2^+ + \text{He}$	1.2
$\rightarrow \text{N}^+ + \text{N} + \text{He}$	
$\text{He}^+ + \text{CH}_4 \rightarrow \text{CH}_4^+ + \text{He}$	0.04
$\rightarrow \text{CH}_3^+ + \text{H} + \text{He}$	0.06
$\rightarrow \text{CH}_2^+ + \text{H}_2 + \text{He}$	0.90
$\rightarrow \text{CH}^+ + \text{H}_2 + \text{H} + \text{He}$	0.20
D. Isotope-exchange reactions	
$\text{D}^+ + \text{H}_2 \rightarrow \text{HD} + \text{H}^+$	1^b
$\text{H}_3^+ + \text{HD} \rightarrow \text{H}_2\text{D}^+ + \text{H}_2$	0.3
$\text{HCO}^+ + \text{HD} \rightarrow \text{DCO}^+ + \text{H}_2$	< 0.02
$\text{CD}_3^+ + \text{H}_2 \rightarrow \text{CD}_2\text{H}^+ + \text{HD}$	0.51
$\rightarrow \text{CDH}_2^+ + \text{H}_2$	
$\text{CH}_3^+ + \text{D}_2 \rightarrow \text{CH}_2\text{D}^+ + \text{HD}$	0.55
$\rightarrow \text{CHD}_2^+ + \text{H}_2$	
$\text{H}_3\text{O}^+ + \text{D}_2 \rightarrow \text{H}_2\text{DO}^+ + \text{HD}$	≤ 0.001
$\rightarrow \text{HD}_2\text{O}^+ + \text{H}_2$	
$\text{H}_2\text{CN}^+ + \text{D}_2 \rightarrow \text{HDCN}^+ + \text{HD}$	< 0.0025
$^{13}\text{C}^+ + ^{12}\text{CO} \rightarrow ^{13}\text{CO} + ^{12}\text{C}^+$	0.2

^a Deduced from the inverse reaction at higher energy by Solomon and Klemperer (1972) and valid only for $T \lesssim 100$ °K.

^b Measured down to 80 K by Fehsenfeld *et al.* (1973).

where μ is the reduced mass, k_0 and k_1 the asymptotic wave numbers, V is the potential energy, and the φ are assumed to be orthogonal. For the energies of interest here, coupled equations analogous to Eqs. (3.7) but formulated in terms of the adiabatic states, are actually more useful.

Unfortunately, no calculations (except $\text{H} + \text{H}^+$) for charge transfer have been performed at the low energies of interest here. The $\text{H}^+ + \text{O}$ charge transfer is of

TABLE XII. Representative data for charge-transfer collisions between atoms.

Charge-transfer	$\alpha(10^{-9} \text{ cm}^3 \text{ s}^{-1})$
$\text{H}^+ + \text{O} \rightarrow \text{O}^+ + \text{H}$	0.38
$\text{O}^+ + \text{H} \rightarrow \text{O} + \text{H}^+$	0.68
$\text{N}^+ + \text{Na} \rightarrow \text{Na}^+ + \text{N}$	Very small
$\text{N}^+ + \text{Ca} \rightarrow \text{Ca}^+ + \text{N}$	1.1
$\text{O}^+ + \text{Na} \rightarrow \text{Na}^+ + \text{O}$	Very small
$\text{O}^+ + \text{Ca} \rightarrow \text{Ca}^+ + \text{O}$	0.76

particular interest as the initial reaction in producing OH and H_2O (Sec. IV.A.3b). It also contributes to neutralizing H^+ (Sec. IV.A.2). In this charge transfer, reaction from the ground states is endothermic by $\Delta E/k = 227$ °K, but the first excited fine-structure state of oxygen is $\Delta E/k = 228$ °K above the ground state. A third fine-structure state is $\Delta E/k = 326$ °K above the lowest state. Laboratory measurements are available only down to temperatures 300 °K and at pressures such that the populations of the fine-structure states are in thermodynamic equilibrium. Representative data on atom-atom charge-transfer are presented in Table XII.

When a molecule is involved in the charge transfer, more states (especially vibrational states) are available to take up the energy. Thus rate coefficients near the usual ion-molecule rate $\alpha \approx 10^{-9} \text{ cm}^3 \text{ s}^{-1}$ normally prevail as suggested by the representative data presented in Table XIII.

C. Radiative association

When two atoms collide, the probability that a molecule will be formed is quite low. The particles enter the collision with a total energy that is positive and will simply dissociate again unless the energy is lost. In laboratory reactions the excess energy is given to a third particle or to a surface. Three-body collisions are absolutely negligible in the interstellar gas. Surface reactions that may occur on interstellar dust grains have been discussed in Sec. II. Another possibility that may be of importance in astrophysics, but is rarely if ever significant in the laboratory, is the emission of energy as radiation during the collision. To be competitive the radiative transition probability A (s^{-1}) must be fast. An electric dipole transition between two electronic states is thus required. The upper electronic state must be attained in collisions between the atoms in their lowest atomic states (including fine

TABLE XIII. Same meaning as Table XII except that collisions involve molecules.

Charge-transfer	$\alpha(10^{-9} \text{ cm}^3 \text{ s}^{-1})$
$\text{H}^+ + \text{O}_2 \rightarrow \text{O}_2^+ + \text{H}$	1.2
$\text{H}^+ + \text{H}_2\text{O} \rightarrow \text{H}_2\text{O}^+ + \text{H}$	8.2
$\text{H}^+ + \text{NH}_3 \rightarrow \text{NH}_3^+ + \text{H}$	5.2
$\text{C}^+ + \text{NH}_3 \rightarrow \text{NH}_3^+ + \text{C}$	1.1
$\text{O}^+ + \text{H}_2\text{O} \rightarrow \text{H}_2\text{O}^+ + \text{O}$	2.3
$\text{N}^+ + \text{CO} \rightarrow \text{CO}^+ + \text{N}$	0.5
$\text{O}_2^+ + \text{Na} \rightarrow \text{O}_2 + \text{Na}^+$	1.4
$\text{H}_2\text{O}^+ + \text{Ca} \rightarrow \text{H}_2\text{O} + \text{Ca}^+$	4.0

s VOLUME 44, NUMBER 26 arations. The upper state must also be attractive, since the transition probability is large only at separations comparable with molecular dimensions.

A detailed treatment of the collision, along with an accurate knowledge of the radiative transition probability $A(r)$ and the potential energy curves, is needed for a reliable determination of the radiative association probability (e.g., Giusti-Suzor, Roueff and van Regemorter, 1976). However an order-of-magnitude estimate can easily be made to provide physical appreciation of the process. For classical motion of the nuclei, the probability to reach a bound state by emission of radiation during a collision is

$$P = 2g \int_a^\infty A(R) [dt/dR] dR \approx gA(R_0)T \quad (3.9)$$

when the upper state is attractive. Here the time t is related to internuclear separation R by the classical orbit described by the turning point a . R_0 is the separation for the potential minimum, g the probability for reaching the upper molecular state from the ground atomic states, and T is the characteristic vibration period for a highly excited vibrational state of the nuclei. With $T \approx 2R_0\sqrt{\mu/2V_{\min}} \approx 2 \times 10^{-14}$ s (V_{\min} = potential well depth, μ = reduced mass), $A(R_0) \approx 10^{16}$ appropriate for a near ultraviolet stabilizing transition such as the $\text{CH}^+(\text{}^1\Sigma - \text{}^1\Pi)$ and $g \approx 1/4$

$$P \approx 10^{-8}.$$

For our purposes a close collision has an impact parameter smaller than the critical value for orbiting Eqs. (3.4) and (3.5) so that for radiative association to form a diatomic

$$\alpha = \langle \sigma v \rangle \approx P\alpha_i \approx 10^{-17} \text{ cm}^3\text{s}^{-1} \quad (3.10)$$

when one particle is ionized.

Astrophysical interest in radiative association has centered mainly on the $\text{C}^+ + \text{H}$ collision with calculations by Kramers and ter Haar (1946), Bates (1951), Solomon and Klemperer (1972) and Smith *et al.* (1973). Electronic energy levels for the CH^+ system are given in Fig. 17. Most recently the semiclassical treatment of Giusti-Suzor *et al.* (1975) includes the calculation of such effects as nonadiabatic transitions between the molecular states and tunneling through the centrifugal barrier. This seems to produce the most accurate cross section presently available (Table XIV). Other radiative associations between atoms are not thought to be important.

It is important in astrophysics that as shown in Fig. 20 the two electronic states of $\text{H}_2(\text{}^3\Sigma_u, \text{}^1\Sigma_g)$ that can be reached in low-energy collisions between ground-state H atoms differ in spin ($\text{}^3\Sigma_u$ is also repulsive). From the oscillator strength estimated by Gould and Salpeter (1963), the radiative association rate coefficient $\alpha \lesssim 10^{-23} \text{ cm}^3\text{s}^{-1}$. Thus the most frequent collisions in the interstellar gas (due to the abundance of hydrogen) cannot lead to radiative association. Radiative association between an atom and a molecule might be much faster for certain systems than for two atoms since the presence of additional modes allows the possibility that a

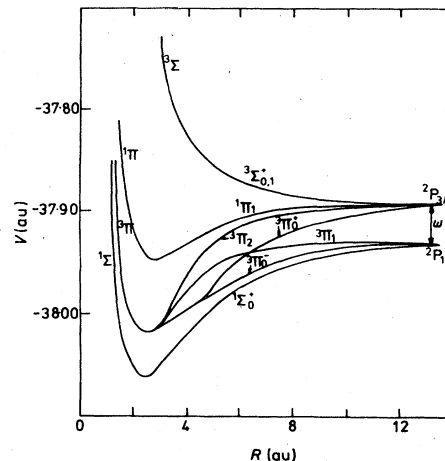


FIG. 17. Correlation of atomic and molecular states in the $\text{C}^+ + \text{H}$ collision. The transition involved in the radiative association is $\text{}^1\Pi \rightarrow \text{}^1\Sigma$. Fine-structure splitting ω is exaggerated (from Giusti-Suzor *et al.*, 1976).

complex can be formed with a lifetime greater than one vibrational period. Black, Dalgarno and Oppenheimer (1975) have suggested that such effects might cause the rate coefficient for



to be as large as $\alpha \approx 10^{-14} \text{ cm}^3\text{s}^{-1}$. Theoretical investigations do indicate that this rate coefficient will be greater than for diatomics (Pearson and Roueff, 1976; Herbst and Delos, 1976), though its actual value has not yet been obtained. Indirect experimental evidence also exists (Fehsenfeld, Dunkin and Ferguson, 1974). Radiative associations involving larger molecules with H_2 have also been estimated (Herbst and Klemperer, 1973; Herbst, 1976). Representative data for radiative associations are summarized in Table XIV.

TABLE XIV. Rate coefficients α for radiative association at gas temperatures $\approx 50\text{--}100^\circ\text{K}$.

Reaction	$\alpha(\text{cm}^3\text{s}^{-1})$
$\text{C}^+ + \text{H} \rightarrow \text{CH}^+ + h\nu$	1.3×10^{-17} ^a
$\text{C} + \text{H} \rightarrow \text{CH} + h\nu$	3×10^{-17} ^b
$\text{O} + \text{H} \rightarrow \text{OH} + h\nu$	4×10^{-19} ^c
$\text{N} + \text{H} \rightarrow \text{NH} + h\nu$	~ 0 ^d
$\text{C} + \text{O} \rightarrow \text{CO} + h\nu$	$10^{-16}\text{--}10^{-18}$ ^d
$\text{N} + \text{O} \rightarrow \text{NO} + h\nu$	$10^{-16}\text{--}10^{-18}$ ^d
$\text{H} + \text{H} \rightarrow \text{H}_2 + h\nu$	≈ 0
$\text{H}^+ + \text{H} \rightarrow \text{H}_2^+ + h\nu$	10^{-18} at 500°K ^e
$\text{HCO}^+ + \text{H}_2 \rightarrow \text{H}_3\text{CO}^+ + h\nu$	10^{-18} ^f
$\text{C}^+ + \text{H}_2 \rightarrow \text{CH}_2^+ + h\nu$	$\approx 4 \times 10^{-17}$ ^g

^a Giusti-Suzor *et al.* (1975), at 100°K .

^b Solomon and Klemperer (1972).

^c Smith and Zweibel 1976; see also Julienne *et al.* (1971).

^d Julienne and Krauss (1973).

^e Bates (1951), rate decreases rapidly at lower temperature.

^f Herbst and Klemperer (1973).

^g Fehsenfeld *et al.* (1974).

D. Electron-ion recombination: Radiative and dissociative

1. Radiative recombination

The radiative recombination coefficient $\alpha_r = \langle \sigma v \rangle$ is usually obtained from the cross section for the inverse process, photoionization (e.g., Bates and Dalgarno, 1962). In thermodynamic equilibrium the number densities of the ionized and neutral form of an atom $[X_i]$ and $[X_0]$ are related by

$$[e][X_i]\alpha_r = [X_0] \int_0^\infty \sigma(\nu)B(\nu)d\nu, \quad (3.12)$$

where $\sigma(\nu)$ is the photoionization cross section at frequency ν , and $B(\nu)$ is the blackbody radiation flux. Use of the Saha equation to obtain the ratio $[X_0]/([e][X_i])$ in equilibrium at temperature T yields

$$\alpha_r(T) = \frac{g_0}{g_i} \frac{\sqrt{2} \exp(I_0/kT)}{c^2 \sqrt{\pi} (mkT)^3} \times \int (h\nu)^2 \sigma(\nu) d(h\nu) / [\exp(h\nu/kT) - 1]. \quad (3.13)$$

Here g_0 and g_i are the statistical weights of the two ionization states, and I_0 is the ionization energy of the neutral atom. For the physical conditions of interest, $I_0 \gg kT$, and $\nu^2 \sigma(\nu)$ remains close to its value at threshold $I_0^2 \sigma_0 / h^2$ in the region that contributes to the integral. Then

$$\alpha_r(T) \approx \frac{g_0}{g_i} \frac{\sqrt{2} I_0^2}{m^{3/2} \sqrt{\pi} k T c^2} \sigma_0 (I_0/h). \quad (3.14)$$

A typical photodissociation cross section (10^{-17} cm^2) and $I_0 = 1 \text{ Ry}$ yields $\alpha_r(100 \text{ K}) \approx 10^{-12} \text{ cm}^3 \text{ s}^{-1}$. If recombinations to all states except the ground state are summed to give α_r^1 for H^+ at temperatures $30 \leq T(\text{K}) \leq 125$,

$$\alpha_r^1(T) = 7.4 \times 10^{-11} / T^{1/2} \text{ cm}^3 \text{ s}^{-1} \quad (3.15)$$

to ten percent accuracy.

Radiative recombination rates for most molecular ions are considered to be comparable with those for atoms. Except possibly for a few special cases, dissociative electron recombination will then dominate by a substantial factor so that the exact radiative rate is unimportant.

2. Dissociative recombination

Dissociative electron recombination competes with other processes, and usually dominates, in the destruction of molecular ions which play a key role in proposed ion-molecule reaction schemes. Dissociative recombination involves capture of an electron to form the neutral molecule in an excited electronic state that can dissociate. In most cases considered, the state is repulsive so that dissociation takes place directly as shown in Fig. 18. Recombination to the state AB in Fig. 18 occurs by a radiationless transition in which an electron of the positive ion is excited to absorb the energy of the recombining electron. Immediately after recombination, state AB has electronic energy greater than the ionization energy. The inverse process (autoionization) can simply ionize the molecule again and

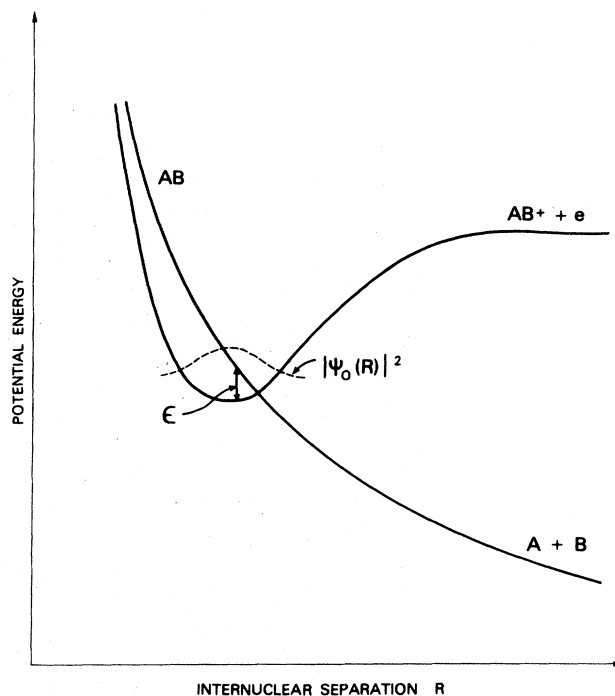


FIG. 18. Illustration of molecular, electronic energy curves involved in the dissociative electron recombination of the molecular ion AB^+ .

nothing has been achieved. However, if the nuclei separate somewhat before the autoionization occurs, the electronic energy will drop below that needed for ionization. Autoionization will not then be probable. The nuclei will continue to move apart and the molecule will dissociate.

The characteristic several orders-of-magnitude difference in reaction rates between radiative and dissociative recombination can be estimated by classical methods following, for example, Bates and Dalgarno (1962) and Bardsley and Biondi (1970). First consider the relative rates for autoionization and dissociation for the state AB in Fig. 18. Autoionization lifetimes are known from experiments with atoms to be typically $t_a \approx 10^{-14} \text{ s}$. A representative force on the nuclei deduced from the slope of the potential energy curve is about $5 \text{ eV}/\text{\AA}$. Then for a reduced mass of $8M_H$, the nuclear kinetic energy is increased by 0.75 eV in classical motion at the expense of the electronic energy in a time $7 \times 10^{-15} \text{ s}$. The separation is increased by approximately 0.15 \AA , roughly the De Broglie wavelength. This is a reasonable estimate for the separation time t_s after which autoionization will not occur, so that $t_s < t_a$ and autoionizing states will dissociate rather than autoionize. The dissociative recombination coefficient $\alpha_{de} = \langle \sigma(\epsilon)v \rangle$ can then be estimated by determining the electron recombination coefficient to an autoionizing state. It is again convenient to determine the recombination coefficient from the inverse process. In thermodynamic equilibrium

$$f(\epsilon)[X_a]/t_a = \sigma(\epsilon)v[X_i]dn(e)/d\epsilon \quad (3.16)$$

for autoionizing state X_a and a differential electron

spectrum $dn(e)/d\epsilon$. Also

$$f(\epsilon)d\epsilon = |\varphi_0(R_\epsilon)|^2 (dR_\epsilon/d\epsilon)d\epsilon \quad (3.17)$$

is the probability that an electron will be ejected with kinetic energy ϵ into the interval $d\epsilon$ as a result of the autoionization process. Only the ground vibrational state of AB^+ [wave function $\varphi_0(R)$] will be populated under the relevant astrophysical conditions. In Eq. (3.17) the variation of the nuclear overlap integral with R is assumed to be mainly due to φ_0 . R_ϵ is the internuclear distance when the separation of the AB and AB^+ curves is ϵ . In the Born-Oppenheimer approximation, only the electronic potentials can contribute to the outgoing energy ϵ for the electron and nuclear position and energy are constant during the transition. By making use of the Saha equation and noting that X_a is higher in energy than X_i by an amount ϵ

$$\alpha_{de}(T) = \frac{g_a}{g_i} \frac{h^3}{(2\pi m k T)^{3/2}} \frac{1}{t_a} \int f(\epsilon) e^{-\epsilon/kT} d\epsilon. \quad (3.18)$$

At energies of interest ($kT \approx 0.01$ eV) essentially all the contributions to the integral come from the point at which the curves for AB and AB^+ cross. Then

$$\alpha_{de}(T) = \frac{g_a}{g_i} \frac{C_0}{T^{3/2}} \frac{f(0)kT}{t_a} \quad (3.19)$$

with $C_0 = 2.1 \times 10^{-16} \text{ cm}^3 (\text{K})^{3/2}$. It is thus clear that the chief criterion for a large dissociative recombination cross section is that the crossing point of AB and AB^+ must be in the region where the lowest vibrational wave function of AB^+ is appreciable. For the favorable case of Fig. 18, α_{de} can be estimated by taking $|\varphi_0(R)|^2 \approx (1 \text{ \AA})^{-1}$, $(d\epsilon/dR_\epsilon) \approx 5 \text{ eV/\AA}$, $t_a \approx 10^{-14} \text{ s}$ and $g_a/g_i = 1$ for which

$$\alpha_{de}(T) \approx 10^{-7} \text{ cm}^3 \text{ s}^{-1}$$

at 100°K .

Thus dissociative recombination can be many orders of magnitude greater than radiative recombination. In fact, it seems that essentially all molecules do have states with favorable crossings for dissociative recombination (Table XV). Equation (3.19) exhibits the characteristic $T^{-1/2}$ dependence usually attributed to the process. This is not always followed, however (e.g., HCO^+ in Table XV). Bardsley and Biondi (1970) have reviewed

TABLE XV. Representative dissociative electron recombination coefficients for positive, molecular ions (from Bardsley and Biondi, 1970; Leu *et al.*, 1973a, b, c).

Ion	$\alpha_{de} (10^{-7} \text{ cm}^3 \text{ s}^{-1})$
H_3O^+	10 (540 K)
H_3^+	3 (205 K) ^a
H_5^+	36 (205 K) ^a
HCO^+	3 (205 K) ^b
He_2^+	<0.1 (300 K)
Ne_2^+	2 (300 K)
N_2^+	3 (300 K)
O_2^+	2 (300 K)
NO^+	4 (300 K)

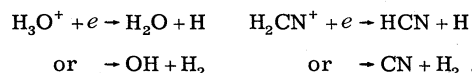
^a Temperature dependence $T^{-1/2}$ indicated.

^b Temperature dependence T^{-1} indicated.

possible arrangements of electronic states that can lead to other than a $T^{-1/2}$ dependence. The representative data given in Table XV are mainly for diatomics. For molecular ions of most interest in dense clouds (e.g., CH_3^+ , H_2CN^+ , NH_4^+), probably $\alpha_{de} (\approx 100^\circ \text{K}) \approx 10^{-6} \text{ cm}^3 \text{ s}^{-1}$ or slightly greater as found for H_3O^+ .

At present one of the most serious problems in understanding molecular abundances is that of CH^+ (see Sec. IV.A.3). For most processes the predicted CH^+ abundance can be analyzed relatively independent of uncertainties in the physical conditions and fails by a considerable factor to reproduce the observed abundances if $\alpha_{de}(\text{CH}^+) \approx 10^{-7} \text{ cm}^3 \text{ s}^{-1}$. Calculations (Bardsley and Junker, 1973; Krauss and Julienne, 1973) indicate that a suitable potential energy curve for excited CH crosses the curve for CH^+ within the region of the lowest vibrational state in CH^+ (see Fig. 19). Hence, a large α_{de} is indicated.

Although the rate coefficients α_{de} for molecular ions can be estimated, the products are highly uncertain when the recombination involves polyatomic ions, e.g.,



Almost certainly HCO^+ and N_2H^+ dissociate to CO and N_2 as a result of the strong binding of these diatomics.

E. Photodissociation/Photoionization

Although direct photo-excitation to a free nuclear state of the ground electronic state is negligible, a change in the electronic state can leave the nuclei in a free state. Specifically, in the Frank-Condon approximation the photoabsorption cross section is proportional to the ma-

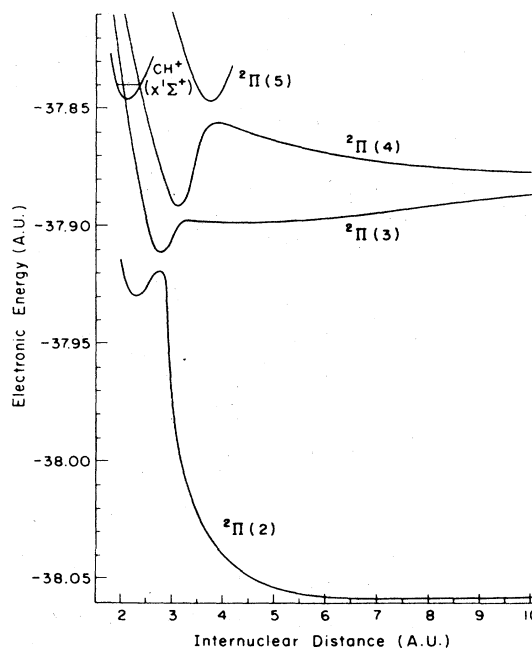


FIG. 19. Electronic energy of excited states of CH that are of interest in the dissociative electron recombination of CH^+ . Energy is in hartrees (27.2 eV) and distance in Bohr radii (from Bardsley and Junker, 1974).

trix element

$$\sigma \propto \left| \langle \varphi_i^e | \sum_s \vec{r}_s | \varphi_f^e \rangle \right|^2 |\langle \psi_i^n | \psi_f^n \rangle|^2, \quad (3.20)$$

where e, n denote electronic and nuclear wave functions in the initial (i) and final (f) states. The sum is over position vectors of the electrons. There then exist three possible dissociation mechanisms.

(i) The nuclear overlap can be appreciable for a continuum state ψ_f^n .

(ii) The electronic state φ_f^e can "cross" a third state for which mixing can occur. The molecule may then dissociate in the third state (predissociation).

(iii) The excited electronic state may decay radiatively to a lower state (e.g., ground) for which the nuclear overlap with a continuum state is appreciable.

The chief quantity of interest in astrophysics is the total photodissociation rate

$$\text{dissociation rate} = \int_0^{13.6 \text{ eV}} F(\nu) \sigma(\nu) d\nu,$$

where the cutoff at 13.6 eV in the interstellar radiation spectrum $F(\nu)$ is due to absorption by the abundant atomic hydrogen. Since $F(\nu)$ at 1000–2000 Å is comparable to that at ~3000 Å, photodissociating transitions in the former wavelength interval normally because of the large number of electronic states well above the dissociation energy and the tendency for far-ultraviolet transitions to be strong.

Photodissociation of type (iii) above is usually less important than (i) and (ii). However, for the most abundant molecule in the interstellar gas—molecular hydrogen—it is the only significant mechanism. As seen from the positions of the electronic energy curves (Fig. 20), a direct transition to a free state [type (i)] is not energetically possible for radiation below 13.6 eV. Predissociation also does not occur. The chief contribution to photodissociation of H_2 arises from excitations to the $^1\Sigma_u$ state (Lyman band) followed by a radiative decay into a free nuclear state of the $^1\Sigma_g$ ground state. After the suggestion by Solomon (see Field *et al.*, 1966), Stecher and Williams (1967) demonstrated quantitatively that this is the dominant dissociation mode. Precise calculations (Dalgarno and Stephens, 1970) show that 23% of the Lyman excitations lead to dissociation in a uniform radiation field and that the contribution of the Werner band ($^1\Pi_u \rightarrow ^1\Sigma_g$) is negligible. Dissociation is probable in the Lyman band only for final vibrational states ≥ 7 which correspond to wavelengths ≤ 1000 Å. Since the natural linebreadth of the Lyman band is due only to the radiative decay, the lines are unusually narrow in comparison with dissociating transitions for most molecules. Along with the large relative abundance of hydrogen, this causes the Lyman bands to become saturated even in interstellar clouds of modest thickness. The photodissociation rate for H_2 is then decreased by factors up to $\sim 10^4$ in the interstellar clouds that have been observed.

With the exception of H_2 and HD, photodissociation data are poor for molecules with which accurate comparisons between prediction and observation might be made (e.g., CO, CH, OH, NH, CN). Although dissociation

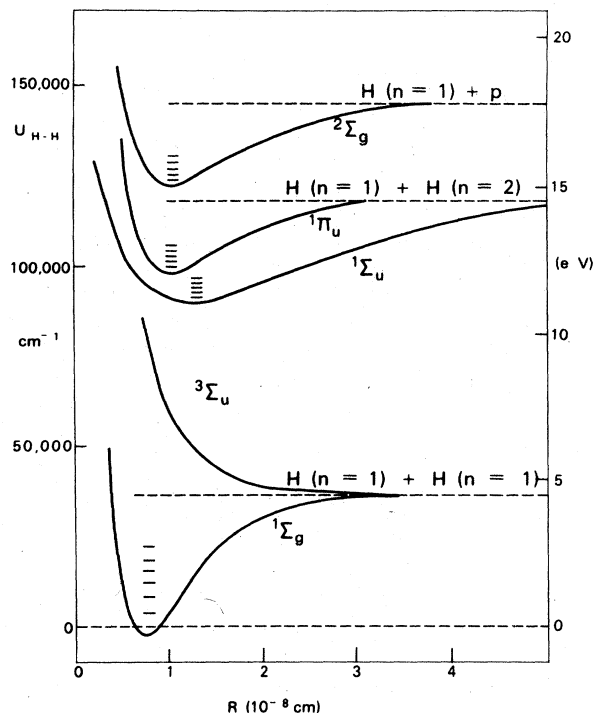


FIG. 20. Electronic energy for low lying states of molecular hydrogen vs internuclear separation.

through the $A^2\Sigma^+ - X^2\Pi$ transition at ~ 3100 Å in OH has been studied extensively in the laboratory, it probably is weaker than the OH transitions in the 1000–2000 Å region. In Table XVI we present representative data for photodissociation. For comparison, an oscillator strength of 0.5 at wavelengths near 1000 Å corresponds to a lifetime of about 10^9 s in the galactic radiation field. We emphasize that many of the rates in Table XVI are only estimates.

Photoionization can also lead to destruction of the molecules, but is typically less important than photo-

TABLE XVI. Representative lifetimes against photo-dissociation for molecules in the galactic radiation field of Habing (1968).

Molecule	Lifetime (sec)
H_2	2×10^{10} ^a
HD	2×10^{10} ^a
CH	1×10^{10} ^b
OH	$\leq 5 \times 10^9$ ^c
CO	10^{11} ^d
CN	10^{10} ^d
H_2CO	10^9 ^e
NH_3	10^9 ^e
H_2O	10^9 ^e
CH_3^+	$\geq 10^{11}$ ^f

^a Hollenbach *et al.* (1971).

^b Smith *et al.* (1973). The time for photoionization is $\approx 0.4 \times 10^{10}$ s for the cross section of Walker and Kelley (1972).

^c Smith and Zweibel (1976).

^d Estimate by Solomon and Klemperer (1972).

^e Steif *et al.* (1971).

^f Blint *et al.* (1976).

dissociation at photon energies below 13.6 eV (Stief *et al.*, 1972). Possible exceptions of astrophysical interest include CH and CH₂. For negative ions which are of potential interest in molecule formation, the photoionization rate is comparable with that for H⁻—about $2 \times 10^{-7} \text{s}^{-1}$.

Lifetimes presented in Table XVI are for unshielded galactic radiation. The extinction for ultraviolet radiation which causes the chief photodissociation is much greater than for visible radiation. However, the relative importance of scattering and absorption in this extinction is not well known. A reasonable estimate for the effective attenuation factor at a point within an interstellar cloud is $\exp(-2.5\tau_v)$, where τ_v is the visual, optical depth from the point to the nearest edge of the cloud (Watson and Salpeter, 1972b).

IV. COMPARISON OF PREDICTED AND OBSERVED MOLECULAR ABUNDANCES IN THE INTERSTELLAR GAS

This section is devoted to indicating the basic aspects of reaction sequences that presently seem to be of chief importance in the general interstellar gas. The two extreme astronomical conditions—diffuse and dense clouds—are considered separately. For molecular reactions, the chief differences result from the fact that galactic starlight easily penetrates diffuse clouds (optical extinction $A_v \lesssim 1$ mag.) to photodissociate molecules and, except for hydrogen, keep the atoms mainly in atomic form. In contrast the dense clouds are sufficiently thick ($A_v \gtrsim 7$) that photodissociation and photoionization by starlight incident on the outside of the cloud is slower than competing processes and can be ignored. There certainly exist intermediate astronomical conditions, though the basic features can be illustrated with less complication by considering the extremes. In practice, we cannot exclude the possibility that most dense clouds which actually occur in the galaxy do contain sufficient numbers of bright stars that photoprocesses influence the reaction sequences. We also do not consider catalysis on hot grains ($T_g \gtrsim 50^\circ \text{K}$) or reactions at elevated temperatures ($T_{\text{gas}} \gtrsim 100^\circ \text{K}$) which may be important in dense interstellar clouds. Indications that these are not, in general, dominant are mentioned in Secs. I.C and IV.B.

Molecular reactions have their greatest importance in dense clouds where they produce the large variety of complex molecules and possibly influence the thermodynamics of the gas relevant to star formation. However, most investigators agree that the diffuse clouds provide the best laboratories in which to test the basic ideas about interstellar reactions. As discussed in Sec. I and above, the physical conditions are quite poorly known in dense clouds. The distance is much greater and the observational angular resolution poorer than in diffuse clouds so that the observational measurements can include contributions from different physical conditions. Finally the possible reaction chains are more numerous and complex in dense clouds due to the slow dissociation rate which even allows the possibility for time-dependent effects. As a result of the rapid photodissociation rate in diffuse clouds, a local steady-state situation

certainly prevails. Abundances in diffuse clouds are measured by the absorption from the spectrum of a bright star. Thus there is no problem with angular resolution. The diffuse clouds that are observed are nearby so that only one or a few condensations of neutral gas occur along the path to the star. Though some uncertainty does exist at present, these can be reasonably well separated by radial velocity data. Information on atomic and molecular abundances, electron density, temperature, ionization rates, starlight intensity, etc., are far more detailed than for dense clouds, despite some disagreements in the precise interpretation. It is expected that a quantitative understanding of reactions in the diffuse clouds will provide a foundation from which studies of dense clouds can proceed. Of course, valuable information is also obtained directly from diffuse clouds—e.g., data on the low-energy cosmic ray/x-ray flux, on the role of surface reactions, on the relation between young stars and the gas, etc.

General information about the interstellar gas is discussed in Sec. I.A and data on molecular abundances is given in Sec. I.B.

A. Diffuse interstellar clouds

1. H₂ abundance

As discussed in Sec. III.C, radiative association of H atoms to produce H₂(H+H→H₂+hν) is strongly forbidden and is completely negligible even for astronomical time scales. Production of H₂ molecules on grains of surface area σ_g and density n_g is predicted to occur at a rate per H atom in the gas (Hollenbach *et al.*, 1971)

$$t_g^{-1} = (n_g \sigma_g v_H S/n) n/2 \equiv \alpha_g S n/2 \text{ s}^{-1}, \quad (4.1)$$

where $\alpha_g S/2 \approx 10^{-17} \text{ cm}^3 \text{ s}^{-1}$. Normally, the fastest gas phase process is (McDowell 1961; Dalgarno and McCray 1973),¹



The critical abundance of H⁻ is determined by

$$\text{H} + e \rightarrow \text{H}^- \quad \alpha(3) = 10^{-18} T(^{\circ}\text{K}) \text{ cm}^3 \text{ s}^{-1}, \quad (4.3)$$

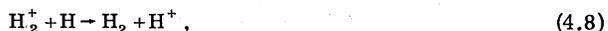
$$\text{H}^- + h\nu \rightarrow \text{H} + e \quad \Gamma_0(4) = 2 \times 10^{-7} \exp(-\tau_v) \text{ s}^{-1}, \quad (4.4)$$

$$\text{H}^- + \text{A}^+ \rightarrow \text{H} + \text{A} \quad \alpha(5) = 4 \times 10^{-6} T(^{\circ}\text{K})^{-1/2} \text{ cm}^3 \text{ s}^{-1}, \quad (4.5)$$

in addition to Eq. (4.2). For standard conditions in diffuse clouds, Eq. (4.5) is always somewhat slower than competing reactions and $\tau_v \lesssim \frac{1}{2}$. The H⁻ rate analogous to Eq. (4.1) can be compared with the expected rate on surfaces

$$\frac{t_g^{-1}}{t_H^{-1}} \approx \frac{n}{[e]} \frac{1 + 150/[H]}{\sqrt{T(^{\circ}\text{K})/100}}. \quad (4.6)$$

Present information on the number densities n , $[H]$, and $[e]$ yields $t_g^{-1}/t_H^{-1} \gtrsim 10^2$. Another possible sequence



¹Rate coefficients are designated $\alpha (= \langle \sigma v \rangle)$ and photoionization/dissociation rates Γ_0 computed in the Habing (1968) galactic radiation field are used throughout.

is unimportant at low temperatures ($T \lesssim 100^\circ\text{K}$) because of the small rate coefficient for Eq. (4.7). It is $\alpha \approx 10^{-18} \text{ cm}^3 \text{ s}^{-1}$ at $T = 500^\circ\text{K}$ and decreases rapidly at low temperatures. At elevated temperatures ($T \gtrsim 1000^\circ\text{K}$) it can compete with the H^- sequence.

Photodissociation of H_2 by the ultraviolet galactic radiation (912–1000 Å) is the dominant destruction mechanism in diffuse clouds. The rate is $\Gamma_0(\text{H}_2) \approx 5 \times 10^{-11} \text{ s}^{-1}$ for the average galactic radiation intensity in the solar neighborhood (Habing 1968) and is expected to vary little throughout the galaxy except near hot stars. There are suggestions that a spatial association exists between diffuse clouds and the bright O and B stars (Sec. I), so that $\Gamma_0(\text{H}_2)$ may be systematically enhanced by factors up to about 10. Shielding of one cloud by another may frequently reduce $\Gamma_0(\text{H}_2)$ by perhaps a factor of two or so. Large fractional abundances of H_2 are not solely a result of the efficient production process, but are due in a large part to the radiative two-step dissociation process that causes the narrow, natural breadth for the absorption lines. Doppler broadening determines the line cores. The radiative transfer of the dissociating radiation is usually simplified to radiation incident perpendicular to the planar interface between the cloud and intercloud medium. If the column density of H_2 molecules from the edge of the cloud to an interior point is N_2 , the dissociation rate at that point is

$$\begin{aligned} \Gamma(\text{H}_2) &= \Gamma_0(\text{H}_2) \sum \frac{mch_i k_i}{\pi e^2 f_i} \\ &\times \int \exp[-N_2 h_i \sigma_i(\nu) - \tau_g] \sigma_i(\nu) d\nu / \sum h_i k_i \\ &= \Gamma_0(\text{H}_2) \exp(-\tau_g) \sum h_i k_i J_i / \sum h_i k_i. \end{aligned} \quad (4.9)$$

The sum is over all lines i (associated with the final vibrational states) of the Lyman band, each of which has oscillator strength f_i , cross section $\sigma_i(\nu)$, probability for dissociation k_i and fractional population h_i in the initial state. Absorption at 1000 Å due to dust grains of optical depth τ_g is also included. Under the time-independent conditions that prevail, the local number density ratio is

$$\frac{[\text{H}_2]}{[\text{H}]} = \frac{\alpha_g S n}{2\Gamma(\text{H}_2)} \equiv \frac{Z(N_2)}{2}. \quad (4.10)$$

To compare with observation

$$\frac{dN_2}{dN} = \frac{1}{2} \frac{Z(N_2)}{1+Z(N_2)} \quad (4.11)$$

must be integrated through the cloud. Here N is the column density of total hydrogen ($\text{H} + 2\text{H}_2$) from the edge of the cloud. To the accuracy of the above treatment for the radiative transfer and to the extent that constant total density n is a good approximation, the ratio $n\alpha_g S / \Gamma_0(\text{H}_2)$ is determined by the observed N_2 and N for an interstellar cloud.

In Fig. 7, part of an absorption spectrum showing the H_2 lines from an interstellar cloud is presented. Some representative observational data in the directions of various stars is given in Table XVII. Molecular hydrogen fractional abundances tend to be either quite small ($\text{H}_2/\text{H} \lesssim 10^{-6}$) or large ($\text{H}_2/\text{H} \gtrsim 0.1$) due to influence of

TABLE XVII. Observed column densities and upper limits for molecular hydrogen [N_0 for $J=0$ state, N_1 for $J=1$ state], and for atomic hydrogen HI in interstellar gas clouds in the directions of various stars. $f = 2(N_0 + N_1) / [N(\text{HI}) + 2(N_0 + N_1)] =$ fractional abundance of molecular hydrogen. From Spitzer *et al.* (1973).

Star	$\log N_0$	$\log N_1$	$\log N(\text{HI})$	f
ζ Per	20.29	20.39	20.78	0.59
ξ Per	20.28	20.21	20.92	0.46
ϵ Per	19.59	19.56	20.56	0.30
δ Per	18.91	19.18	20.18	0.24
α Cam	19.81	19.94	20.72	0.37
ζ Ori	15.2	...	20.26	1.8×10^{-5}
ζ Oph	20.46	20.10	20.61	0.67
10 Lac	19.12	19.26	20.84	0.082
τ Sco	<12.54	...	20.58	$<1.8 \times 10^{-8}$
α Eri	<12.51	...	20.17	$<4.3 \times 10^{-8}$
σ Sgr	<12.63	...	20.58	$<2.3 \times 10^{-8}$

self-shielding on the dissociating radiation. From the observed N_2 and N , the formation rate is deduced by the methods described above and is presented in Table XVIII. Since the number densities are $n \approx 10^2 - 10^3 \text{ cm}^{-3}$, $\alpha_g S$ is in semiquantitative agreement with predictions. Limits for $\alpha_g S$ have also been obtained by Jura (1974) from data on the ISM where $N_2/N \ll 1$.

2. HD abundance

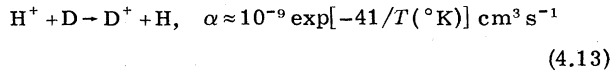
Observations by the *Copernicus* satellite in 1973 determined an abundance ratio $\text{HD}/\text{H}_2 \approx 10^{-6}$ as typical for diffuse clouds with appreciable H_2 . However, as a result of the severe self-shielding which occurs for H_2 but not for HD, the destruction rate is slower for H_2 by a factor of about 10^4 . The production rates t_{HD}^{-1} and $t_{\text{H}_2}^{-1}$ (s^{-1}) per D or H atom are then related to the number densities for the atoms [D] and [H],

$$[\text{D}] t_{\text{HD}}^{-1} / [\text{H}] t_{\text{H}_2}^{-1} \approx 10^{-2}. \quad (4.12)$$

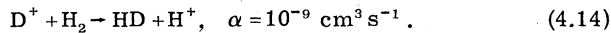
Subsequently, atomic deuterium has been measured in the interstellar gas to have an abundance $[\text{D}]/[\text{H}] \approx 10^{-5}$ so that $t_{\text{HD}}^{-1} \approx 10^3 t_{\text{H}_2}^{-1}$. If atomic H is converted to H_2 at about one-third of its collisions with grains as is predicted and is indicated by analysis of the observations (Table XVIII), then HD must be produced mainly by reactions in the gas. These are generally accepted to be (Watson 1973; Black and Dalgarno 1973)

TABLE XVIII. Formation rate $n\alpha_g S/2$ for molecular hydrogen on grain deduced for interstellar gas clouds in the directions of various stars. Constant gas density and $\Gamma_0(\text{H}_2) = 5 \times 10^{-11} \text{ s}^{-1}$ are assumed (O'Donnell and Watson, 1974). The analogous rate t_{H}^{-1} from Eq. (4.6) for formation by the H^- chain is also given for $n = 10^2 \text{ cm}^{-3}$, $T = 100^\circ\text{K}$, and electron density $= 5 \times 10^{-4} n + n(\text{H}^+)$ [obtained using methods of Sec. IV.A.2].

Star	$n\alpha_g S/2(10^{-11} \text{ s}^{-1})$	$t_{\text{H}}^{-1}(10^{-11} \text{ s}^{-1})$
10 Lac	75	0.5
λ Ori A	110	0.05
ξ Per	190	0.05
α Cam	230	0.05
ζ Oph	530	0.05



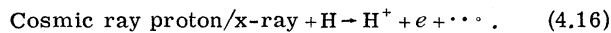
followed by



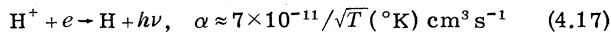
The rate coefficient for reaction (4.14) has been measured down to 90 °K as a result of its astrophysical importance. It has no energy barrier, unlike the analogous reaction between neutrals (Fig. 16),



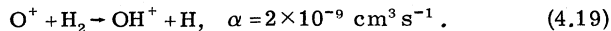
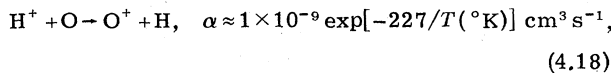
Since HD is produced directly by reaction of H^+ , the abundance of HD serves as an indicator for the H^+ abundance and thus for the intensity of unobserved, low-energy x rays or cosmic ray particles that are the chief cause for hydrogen ionization.



Ionization of H_2 leads mainly to H_2^+ , not H^+ . To deduce an ionization rate from the H^+ abundance, it is also necessary to consider the neutralization processes



and



Reaction (4.19) is followed by a number of possible reactions which usually have the net effect of neutralizing the ions without further ionizing hydrogen (see O'Donnell and Watson 1974). The rate coefficient α for Eq. (4.18) is uncertain under astrophysical conditions (see Sec. III.B), though the observed OH abundance can be interpreted to support the rate coefficient suggested above (see Sec. IV.A.3). Since this value is near the maximum reasonable cross section, an upper limit to the ionization rate of hydrogen $\xi(\text{H atom s})^{-1}$ can be obtained. These limits are shown in Fig. 21 as a function of gas density for diffuse interstellar clouds located in the directions of several stars. Actual gas densities are not known accurately, though probably $10^2 \lesssim n \text{ (cm}^{-3}) \lesssim 10^3$. The limits on ξ in Fig. 21 are well below that apparently required for heating and ionizing the general interstellar gas (Sec. I.A).

3. Diatomic hydrides (CH, CH^+ , OH, NH)

Representative abundances for these molecules observed in diffuse interstellar clouds are presented in Table II.

a. Surface processes

Consider first the abundance of the neutrals (CH, NH, OH) that can result from reactions on grain surfaces followed by efficient ejection back to the gas. It is unclear whether these will be ejected mainly as diatomics or in the chemically saturated form (CH_4 , NH_3 , H_2O). At lower densities ($n \lesssim 10^3 \text{ cm}^{-3}$, for the galactic average starlight intensity), this is relatively unimportant as photo-dissociation or photo-ionization followed by disso-

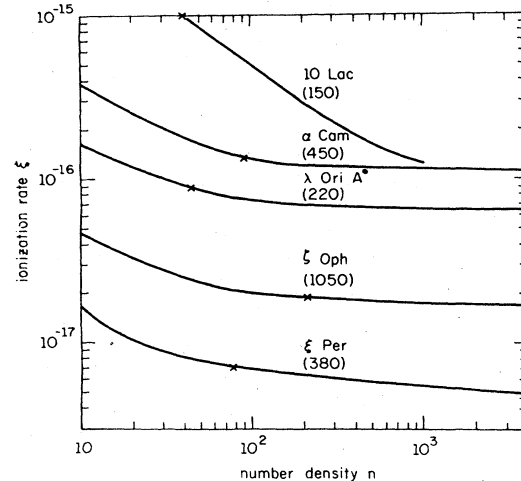
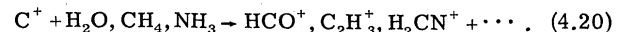
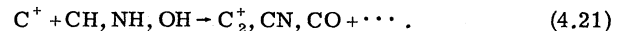


FIG. 21. Upper limits to the ionization rate $\xi(\text{H-atom s})^{-1}$ as a function of total number density n in interstellar gas clouds located toward the indicated stars. The value of $\alpha_g S n / \Gamma_0(\text{H}_2)$ derived for each cloud is given in parenthesis and an x marks the minimum likely value of n . In these calculations $\Gamma_0(\text{HD}) = \Gamma_0(\text{H}_2) = 10^{-10} \text{ s}^{-1}$.

ciative electron recombination are expected to convert the saturated forms to diatomics with good efficiency. At higher densities, reactions can dominate over radiative processes and reduce this efficiency, e.g.,



Similarly, destruction of the diatomics will be mainly by photo-dissociation at lower densities and by reactions at higher densities



Although the overall energetics are favorable, reaction of these hydrides with the abundant atomic H is thought to be excluded by activation energy barriers. For OH, a barrier is known to be present. By employing the rate at which heavy atoms stick to grains,

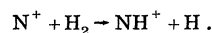
$$\frac{[\text{OH}][\Gamma_0(\text{OH}) + 10^{-9}[\text{C}^+]\sqrt{16}]}{[\text{O}]} \lesssim n\alpha_g, \quad (4.22)$$

for number densities n , a photodissociation rate $\Gamma_0(\text{OH})$ and α_g defined by Eq. (4.1). Similar relations hold for NH and CH, though the sticking of C^+ may be severely altered by positive grain charges. Thus the likely abundance ratios for these diatomic hydrides to hydrogen are about 10^{-8} under typical conditions in diffuse interstellar clouds. CH^+ will not, of course, be ejected directly from grain surfaces but may be produced by photo-ionization of the CH.

b. OH abundance due to gas phase reactions

After reaction (4.19) the OH^+ continues to react at every collision with H_2 until H_3O^+ , which does not react with H_2 , is produced. Conversion of H_3O^+ to OH is expected to be relatively efficient



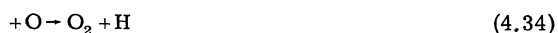


Reactions (b) and (c) will be followed by rapid reaction with H_2 until NH_3^+ is reached. NH_3^+ is likely to be converted into NH with good efficiency by dissociative electron recombination and possibly photodissociation. However, in diffuse interstellar clouds the H_3^+ abundance is not expected to be high enough to make (b) competitive. A large charge-transfer cross section, which seems unlikely, is needed in (c). For nitrogen the charge transfer analogous to (4.18) is endothermic. Finally, the rate coefficient for (a) has been found to be small.

If the observed OH is a result of surface reactions, according to Secs. II and IV.A.3a, NH should be produced at about the same rate per atom if grains have inert surfaces as expected. Then, NH will be present in diffuse clouds at a level which can be roughly predicted from the OH abundance and in Eq. (4.22) for NH as well as OH. Uncertainties do arise concerning photodissociation rates, especially in determining the expected abundance of NH if most nitrogen is ejected from grains as NH_3 . Such questions have been analyzed in detail by Crutcher and Watson (1976b). These authors conclude that the observed NH/OH upper limit (Table II) is inconsistent with the formation of NH at the same rate per particle as OH. It is thus considered to be evidence against formation of OH on grains. The conclusion does assume that atomic nitrogen is not depleted in the gas below the abundance given in Table I in relation to oxygen. There is reason to believe that no such depletion occurs.

4. Other diatomics (CO , CN , C_2 , N_2 , NO , O_2)

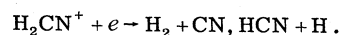
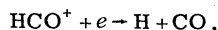
Although the dominant reactions producing the diatomic hydrides for the initial step in converting atoms to molecules might be either surface or gas phase, the diatomics with two "heavy" atoms are almost certainly produced mainly by gas phase reactions. Exchange collisions of a hydride with a heavy atom are energetically favorable, e.g.,



though probably,



The product molecule in (4.30)–(4.32) may also be ionized. It, however, will be neutralized by charge exchange with hydrogen or in a series of reactions with H_2 . At the higher densities ($n \geq 10^3 \text{ cm}^{-3}$), reaction of C^+ with NH_3 (or possibly NH_2) and H_2O produced in surface reactions or in ion-molecule reactions terminating as in Eq. (4.23) becomes competitive:



Certain of the products in the above are also susceptible to further exchange reactions:



Here CN is apparently protected by activation energy barriers from destruction through reaction with N and O. Photodissociation is then the chief destruction mechanism for CO, CH and N_2 , and at the lower densities for NO, C_2 , and O_2 . Unfortunately, the cross sections are poorly known so that a precise test of the proposed reactions is severely hindered. Estimated photodissociation rates are $\Gamma_0(\text{CO}) \approx \Gamma_0(\text{CN}) \approx 10^{-11} \text{ s}^{-1}$ in the galactic average radiation field (Sec. III.E). If these are employed, it is clear that the observed $[\text{CO}]/n \approx 10^{-7} - 10^{-8}$ and $[\text{CN}]/n \approx 10^{-8}$ [see Table II] can be produced at gas densities $n \approx 10^2 - 10^3 \text{ cm}^{-3}$ appropriate for diffuse interstellar clouds. Exchange reactions with the CH, CH^+ , and OH at their observed abundance is adequate.

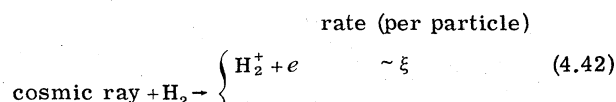
B. Dense interstellar clouds

Since these regions are assumed to exclude starlight, the gas is mostly neutral and in molecular form. The slow ionization due to high-energy ($\approx 100 \text{ MeV/nucleon}$) cosmic rays occurs at a rate $\xi \approx 10^{-17} - 10^{-18}$ ionizations (H_2 molecule sec^{-1}). The relative abundance of C, N, O, etc., elements is unknown by direct observation and particularly uncertain due to the possible influence of freezing onto grains. Total gas densities n are greater than 10^4 cm^{-3} . The role of grains is especially uncertain. Grains are negative and certainly neutralize positive ions that hit them. In view of the inability to make precise predictions from surface reactions (except H_2 production) and the uncertainty concerning the ejection mechanism (if one exists) for the reaction products in dense clouds, current models for dense clouds often simply ignore the grains altogether. Certain gas reactions are faster than the time for a particle to hit a grain so that ignoring effects of surface reactions can be justified. A possible way to avoid severe depletion of heavy elements from the gas by freezing is the rapid conversion of these elements to CO, O_2 , and N_2 . The vapor pressure of these is high enough that freezing onto the grains may not occur. Slow dissociation of the CO, O_2 and N_2 might then provide the constituents of less abundant molecules for time scales comparable with a lifetime for a dense interstellar cloud. Predicted molecular abundances from the pure gas phase models can be compared with observations as a test of the assumptions. The above viewpoint for reactions in dense interstellar clouds is the basis for the "ion-molecule" scheme (Herbst and Klemperer, 1973; Watson, 1973d, 1974a) presented in the following. Most atoms are tied up in unreactive molecular forms in dense clouds so that further reactions with neutrals are severely inhibited by activation energy barriers and the absence of exothermic reactions. In contrast, reaction with an

ion usually does not involve an activation energy and is more often exothermic. The strength of the ion-molecule scheme is based upon transferring most of the ionization of hydrogen and helium to less abundance species. In a manner similar to the ionization of D and O in diffuse clouds, these particles are then ionized at a much greater rate by this indirect process than from the direct ionization by cosmic rays. Steady-state abundances are assumed to prevail, though this is somewhat less well established than for diffuse clouds. Langer and Glassgold (1976) have questioned the use of steady-state abundances. Except in subsection 1. below, the discussion of reactions in dense clouds is limited here to delineating the major reactions. The uncertainties in physical conditions and the close coupling between most reaction chains makes detailed abundance predictions questionable at present. Extensive numerical calculations have been performed by Herbst and Klemperer (1973).

1. Ionization state

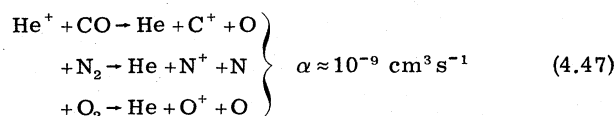
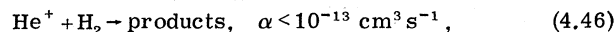
The initial step is



Equation (4.42) is followed immediately by



Rates for dissociative electron recombination of molecules are much larger than the radiative electron recombination rates for atoms. Hence H_3^+ is lost rapidly, and H^+ and He^+ that are produced at a slower rate than the H_2^+ can be the determining factors for initiating reactions and for the electron density. These may, however, be converted to molecular ions, e.g.,



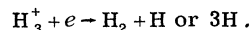
and



depending upon the exact abundances. The O^+ and N^+ produced will be converted to molecular ions immediately by reaction with H_2 . Neutralization by hitting negative grains also occurs, though at a somewhat slower rate. The abundance of free atoms with low ionization energy (e.g., Si, Ca, Na, Mg) might be sufficient in dense clouds that charge exchange between these and molecular ions will transfer appreciable ionization back to atoms (Oppenheimer and Dalgarno 1974). Neutrali-

zation through the slow radiative recombination will again be necessary and the predicted electron abundance will be raised.

For simplicity consider the minimum fractional ionization obtained by assuming that the rate limiting step in neutralization of the gas is the dissociative electron recombination of the dominant ion H^+ produced,



Then,

$$[e] \approx [\text{H}_3^+] \approx 6 \times 10^{-6} \sqrt{(\xi/10^{-17} \text{ s}^{-1})} [\text{H}_2] \text{ cm}^{-3}. \quad (4.50)$$

The fractional ionization can be increased by one to two orders of magnitude as a result of the effects mentioned above.

2. Abundances of certain small molecules

Except for HCO^+ and N_2H^+ in (a) below, the generation of interstellar molecules depends more on the ionization of helium than on the ionization of hydrogen. Because neutralization of He^+ is slow due to the small rate coefficient for Eq. (4.46), most initial ionizations of helium are employed in the breaking up and ionizing unreactive molecules such as CO, N_2 , and O_2 [Eq. (4.47)]. The products then enter into reactions to produce molecules.

a. HCO^+ , N_2H^+

In practice, the proton transfer



can compete with electron recombination in the destruction of H_3^+ . A large fraction of all cosmic ray ionizations [Eq. (4.42)] then lead to HCO^+ . No other molecule is sufficiently abundant (except possibly H_2O which is unobservable) to compete with the electron recombination. Hence the abundance of HCO^+ is given approximately by Eq. (4.50). The presence of HCO^+ in dense clouds was thus recognized as the basic test for the influence of reactions involving ions (Herbst and Klemperer 1973; Watson 1974a). At the time of these investigations, one of the strongest radio lines from dense clouds was an unidentified emission at 89,189 MHz (Buhl and Snyder 1970). Without consideration of its significance in the above reactions, Klemperer (1970) had suggested HCO^+ as the source of this unidentified feature based on its approximate moment of inertia. Before progress was made in the identification of HCO^+ , a group of microwave emission lines from dense clouds was detected and identified as due to N_2H^+ (Green *et al.* 1974). Due to the lack of observational information on N_2 in dense clouds, N_2H^+ had not previously been emphasized as a basic indicator for "ion-molecule" reactions. Clearly, if the abundance of N_2 is comparable with that of CO, N_2H^+ has a parallel position to HCO^+ since the relevant reaction cross sections for proton transfer from H_3^+ are similar. Subsequently, a radio line was detected at the estimated frequency for the isotope substituted form H^{13}CO^+ (Snyder *et al.*, 1976). Finally, the H^{12}CO^+ ($J=1 \rightarrow 0$) frequency was measured in the

laboratory (Woods *et al.*, 1975) and found to be in excellent agreement with the best astronomical frequency 89,188.55 MHz for the proposed H^{12}CO^+ line (Snyder and Hollis, 1976).

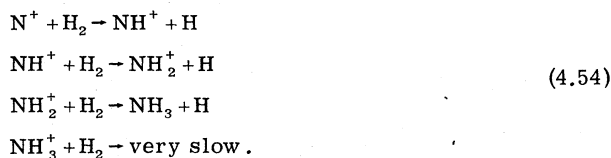
A difference between HCO^+ and N_2H^+ is that the reactions



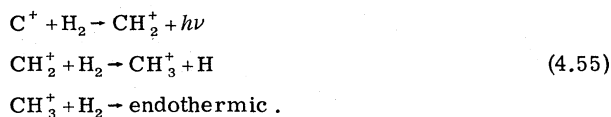
provides a destruction mode that is unavailable to HCO^+ . As the total gas density n of a dense interstellar cloud is increased, the CO abundance probably increases almost linearly whereas the electron density probably increases more slowly— as \sqrt{n} according to Eq. (4.50). Thus at higher gas densities Eq. (4.53) can dominate the destruction of N_2H^+ and reduce its abundance in relation to that of HCO^+ . This effect is apparently present in the observations. Reaction with certain other molecules such as CO_2 whose abundance is unknown is also possible for N_2H^+ , but not for HCO^+ .

b. CH_4 , NH_3 , H_2O

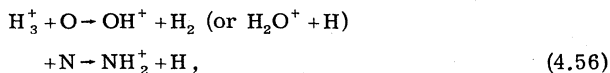
Of these, H_2O is produced in a straightforward manner as in Eq. (4.23) from the O^+ generated in Eqs. (4.47) if O_2 is abundant. Equations (4.47) also produce N^+ and C^+ . For NH_3 the reactions with H_2 apparently terminate at NH_3^+



The last reaction is quite slow ($\alpha = 5 \times 10^{-13} \text{ cm}^3 \text{ s}^{-1}$) at 300 °K and exhibits a strong temperature dependence that suggests it is unimportant under astrophysical conditions (Fehsenfeld *et al.*, 1975). Similarly,



Thus the sequences terminate before a molecular ion is reached that can dissociatively recombine with an electron to produce NH_3 and CH_4 . This is currently a problem in understanding the NH_3 abundance. One possibility is neutralization of the NH_3^+ by charge transfer to atoms with low ionization potential (Si, Ca, Mg, Na, etc.; see Sec. IV.B.1). The initiating reactions in the H_2O and NH_3 chains can also be



if atom O and N is in sufficient abundance.

c. CCH

CCH, which has now been widely observed, is almost as basic to "ion-molecule" schemes as HCO^+ and N_2H^+ . It was identified without laboratory measurements for the line frequencies by considering the relative spacings and strengths of the lines in the multiplet (Tucker, Kutner and Thaddens, 1974). CCH is expected to be a natu-

ral product of the presence of C^+ and any of the CH, CH_2 , CH_3 , CH_4 group. One such reaction chain is



Quantitative predictions for the abundance of CCH are in agreement with the subsequent observation.

d. HCN, HNC

With the presence of an appreciable abundance of NH_3 established by observation and C^+ as a direct product from Eqs. (4.47), the reactions that are expected to dominate are



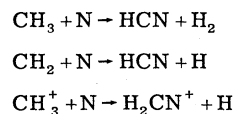
Reaction with C^+ also destroys HCN



Then in the time-independent situation that is assumed to prevail, a constraint exists on the abundances

$$\begin{aligned} n(\text{HCN})/n(\text{NH}_3) &< \alpha(4.58)/\alpha(4.60) \\ &\approx 0.6. \end{aligned} \quad (4.61)$$

Rate coefficients α for the designated reactions are due to Anicich and Huntress (1976). Whether Eq. (4.61) is satisfied seems unclear at present from the observations. Other processes that might produce HCN are

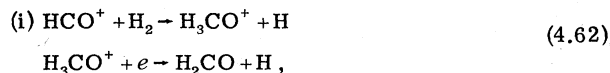


followed by Eq. (4.59). The presence of the isomer HNC in an abundance comparable with that of HCN seems to support the presence of reaction (4.59) in the formation of HCN and HNC. Since the structure is HCNH^+ , it is expected to dissociate frequently to HNC in reaction (4.59). HNC is rearranged easily by collision to HCN as evidenced by the difficulty with which it is prepared in the laboratory. Its occurrence is thus a strong indication that nonthermal reactions at low gas density and temperature dominate the interstellar molecule reactions. This excludes reactions in circumstellar shells of gas and in shock waves through the gas, as well as surface reactions in which the products are thermalized at the grain temperature. Until the laboratory measurement of Saykally *et al.* (1976), the interstellar HNC emission was another strong, unidentified line. Additional astronomical evidence obtained prior to the laboratory data had strengthened the identification HNC (Snyder and Hollis, 1976).

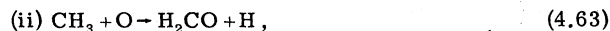
e. H_2CO

Formaldehyde is widely observed throughout the galaxy at radio wavelengths. It occurs in both high and relatively low density interstellar clouds. Thus the re-

actions that produce formaldehyde must be operative under a range of physical conditions. Also, formaldehyde is perhaps the most complex interstellar molecule for which specific gas phase reaction sequences have been proposed. It thus becomes a test case for whether the more complex molecules are likely to be generated in gas phase reactions or whether reactions on surfaces are necessary. The basic reactions of the chief gas-phase possibilities are the following



(Herbst and Klemperer, 1973),



or



(Dalgarno *et al.*, 1973). Indirect laboratory studies of Eqs. (4.62) are not encouraging (Fehsenfeld *et al.*, 1974). For Eqs. (4.63) and (4.64) a serious problem is the neutralization of the molecular ion without its destruction. In Eq. (4.63), CH_3^+ must apparently be neutralized to obtain the necessary CH_3 since CH_3^+ does not react with H_2 . The rate coefficient for reaction of H_2CO^+ with H_2 is slow and probably negligible (Huntress and Anicich, 1976). One possibility for neutralization of CH_3^+ and H_2CO^+ is charge-transfer with atoms such as Si, Mg, Na, etc. (Dalgarno *et al.*, 1973). If CH_3^+ is an intermediate in the formation of formaldehyde as postulated in (ii) and (iii) above, the reaction of Eq. (4.69) must enhance the abundance ratio $[\text{HDCO}]/[\text{HCO}]$ substantially over the total D/H ratio. Observations seem to be inconsistent with the required enhancement (Watson *et al.*, 1975). Recent laboratory measurements also find that the product in reaction (4.64) is HCO^+ in more than ninety percent of the reactions (Fehsenfeld, 1976).

C. Fractionation of isotopes (dense clouds)

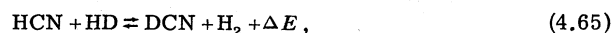
As discussed in Sec. I.B, radio observation of less abundant isotopes in interstellar molecules provides the only means for studying the abundance of these isotopes in the ISM throughout the galaxy. Isotope ratios yield information on nuclear processes in the astrophysical environment. The basic uncertainty is to what extent the ratios of isotopes in molecules can be relied upon to give information about the actual ratio in the ISM. In the case of deuterium, the DCN/HCN ratio detected in six locations is roughly a factor of 200 greater than the D/H ratio in the neighborhood of the sun, whereas the $\text{DCO}^+/\text{HCO}^+$ ratio seems to reflect a 10^4 to 10^5 enhancement. Although the actual D/H ratio is unknown in these regions, the possibility that the deuterium abundance is larger by these factors is not considered seriously. A fractionation process that favors deuterium in HCN and HCO^+ is indicated. In view of the extreme fractionation of the hydrogen isotopes, the "factor of 2" deviations from the solar system value $\text{C}^{13}/\text{C}^{12} = 1/90$ that have now been established for interstellar molecule ratios in certain locations must be examined carefully for fractionation effects. Although fractionation in favor of deu-

terium is widely accepted, until recently the possible enhancement of other less abundant isotopes has received little attention. While the alteration of molecular properties associated with exchanging carbon isotopes is much smaller than that for hydrogen isotopes, the magnitude ($\approx 25\%$) of the fractionation which will influence the interpretation of observations is also much smaller. The observations and the discussion here concerning isotope fractionation are limited to dense cloud conditions. In diffuse clouds only the enhancement of the $^{13}\text{CO}/^{12}\text{CO}$ ratio is likely to be of practical interest (Watson, Anicich and Huntress 1976). Observations are not yet sufficiently sensitive to detect this effect.

1. Hydrogen/deuterium

Observational data for deuterium in interstellar molecules are summarized in Sec. I.B.3. The most direct cause for fractionation is the difference in binding energies of molecules related by isotope substitution. At ISM temperatures this energy is comparable with or greater than the gas kinetic energy. Then if isotope exchange reactions occur which approach thermodynamic equilibrium, an isotope selection is introduced. Normally, interstellar molecule abundances are far from thermodynamic equilibrium. It is thus not at all evident that the small differences in binding energy can be important. A detailed examination does, however, indicate that certain isotope exchanges are likely to approach equilibrium. Although we limit the following discussion to these isotope-selection processes, nonthermal selection effects might also be important especially for deuterium (Watson, 1973b).

Solomon and Woolf (1973) suggested that the reaction



or



in the gas or on grain surfaces might produce the enhancement of DCN. These choices appear less likely to approach equilibrium at ISM temperatures due to likely activation energy barriers and to the low abundance of atomic deuterium expected in dense clouds. Ion-molecule reactions which do not have the activation energy barriers are more plausible candidates (Watson, 1974; Watson, Crutcher and Dickel, 1975). The first such reaction to consider is (see also Dalgarno, Black and Weisheit, 1973)



However, the low abundance of D^+ as a result of its rapid loss through reaction with H_2 [Eq. (4.14)] probably cause this exchange to be unimportant. Essentially all deuterium is thought to exist as HD in dense interstellar clouds so that reactions of the form



where X is any molecular structure are likely candidates. In this case the neutral molecule which is observed would be produced through a subsequent electron recombination or charge exchange. These neutralizations occur far from equilibrium conditions and should

normally exhibit little or no isotope selection. Intermediate reactions that alter XD^+ may occur between reaction (4.67) and the neutralization. Then the molecular structure involved in the isotope exchange and that which is observed are only indirectly related. For polyatomics XH^+ , reaction (4.67) is exothermic by a few hundredths eV or so for all cases that have been examined. Since H_3^+ initiates a major chain of reactions and is a source for hydrogen atoms to a number of molecules (see especially Sec. IV.B.1 and IV.B.2), the reaction



can influence the deuterium in many molecules. Its rate coefficient has been measured to be $\alpha = 3 \times 10^{-10} \text{ cm}^3 \text{ s}^{-1}$ at 300 °K (Anicich and Huntress, 1976). However, the energy difference $\Delta E/k \approx 178 \text{ }^\circ\text{K}$ for reaction in the lowest states is marginal at the indicated gas temperatures to produce the large observed enhancements. This ΔE is obtained from the H_3^+ vibrational frequencies of Borkman (1970) which are supported by experiment (Petty and Moran 1970). Standard relations given by Herzberg (1945) are employed to relate the frequencies of H_2D^+ to those of H_3^+ . A measurement of the zero-point energy for H_2D^+ will be valuable.

Other reactions of the form in Eq. (4.67) have been examined at 300 °K for $\text{X} = \text{H}_2\text{O}$, HCN , NH_3 , CO , and CH_2 (Anicich and Huntress, 1976; also Harrison and Keyes, 1973; Kim, Theard and Huntress, 1974). Only the reaction



for which $\alpha = 5 \times 10^{-10} \text{ cm}^3 \text{ s}^{-1}$ has a large rate coefficient ($\geq 10^{-10} \text{ cm}^3 \text{ s}^{-1}$). Calculations yield $\Delta E/k \sim 300 \text{ }^\circ\text{K}$ for Eq. (4.69) (Blint, Marshall and Watson, 1976), though this might be an underestimate. Reaction (4.69) will then influence the observed abundances through, for example



followed by reaction (4.76). Another possibility is



after which



The natural reaction to cause the enhancement of deuterium in DCO^+ is

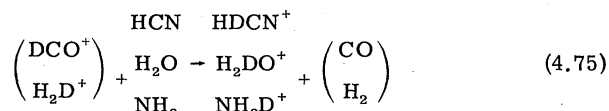


for which $\Delta E/k$ should be approximately the same as for the exchange with isoelectronic HCN ($\approx 460 \text{ }^\circ\text{K}$). Measurements for the analogous reaction with D_2 , which should normally be accurate for HD , yield a small rate coefficient ($2 \times 10^{-11} \text{ cm}^3 \text{ s}^{-1}$, Huntress and Anicich, 1976). There also exists the possibility for which there is some evidence (Herbst *et al.*, 1976) that the isomer COH^+ is produced in large abundance from $\text{H}_3^+ + \text{CO}$ or other reactions in the ISM. Then the exchange analogous to Eq. (4.73) for COH^+ might be rapid. The COH^+ presumably is rearranged into the observed HCO^+ in collisions with CO . It is also possible that the abundant CH_2D^+ produced in Eq. (4.69) leads to the DCO^+ through

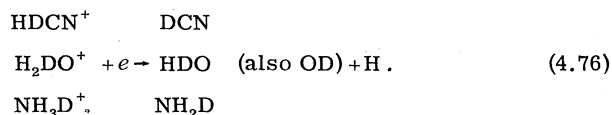


However, the most likely cause for the enhancement of DCO^+ is probably reaction (4.77) below.

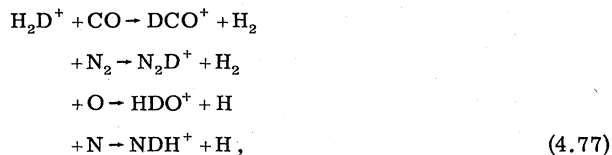
The observed abundance of DCO^+ and the probable high abundance of H_2D^+ influences other molecules through reactions such as



followed by



In addition, H_2D^+ can participate in other reactions



etc.

Knowledge of the physical conditions in dense interstellar clouds is not yet sufficient to determine which of the above possibilities is primarily responsible for enhancement of deuterium in particular molecules. To illustrate how the fractionation depends upon parameters, consider a simplified case. A molecular species ultimately is produced from a molecular ion that exchanges with HD as in reaction (4.67) with a rate coefficient α_x . The molecular ion can be destroyed in dissociative electron recombination (rate coefficient α_e) and in reactions with particular neutral particles M (rate coefficient α_M). If g is a statistical factor of order unity that represents the probability for a deuteron in the molecular ion to reach the molecular species of interest, then the ratio of deuterium to hydrogen in the resulting molecule is

$$\left(\frac{\text{D}}{\text{H}}\right)_{\text{mol}} \approx \frac{g\alpha_x[\text{HD}]}{\alpha_x[\text{H}_2]h + \alpha_e[e] + \alpha_M[M]}. \quad (4.78)$$

Here $h = \exp(-\Delta E/kT)$ for an energy ΔE arising in the exchange reaction analogous to reaction (4.67). It is evident that a strong temperature dependence in $(\text{D}/\text{H})_{\text{mol}}$ is a possible, though not a necessary consequence if reactions similar to Eq. (4.67) lead to the observed fractionation in favor of deuterium. For $\Delta E/k \approx 400 \text{ }^\circ\text{K}$, $\alpha_x = 5 \times 10^{-10} \text{ cm}^3 \text{ s}^{-1}$, $\alpha_e = 10^{-6} \text{ cm}^3 \text{ s}^{-1}$, and $g = 1$, the above expression for $(\text{D}/\text{H})_{\text{mol}}$ predicts an enhancement factor of about 200 above the actual (D/H) ratio in the ISM. This factor is essentially constant at $T \lesssim 60 \text{ }^\circ\text{K}$ when $[e]/[\text{H}_2] \approx 10^6$ —a reasonable electron density in dense clouds. Similarly, the degree of enhancement may be not the same for all molecules since a single reaction (4.67) probably is not responsible for all molecules. Even the observed temperature dependence of the fractionation may not be the same. For example, if reaction (4.70) produces DCN and (4.77) generates the DCO^+ , α_e for CH_2D^+ is probably a factor of 10 or so greater than for H_2D^+ , and ΔE for the two is quite different. Temperature variations within interstellar clouds and the possibility that more than one reaction

chain contributes significantly to the abundance of a particular molecule provide further complications for interpretation of the observational data in terms of particular fractionation processes. The relative constancy of DCN/HCN in a number of dense clouds (Penzias *et al.*, 1976) is quite consistent, and the increase in DCO⁺/HCO⁺ that is indicated for decreasing gas temperature (Hollis *et al.*, 1976) is strong support for the type fractionation process described above.

2. Carbon isotopes

The reaction



where $\Delta E/k = 35^\circ\text{K}$ has been measured at 300°K to have a rate coefficient $\alpha = 2 \times 10^{-10} \text{ cm}^3 \text{ s}^{-1}$ (Watson, Anicich and Huntress, 1976). Since the reaction rate (two times exchange) is large (about one-third of the total collision rate), the rate coefficient is probably of the usual temperature independent form that is characteristic of ion-molecule reactions. Then Eq. (4.79) will approach thermodynamic equilibrium if other molecules with which C⁺ can react rapidly are less abundant than CO by a factor of about 10. All molecules that have been observed satisfy this requirement. However, certain potentially abundant molecules are effectively unobservable at present, e.g., O₂, H₂O, CO₂, and CH₄. Since carbon that is incorporated into most molecules other than CO will probably have existed more recently as C⁺ than as CO (see Secs. IV.A.3, .4 and IV.B), the carbon isotope ratio in these molecules will reflect that of C⁺. If the exchange of carbon isotopes between CO and other molecules is fast in comparison with changes in the physical conditions and only reaction (4.79) is effective in exchanging carbon isotopes, an equation exactly analogous to Eq. (4.78) relates the ¹³C/¹²C ratio in most molecules other than CO to the ¹³CO/¹²CO ratio. This predicts that the ratio in CO should be increased over the actual ISM value, whereas in other molecules ¹³C/¹²C should be below the ISM value. However, observationally the ¹³C/¹²C ratio seems to be increased from the solar system value in most molecules in most locations.

This general increase might be due to the following. There is evidence of various types that an appreciable fraction of the atoms and molecules other than hydrogen and helium freeze out of the gas onto dust grains (Secs. I.A and II) in interstellar clouds. Of the carbon-bearing molecules, CO has the highest vapor pressure with a critical temperature $\approx 14^\circ\text{K}$ for vaporization in interstellar clouds. Since grain temperatures are no lower than $10\text{--}20^\circ\text{K}$, the carbon which freezes onto grains is likely to do so in molecular species other than CO. These molecules are deficient in carbon-13 according to the above discussion. Thus carbon-12 is preferentially lost from the gas, and the carbon which remains in the gas is enriched in carbon-13 above the actual ISM value. The exact increase depends upon additional considerations, though depletion of carbon by a factor of 3 to 10 which is consistent with data on depletion can easily give a factor of 2 or so increase in the ¹³C/¹²C ratio in all molecules in the gas (see Watson *et al.*, 1976). For reasons similar to those in D/H fractionation as well as other factors, an observable temperature de-

pendence is not a necessary consequence of this ¹³C/¹²C fractionation process. The temperature dependence in the DCO⁺/HCO⁺ observations lends qualitative support to the idea for the analogous effect among carbon isotopes. Isotope studies of HC₃N do, of course, indicate a fractionation process (Sec. I.C).

V. SUMMARY

Although the abundances of molecules in the ISM are far from thermodynamic equilibrium, a steady-state situation is likely to be a good approximation, at least for the abundant molecules. Starlight and cosmic rays prevent equilibrium abundances from being attained at the kinetic temperature of the gas.

By coincidence, the rate at which atoms stick to dust grains typically is comparable to rates of molecule formation by various gas phase reactions. Uncertainties concerning the surface processes—especially the ejection to return the molecule to the gas—make it unclear whether dust grains are, in fact, of major importance for reactions other than H+H in the ISM. For formation of H₂, theoretical investigations that predict almost every H atom that hits a grain will be converted to a molecule are compelling. The required rate of formation deduced from observation agrees well with the prediction. Possible gas phase processes are orders-of-magnitude slower. For formation of other “small” molecules, however, studies in the past few years have found that reactions between positive ions and molecules are comparable or faster than the possible rate due to surface processes on grains. To be effective at the low kinetic temperatures of the ISM, reactions must be exothermic and have no activation energy barrier. In contrast with neutral-neutral reactions, those between positive ions and molecules almost always satisfy the latter, and more frequently satisfy the former requirements.

To discuss molecule reactions in the ISM, it is convenient to consider limiting conditions in the gas, designated as “diffuse” and “dense” clouds. Except for hydrogen, the gas in the diffuse type is mainly atomic since these are transparent to the starlight which dissociates molecules. Dense clouds are opaque and are thus mainly molecular. Due to our better knowledge of the physical conditions in the diffuse clouds, observational tests of theories for molecule reactions are most precise in these regions. In addition to confirmations of the predicted formation rate for H₂, the rate for formation of HD is found to be much greater ($\times 10^3$) than the rate of sticking to grains. It can only be understood in terms of gas phase, ion-molecule reactions. There are indications from the abundances of NH and OH that gas phase reactions are dominant in the diffuse clouds. In dense clouds, the presence of certain molecules that are especially indicative of proposed ion-molecule reaction schemes—HCO⁺, N₂H⁺, CCH, HNC—is strong evidence in their favor. In addition to these molecules, the isotope fractionation that enhances deuterium in molecules is a further indication that the molecule formation process does occur under the low temperature/density conditions where the molecules are observed. High-energy cosmic rays are assumed to produce the ionization required to initiate the reactions.

Understanding the formation processes for the com-

plex molecules is the chief problem at present. Formaldehyde (H_2CO) is perhaps the most complex species for which specific processes have been proposed. No proposals seem to be in agreement with the observational constraints. Other current questions include the possible fractionation of carbon isotopes in molecules and understanding how CH^+ can be abundant and ubiquitous in diffuse clouds.

Laboratory investigations to determine microwave frequencies for molecules and to measure ion-molecule reaction cross sections have been especially valuable to the progress in understanding reactions in the ISM. Further studies in these areas, as well as for photodissociation cross sections, oscillator strengths at ultraviolet wavelengths and surfaces relevant to astrophysical conditions are needed.

ACKNOWLEDGMENTS

I am grateful to R. Crutcher, E. Herbst, E. Salpeter and L. Snyder for helpful discussions during the preparation of this manuscript.

REFERENCES

- Aannestad, P., 1973a, *Astrophys. J. Suppl. Ser.* **25**, 205.
 Aannestad, P., 1973b, in *I. A. U. Symposium No. 52 "Interstellar Dust and Related Topics,"* edited by J. M. Greenberg and H. C. van de Hulst (D. Reidel, Dordrecht).
 Aannestad, P., and E. M. Purcell, 1973, *Annu. Rev. Astron. Astrophys.* **11**, 309.
 Allen, C. W., 1973, *Astrophysical Quantities* (Athlone Press, London), 3rd ed.
 Allen, M., D. Cesarsky, and R. Crutcher, 1974, *Astrophys. J.* **188**, 33.
 Allen, M., and G. W. Robinson, 1975, *Astrophys. J.* **195**, 81.
 Anders, E., R. Hayatsu, and M. H. Studier, 1974, *Astrophys. J. Lett.* **192**, L101.
 Anicich, V. G., and W. T. Huntress, 1976, "Laboratory Studies of Ion-Neutral Reactions in Interstellar Regions: Gas Phase Equilibrium between HCN and NH_3 in Dense Clouds," *Astrophys. J.*, in press.
 Augustin, S. D., and W. H. Miller, 1974, *J. Chem. Phys.* **61**, 3155.
 Balian, R., P. Encrenaz, and J. Lequeux, editors, 1975, *The Proceedings of the Les Houches Summer School of Theoretical Physics XXVI, "Atomic and Molecular Physics and the Interstellar Matter"* (North-Holland, Amsterdam).
 Bardsley, J. N., and B. R. Junker, 1973, *Astrophys. J. Lett.* **183**, L135.
 Bardsley, J. N., and M. A. Biondi, 1970, *Adv. At. Mol. Phys.* **6**, 1.
 Bar-Nun, A., 1975, *Astrophys. J.* **197**, 341.
 Bartolot, V. J., and P. Thaddeus, 1969, *Astrophys. J. Lett.* **155**, L17.
 Bates, D., 1951, *Mon. Not. R. Astron. Soc.* **111**, 303.
 Bates, D., and A. Dalgarno, 1962, in *Atomic and Molecular Processes*, edited by D. Bates (Academic, New York).
 Bates, D., and L. Spitzer, 1951, *Astrophys. J.* **113**, 441.
 Bertojo, M., M. F. Chui, and C. H. Townes, 1974, *Science* **184**, 619.
 Black, J. H., and A. Dalgarno, 1973, *Astrophys. J. Lett.* **184**, L101.
 Black, J. H., A. Dalgarno, and M. Oppenheimer, 1975, *Astrophys. J.* **199**, 633.
 Bless, R. C., and B. D. Savage, 1972, *Astrophys. J.* **171**, 293.
 Blint, R. J., R. F. Marshall, and W. D. Watson, 1976, *Astrophys. J.* **206**, 627.
 Borkman, R. F., 1970, *J. Chem. Phys.* **53**, 3153.
 Brecher, A., and G. Arrhenius, 1971, *Nature Phys. Sci.* **230**, 107.
 Bretz, M., and J. G. Dash, 1971, *Phys. Rev. Lett.* **26**, 963.
 Buhl, D., and L. E. Snyder, 1970, *Nature (Lond.)* **228**, 267.
 Cheung, A. C., D. M. Rank, C. H. Townes, D. D. Thornton, and W. J. Welch, 1968, *Phys. Rev. Lett.* **21**, 1701.
 Cheung, A. C., D. M. Rank, C. H. Townes, D. D. Thornton, and W. J. Welch, 1969, *Nature (Lond.)* **221**, 626.
 Churchwell, E., W. Walmsley, and G. Winnewisser, 1976, Paper presented at the meeting of the Deutsche Astronomische Gesellschaft, 10-12 March.
 Crutcher, R. M., and W. D. Watson, 1975a, *Astrophys. J. Lett.* **203**, L123.
 Crutcher, R. M., and W. D. Watson, 1976b, "Upper Limit and Significance of the NH Molecule in Diffuse Interstellar Clouds," *Astrophys. J.*, in press (Nov., 1976).
 Dalgarno, A., and J. H. Black, 1976, "Molecule Formation in the Interstellar Gas," *Rep. Prog. Phys.*, in press.
 Dalgarno, A., J. H. Black, and J. Weisheit, 1973, *Astrophys. Lett.* **14**, 77.
 Dalgarno, A., M. Oppenheimer, and J. Black, 1973, *Nature Phys. Sci.* **245**, 100.
 Dalgarno, A., and R. McCray, 1972, *Annu. Rev. Astron. Ap.* **10**, 375.
 Dalgarno, A., and R. McCray, 1973, *Astrophys. J.* **181**, 95.
 Dalgarno, A., and T. L. Stephens, 1970, *Astrophys. J. Lett.* **160**, L107.
 Dash, J. G., 1968, *J. Chem. Phys.* **48**, 2820.
 Day, K. L., 1973, in *I. A. U. Symposium No. 52 "Interstellar Dust and Related Topics,"* edited by J. M. Greenberg and H. C. van de Hulst (D. Reidel, Dordrecht).
 Dickel, J., and R. Radick, 1976, unpublished result.
 Dormant, L. M., and A. N. Adamson, 1968, *J. Colloid. Interface Sci.* **28**, 459.
 Duley, W. W., 1973, *Astrophys. Space Sci.* **23**, 43.
 Evans, N., 1975, *Astrophys. J.* **201**, 112.
 Fehsenfeld, F. C., 1976, "Ion Reactions with Atomic Oxygen," *Astrophys. J.*, in press.
 Fehsenfeld, F. C., D. B. Dunkin, and E. E. Ferguson, 1974, *Astrophys. J.* **188**, 43.
 Fehsenfeld, F. C., D. B. Dunkin, E. E. Ferguson, and D. L. Albritton, 1973, *Astrophys. J. Lett.* **183**, L25.
 Fehsenfeld, F. C., W. Lindinger, A. L. Schmeltekopf, D. L. Albritton, and E. E. Ferguson, 1975, *J. Chem. Phys.* **62**, 2001.
 Field, G. B., 1969, *Mon. Not. R. Astron. Soc.* **144**, 411.
 Field, G. B., 1975, in *The Proceedings of the Les Houches Summer School of Theoretical Physics XXVI, "Atomic and Molecular Physics and the Interstellar Matter,"* edited by R. Balian, P. Encrenaz, and J. Lequeux (North-Holland, Amsterdam).
 Field, G. B., W. B. Sommerville, and K. Dressler, 1966, *Annu. Rev. Astron. Astrophys.* **4**, 207.
 Folman, M., and R. Klein, 1968, *Surf. Sci.* **11**, 430.
 Fujihira, M., T. Hirooka, and H. Inokuchi, 1973, *Chem. Phys. Lett.* **19**, 584.
 Garrison, B. J., W. A. Lester, W. H. Miller, and S. Green, 1975, *Astrophys. J. Lett.* **200**, L175.
 Giusti-Suzor, A., E. Roueff, and H. van Regemorter, 1976, *J. Phys.* **B 9**, 1021.
 Goldreich, P., and N. Scoville, 1976, *Astrophys. J.* **205**, 144.
 Gomer, R., 1959, *Discuss Faraday Soc.* **28**, 23.
 Gomer, R., R. Wortman, and R. Lundy, 1957, *J. Chem. Phys.* **26**, 1147.
 Goodman, F. O., 1966, *Proc. Intern. Symp. Rarefied Gas Dynamics*, 4th Suppl. **2**, 383.
 Gordon, M. A., and W. B. Burton, 1976, "Carbon Monoxide in the Galaxy. I. The Radial Distribution of CO, H_2 and Nucleons," *Astrophys. J.*, in press (Sept., 1976).
 Green, S., J. A. Montgomery, and P. Thaddeus, 1974, *Astro-*

- phys. J. Lett. **193**, L89.
- Greenberg, J. M., 1971, *Astron. Astrophys.* **12**, 240.
- Greenberg, J. M., and S. Hong, 1974, *Bull. Am. Astron. Soc.* **5**, 380.
- Greenberg, L., 1973, in *I. A. U. Symposium No. 52 "Interstellar Dust and Related Topics,"* edited by J. M. Greenberg and H. C. van de Hulst (D. Reidel, Dordrecht).
- Habing, H. J., 1968, *Bull. Astron. Inst. Neth.* **19**, 421.
- Harrison, A. G., and B. G. Keyes, 1973, *Can. J. Chem.* **51**, 1265.
- Heiles, C., 1971, *Annu. Rev. Astron. Astrophys.* **9**, 293.
- Herbst, E., 1976, *Astrophys. J.* **205**, 94.
- Herbst, E., and J. B. Delos, 1976, "Dynamic Renner Effect in Collisions of C* with H₂," *Chem. Phys. Lett.*, in press.
- Herbst, E., and W. Klemperer, 1973, *Astrophys. J.* **185**, 505.
- Herbst, E., and W. Klemperer, 1976, *Phys. Today* **29**, 32.
- Herzberg, G., 1945, *Molecular Spectra and Molecular Structure* (van Nostrand, New York).
- Hobbs, L. M., 1973, *Astrophys. J. Lett.* **181**, L79.
- Hollenbach, D., and E. E. Salpeter, 1970, *J. Chem. Phys.* **53**, 79.
- Hollenbach, D., and E. E. Salpeter, 1971, *Astrophys. J.* **163**, 155.
- Hollenbach, D., M. Werner, and E. E. Salpeter, 1971, *Astrophys. J.* **163**, 165.
- Hollis, J. M., L. E. Snyder, F. J. Lovas, and D. Buhl, 1976, "Radio Detection of Interstellar DCO*," *Astrophys. J. Lett.*, in press.
- Huntress, W. T., and V. G. Anicich, 1976, unpublished result.
- Iguchi, T., 1975, *Pub. Astron. Soc. Jpn.* **27**, 515.
- Jefferts, K. B., A. A. Penzias, and R. W. Wilson, 1973, *Astrophys. J. Lett.* **179**, L57.
- Johnson, H. L., 1968, in *Star and Stellar Systems: Nebulae and Interstellar Matter*, edited by B. M. Middlehurst and L. H. Aller (University of Chicago, Chicago, Ill.) Vol. VII.
- Julienne, P., and M. Krauss, 1973 in "Molecules in the Galactic Environment," edited by M. Gordon and L. Snyder (Wiley, New York).
- Julienne, P., M. Krauss, and B. Donn, 1971, *Astrophys. J.* **170**, 65.
- Jura, M., 1974, *Astrophys. J.* **191**, 375.
- Kaplan, S. A., and S. B. Pikelner, 1970, *The Interstellar Medium* (Harvard University, Cambridge, Mass.), translated from *Mezhzvezdnaya Sreda* (Moscow, 1963).
- Kerr, F. J., and S. C. Simonson, editors, 1974, *I. A. U. Symposium No. 60, "Galactic Radio Astronomy"* (D. Reidel, Dordrecht).
- Kim, J. K., L. P. Theard, and W. T. Huntress, 1974, *J. Chem. Phys.* **62**, 45.
- Klein, R., 1968, *Surf. Sci.* **11**, 227.
- Klemperer, W., 1970, *Nature (Lond.)* **227**, 1230.
- Kramers, H. A., and D. ter Haar, 1946, *Bull. Astron. Inst. Neth.* **10**, 137.
- Krauss, M., and P. Julienne, 1973, *Astrophys. J. Lett.* **183**, L139.
- Langer, W. D., and A. E. Glassgold, 1976, *Astron. Astrophys.* **48**, 395.
- Lee, T. J., 1972, *Nature Phys. Sci.* **237**, 99.
- Leu, M. T., M. A. Biondi, and R. Johnsen, 1973a, *Phys. Rev. A* **7**, 292.
- Leu, M. T., M. A. Biondi, and R. Johnsen, 1973b, *Phys. Rev. A* **8**, 413.
- Leu, M. T., M. A. Biondi, and R. Johnsen, 1973c, *Phys. Rev. A* **8**, 420.
- Linke, R. A., A. A. Penzias, R. W. Wilson, and P. G. Wannier, 1975, *Bull. Am. Astron. Soc.* **7**, 521.
- McDowell, M. R. C., 1961, *Observatory* **81**, 240.
- Marenco, G., A. Schutte, G. Scoles, and F. Tommasini, 1972, *J. Vac. Sci. Technol.* **9**, 824.
- Mathewson, D. S., and V. L. Ford, 1970, *Mem. R. Astron. Soc.* **74**, 139.
- Matsakis, D. N., M. F. Chui, P. F. Goldsmith, and C. H. Townes, 1976, *Astrophys. J. Lett.* **206**, L63.
- Mitchell, D. N., and D. J. Leroy, 1973, *J. Chem. Phys.* **58**, 3449.
- Morton, D. C., 1975, *Astrophys. J.* **197**, 85.
- Mott, N. F., and H. S. W. Massey, 1965, *Theory of Atomic Collisions* (Clarendon, Oxford).
- O'Donnell, E. J., and W. D. Watson, 1974, *Astrophys. J.* **191**, 89.
- Oppenheimer, M., and A. Dalgarno, 1974, *Astrophys. J.* **192**, 29.
- Osterbrock, D. E., 1974, *Astrophysics of Gaseous Nebulae* (Freeman, San Francisco).
- Pasachoff, J. M., and D. Cesarsky, 1974, *Astrophys. J.* **193**, 65.
- Pearson, P., and E. Roueff, 1976, *J. Chem. Phys.* **64**, 1240.
- Penzias, A. A., 1975, in *The Proceedings of the Les Houches Summer School of Theoretical Physics XXVI "Atomic and Molecular Physics and the Interstellar Matter,"* edited by R. Balian, P. Encrenaz and J. Lequeux (North-Holland, Amsterdam).
- Penzias, A. A., P. G. Wannier, R. W. Wilson, and R. A. Linke, 1976, "Deuterium in the Galaxy," in press.
- Petty, F., and T. F. Moran, 1970, *Chem. Phys. Lett.* **5**, 64.
- Pinkau, K., 1974, *The Interstellar Medium* (D. Reidel, Dordrecht).
- Purcell, E. M., 1969, *Astrophys. J.* **158**, 433.
- Purcell, E. M., 1976, *Astrophys. J.*, in press.
- Ray, S., and H. P. Kelly, 1975, *Astrophys. J. Lett.* **202**, L57.
- Ricca, F., C. Pisani, and E. Garrone, 1969, *J. Chem. Phys.* **51**, 4079.
- Rogerson, J. B., and D. G. York, 1973, *Astrophys. J. Lett.* **186**, L95.
- Saykally, R. J., P. G. Szanto, T. G. Anderson, and R. C. Woods, 1976, *Astrophys. J. Lett.* **204**, L143.
- Schaefer, H. F., 1972, *The Electronic Structure of Atoms and Molecules* (Addison-Wesley, Reading, Mass.).
- Simonson, S. C., 1970, *Astron. and Astrophys.*, **9**, 163.
- Smith, W. B., and E. G. Zweibel, 1976, *Astrophys. J.*, in press.
- Smith, W. B., H. S. Liszt, and B. L. Lutz, 1973, *Astrophys. J.* **183**, 69.
- Snow, T. P., 1976, *Astrophys. J. Lett.* **204**, L127.
- Snyder, L. E., D. Buhl, B. Zuckerman, and P. Palmer, 1969, *Phys. Rev. Lett.* **22**, 679.
- Snyder, L. E., and J. M. Hollis, 1976, *Astrophys. J. Lett.* **204**, L139.
- Snyder, L. E., J. M. Hollis, F. J. Lovas, B. L. Ulich, 1976, *Astrophys. J.*, in press.
- Solomon, P., and N. J. Woolf, 1973, *Astrophys. J. Lett.* **180**, L89.
- Solomon, P., and W. Klemperer, 1972, *Astrophys. J.* **178**, 389.
- Spitzer, L., 1948, *Astrophys. J.* **107**, 6.
- Spitzer, L., 1968, *Diffuse Matter in Space* (Wiley, Interscience, New York).
- Spitzer, L., and E. B. Jenkins, 1975, *Annu. Rev. Astron. Astrophys.* **13**, 133.
- Spitzer, L., J. F. Drake, E. B. Jenkins, D. C. Morton, J. B. Rogerson, and D. G. York, 1973, *Astrophys. J. Lett.* **181**, L116.
- Stecher, T. P., and D. A. Williams, 1967, *Astrophys. J. Lett.* **149**, L29.
- Stief, L. J., B. Donn, S. Glicker, E. P. Gentieu, and J. E. Mentall, 1972, *Astrophys. J.* **171**, 21.
- Townes, C. H., and A. C. Cheung, 1969, *Astrophys. J. Lett.* **157**, L103.
- Tucker, K. D., M. L. Kutner, and P. Thaddeus, 1974, *Astrophys. J. Lett.* **193**, L115.
- Turner, B. E., 1974, in *Galactic and Extra-Galactic Radio Astronomy*, edited by G. L. Verschuur and K. I. Kellerman

- (Springer-Verlag, Berlin).
- Turner, B. E., B. Zuckerman, N. Farinkis, M. Morris, and P. Palmer, 1975, *Astrophys. J. Lett.* **198**, L125.
- van de Hulst, H. C., 1957, *Light Scattering from Small Particles* (Wiley, New York).
- van den Bout, P. A., 1972, *Astrophys. J. Lett.* **176**, L127.
- Verschuur, G. L., and K. I. Kellerman, editors, 1974, *Galactic and Extra-Galactic Radio Astronomy* (Springer-Verlag, Berlin).
- Walker, T. E. H., and H. P. Kelly, 1972, *Chem. Phys. Lett.* **16**, 511.
- Wannier, P. G., A. A. Penzias, R. A. Linke, R. W. Wilson, 1976a, *Astrophys. J.* **204**, 26.
- Wannier, P. G., R. Lucas, R. A. Linke, P. J. Encrenaz, A. A. Penzias, and R. W. Wilson, 1976b, *Astrophys. J. Lett.* **205**, L169.
- Watson, W. D., 1972, *Astrophys. J.* **176**, 103.
- Watson, W. D., 1973a, in *I. A. U. Symposium No. 52 "Interstellar Dust and Related Topics,"* edited by J. M. Greenberg and H. C. van de Hulst (D. Reidel, Dordrecht).
- Watson, W. D., 1973b, *Astrophys. J. Lett.* **181**, L129.
- Watson, W. D., 1973c, *Astrophys. J. Lett.* **182**, L69.
- Watson, W. D., 1973d, *Astrophys. J. Lett.* **183**, L17.
- Watson, W. D., 1974, *Astrophys. J.* **188**, 35.
- Watson, W. D., 1975, in *The Proceedings of the Les Houches Summer School of Theoretical Physics XXVI "Atomic and Molecular Physics and the Interstellar Matter,"* edited by R. Balian, P. Encrenaz, and J. Lequeux (North Holland, Amsterdam).
- Watson, W. D., V. G. Anicich, and W. T. Huntress, 1976, *Astrophys. J. Lett.* **205**, L165.
- Watson, W. D., and E. E. Salpeter, 1972a, *Astrophys. J.* **174**, 321.
- Watson, W. D., and E. E. Salpeter, 1972b, *Astrophys. J.* **175**, 659.
- Watson, W. D., R. M. Crutcher, and J. R. Dickel, 1975, *Astrophys. J.* **201**, 102.
- Weinreb, S., 1962, *Nature (Lond.)* **195**, 367.
- Weinreb, S., A. H. Barrett, M. L. Meeks, and J. C. Henry, 1963, *Nature (Lond.)* **200**, 829.
- Werner, M., and E. E. Salpeter, 1969, *Mon. Not. R. Astron. Soc.* **145**, 249.
- Wilson, R. W., A. A. Penzias, P. G. Wannier, and R. A. Linke, 1976, *Astrophys. J. Lett.* **204**, L135.
- Wilson, T. L., and D. Downes, editors, 1975, *Lecture Notes in Physics No. 42 "HII Regions and Related Topics"* (Springer-Verlag, Berlin).
- Wilson, T. L., J. Bieging, D. Downes, and F. F. Gardner, 1976, "Observation of the Carbon-13 Isotope of Formaldehyde," *Astron. Astrophys.*, in press.
- Woods, R. C., T. A. Dixon, R. J. Saykally, and P. G. Szanto, 1975, *Phys. Rev. Lett.* **35**, 1269.
- Zuckerman, B., and P. Palmer, 1974, *Ann. Rev. Astron. Astrophys.* **12**, 279.

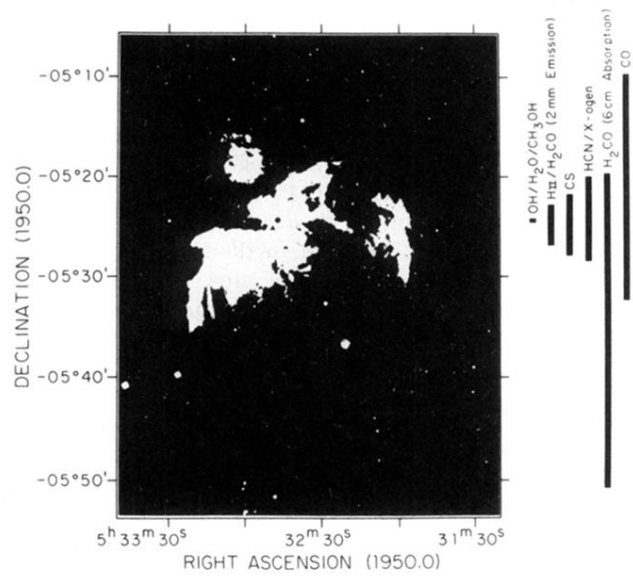


FIG. 9. The Orion Nebula. A region of bright stars and ionized gas with which a molecular cloud is associated. The extents along one axis of the emission from various molecular transitions are indicated by the bars. Axes are astronomical coordinates in degrees and minutes, and hours, minutes and seconds, of arc.